Value of Transport Flexibility under Supply Uncertainty in OCCUS Supply Chains

A Real Options approach

MSc Marine Technology Thesis

Lars de Jong

Delft University of Technology

TU Delft

VM
Value Maritime

Thesis for the degree of MSc in Marine Technology in the specialization of
Maritime Operations and Management

Value of Transport Flexibility under Supply Uncertainty in OCCUS Supply Chains

A Real Options approach

by

Lars de Jong

Performed at

Value Maritime

to obtain the degree of Master of Science
at the Delft University of Technology,
to be defended publicly on Monday July 7, 2025 at 15:00 PM

This thesis MT.24/25/041.M is classified as confidential in accordance with the general conditions for projects performed by the TU Delft

Thesis exam committee:

Chair/Responsible Professor:	Dr. ir. J.F.J. Pruijn
Staff Member:	Dr. B. Atasoy
Company Member:	J. Guljé
Company Member:	R. Bakker

Thesis details:

Student number:	5625041
Thesis number:	MT.24/25/041.M
Thesis duration:	September 4, 2024 – July 7, 2025
Faculty:	Faculty of Mechanical Engineering, TU Delft

TU Delft

VM
Value Maritime

Preface

Dear reader,

This thesis marks the end of my journey as a student, which began eight years ago at Hogeschool Rotterdam, where I set out to become a Bachelor of Science in Marine Technology. At that time, I could not have foreseen all the exciting challenges and invaluable lessons that lay ahead. After completing my bachelor's degree in Rotterdam, I realized I was not yet ready to stop studying and was eager to learn more. Pursuing a Master of Science at TU Delft was the logical next step. Now, after a few challenging extra years, I find myself writing the final sentences of this report.

One of my goals throughout my studies was to broaden my technical background, which led me to specialize in Maritime Operations & Management. During the master's program, I was fortunate to gain practical experience by working part-time at Value Maritime. Finding a suitable thesis topic happened swiftly, though refining the research focus took a bit more time. The result is this thesis, "Value of Transport Flexibility under Supply Uncertainty in OCCUS Supply Chains." I hope you enjoy reading it.

I would like to conclude by thanking everyone who supported me during my studies. I am grateful to my TU Delft supervisor, Jeroen Pruijn, for his guidance, quick feedback, and insightful input. I would also like to thank Value Maritime for the opportunity to work alongside my studies and for enabling me to write this thesis in collaboration with them. Special thanks go to my daily supervisors, Rolf Bakker and Jurriaan Gulé, for their encouragement and assistance throughout this process. Last but not least, I want to thank my family, friends, and girlfriend for their steady support, motivation, and help over the years. Without their support, this would not have been possible.

Lars de Jong
Rotterdam, June 2025

AI statement: AI-tools such as ChatGPT were used to improve readability and writing but are checked by the author, which takes responsibility for the content of this report.

Summary

This research investigates the value of transport mode flexibility in OCCUS supply chains, particularly under uncertain CO_2 supply during the early phases of CCUS development. This study aims to develop a strategic decision support model that quantifies the economic and environmental benefits of transport flexibility within the supply chain.

The literature review provides two key insights. First, it identifies the essential steps in the CO_2 supply chain: CO_2 is captured onboard ships, temporarily stored onboard in solvent, and transported to onshore facilities for regeneration and liquefaction, after which the liquefied CO_2 is transported to permanent underground storage. Second, the review reveals that no comprehensive studies currently model the full OCCUS supply chain while incorporating uncertainty in CO_2 supply. Consequently, no established approaches exist to address transport flexibility under such uncertainty within this context. However, real options analysis has been successfully applied in land-based CCUS projects to value investment and operational flexibility under uncertainty. Building on this proven methodology, the present research adopts a real options approach to quantify the value of the option to switch between transport modes.

This research applies the developed real options model to a case study centered on the Port of Rotterdam. The supply chain model follows the Value Maritime approach: CO_2 is captured onboard ships, stored in CO_2-rich solvent and offloaded at the Maasvlakte terminal. Transport from the port to the regeneration and liquefaction facility is done with containerized trucks, with the option to switch to barges. Two barge types are considered: the smaller CEMT-IVa and the larger CEMT-Va or a combination of the two. The LCO_2 is subsequently transported by truck to an underground storage site. The model evaluates scenarios under both a fixed average CO_2 price (€136/t) and a variable CO_2 price increasing over time based on market forecasts.

The results indicate that while the average CO_2 price is insufficient to achieve economic viability at any time and outcome, incorporating the option to switch from truck to barge transport adds value if CO_2 supply grows. The option to switch to the smaller CEMT-IVa (€630345) barge shows greater economic benefits compared to the larger CEMT-Va (€131555), mainly due to its better alignment with expected supply volumes during the early implementation phase. The combined switching option (€632010) only yields a marginal additional value, as the larger barge is only required at the highest and least probable supply scenario.

Under the variable CO_2 price scenario, the truck-only strategy reaches a positive total value by 2031 with a 30% probability. Introducing the option to switch to the smaller CEMT-IVa barge accelerates this to 2029 with a 55% probability, reflecting earlier and more frequent switching. The larger CEMT-Va barge lags behind, with switching and positive value only occurring from 2030 onward and at a lower 11% probability, indicating less frequent and delayed use.

The break-even price for the truck-only transport strategy is €184.21/tCO_2. The inclusion of switching options reduces this threshold across all configurations: the CEMT-IVa barge option achieves a 4.35% reduction to €176.19/tCO_2, while the CEMT-Va barge provides a modest 0.92% reduction to €182.52/tCO_2. The combined strategy yields the largest reduction of 4.36%, lowering the break-even price to €176.17/tCO_2.

Contents

List of Figures

List of Tables

Acronyms

CAPEX Capital Expenditure. 8, 24, 25
CCUS Carbon Capture Utilization and Storage. iii, 2, 7, 8, 13, 15–18, 25, 72, 73

DCF Discounted Cash Flow. 28, 29, 48, 49, 51, 53, 58, 60, 61
DNV Det Norske Veritas. 13
DOGF Depleted Oil&Gas Field. 43

EOR Enhanced Oil Recovery. 9
EU ETS European Emissions Trading System. 1, 9, 10, 22, 23, 31, 32, 59

FPSO Floating Production, Storage and Offloading. 33

GBM Geometric Brownian Motion. 16–18
GFI GHG Fuel Intensity. 9
GHG Greenhouse gas. 1, 8, 9, 15
GWP Global Warning Potential. 14

IMO International Maritime Organization. 1, 32, 35, 36

LCA Life Cycle Assessment. 10, 11, 14, 15, 23
LNG Liquefied Natural Gas. 1, 14
LPG Liquefied Petroleum Gas. 1

MILP Mixed Integer Linear Programming. 15, 16, 18, 73
MRV Monitoring Reporting and Verification. vi, 9, 33–36

NPV Net Present Value. 16, 18

OCC Onboard Carbon Capture. 2, 4, 5, 8, 11–14, 32, 35, 36, 66, 70–72
OCCUS Onboard Carbon Capture Utilization and Storage. iii, 2–4, 7, 11, 13–15, 18, 22, 31, 37, 46, 60, 66, 70, 72–75
OPEX Operational Expenses. 8, 24, 25

RO Real Options. 15, 16, 18, 20, 36, 73

TEA Techno-Economic Assessment. 5, 14

WTW Well-to-Wake. vi, 36

1

Introduction

In recent years, the global population has increasingly witnessed the tangible impacts of climate change, including widespread forest fires, severe heatwaves, and intense storms. These phenomena are driven by global warming, a consequence of the enhanced greenhouse effect resulting from the combustion of fossil fuels, which releases significant amounts of greenhouse gasses into the atmosphere (Graus et al., 2024).

In today's globalized economy, international trade is crucial for meeting societal needs, with the maritime industry facilitating over 80% of worldwide trade (The Economist Group, 2023). However, the industry faces significant challenges in reducing its carbon footprint. Currently, only around 2% of vessels sail on alternative fuels. In the new building order book, 27% of vessels are propelled by alternative fuels. This category includes Liquefied Natural Gas (LNG), Liquefied Petroleum Gas (LPG), and methanol. (ABS, 2024). While these fuels are less carbon-intensive on a well-to-wake basis compared to traditional fossil fuels, their combustion still results in the release of CO_2 into the atmosphere.

According to the fourth International Maritime Organization (IMO) Greenhouse gas (GHG) study, international shipping was responsible for 1,076 million tons of GHG emissions in 2018, which is expressed in CO_{2e}. To put this in perspective, this is approximately 2.89% of total global emissions. Without additional measures, emissions from international shipping were about 90% of 2008 levels in 2018 and are projected to increase to between 90% and 130% of 2008 levels by 2050, depending on economic and energy developments (IMO, 2020).

To reduce emissions in the shipping industry, governments and regulatory bodies, such as the IMO and the European Union, have set reduction targets and regulations. In the revised IMO GHG Strategy, two indicative checkpoints are mentioned: at least 20%, striving for 30% by 2030, and at least 70%, striving for 80%, by 2040 compared to 2008 levels (IMO, 2023). Additionally, during MEPC83, the committee approved a new pricing and reward mechanism based on well-to-wake GHG fuel intensity standards, set to come into force in 2027 (IMO, 2025). Under this mechanism, penalties could rise to as much as $385 per tonne of CO_{2eq}. Besides the IMO, the European Union has included shipping in its "Fit for 55" package. Ships above 5000 GT are included in the European Emissions Trading System (EU ETS) and FuelEU, which introduces penalties based on the GHG intensity of energy usage onboard (Faber et al., 2022).

Various decarbonization technologies and solutions are being researched, including energy-saving devices, biofuels, low or zero-carbon fuels, and carbon capture. While sustainable fuels are key to reaching net-zero emissions, their limited availability and high prices hinder short to medium-term adoption (BV, 2024). Although carbon capture does not result in net-zero emissions, increases fuel consumption and is limited by available space, research indicates the technological and economic viability of onboard carbon capture systems to reduce GHG emissions in the short and medium term. This makes carbon capture technology an interesting decarbonization option (Ros et al., 2022; Tavakoli et al., 2024).

Carbon Capture is an element of the broader concept of Carbon Capture Utilization and Storage (CCUS) strategy, recognized by the International Energy Agency as one of the four pillars of the energy transition (IEA, 2020). Currently, Europe is in the early stages of developing this necessary infrastructure. There are 119 commercial-scale CCS facilities in various stages of progress across the continent (Gerrits & Blanchard, 2023). Many industrial emitters are located in or near ports, which enhances the feasibility of integrating ship-based carbon capture with land-based systems, making this an attractive option for the maritime industry (DNV, 2024). Regulations regarding carbon capture are uncertain for both shipping and land-based CCUS projects, leading to uncertainties that impact the total CO_2 flow (IEA, 2020).

Given that vessels berth at ports, while outlet locations are located across Europe, the transportation and handling of captured CO_2 becomes essential. For Onboard Carbon Capture (OCC) an efficient Onboard Carbon Capture Utilization and Storage (OCCUS) supply chain around ports is crucial to maximize outlet possibilities and reduce overall costs (BV, 2024; DNV, 2024; LR, 2023). However, transport infrastructure is currently lacking, making it difficult for early adapters of carbon capture to move their captured CO_2 to suitable outlet locations (Oeuvray et al., 2024). On the other side, a network will only be developed if sufficient CO_2 is captured and transported, making a decision about which transport mode to use difficult (Becattini et al., 2024).

Value Group, consisting of two daughter companies, Value Maritime and Value Carbon, is one of the first companies to develop, build and commercially sell onboard carbon capture technologies. A key difference with respect to other competitors is that Value Group regenerates CO_2 from the captive liquid on the landside instead of on the vessel itself. Necessitating the transport of solvent with CO_2 from vessels to conditioning hubs. Due to the above-mentioned constraint, it is uncertain how much CO_2 must be transported. Hence, they are interested in what possible transport options are and how uncertainty influences the decisions to deploy a transport mode.

1.1. Research Objective

The objective of this research is to enhance understanding of OCCUS supply chains by exploring key technologies, process steps, and associated uncertainties. It further aims to develop a strategic decision support model to evaluate economic and environmental feasibility, with a focus on the value of transport mode flexibility under uncertain CO_2 supply during early implementation. Additionally, the study provides insights into total supply chain costs, estimates the minimum required CO_2 price for break-even, and supports decision-making on the timing and selection of transport modes based on expected and uncertain CO_2 volumes.

1.2. Research Questions

To achieve the stated research objective in section 1.1, the following main research question is formulated:

How does transport mode flexibility affect the economic and environmental feasibility of onboard carbon capture utilization and storage supply chains during the early implementation phase under uncertain CO_2 supply to a port?

To answer the main research question, the following sub-research questions are formulated:

1. What are the required steps, technologies, and sources of uncertainty associated with OCCUS supply chains?
2. How have previous studies modelled OCCUS supply chains, and what methodologies have been used to incorporate uncertainty in CO_2 supply?
3. Which parameters and criteria are needed to evaluate the influence of flexibility on the economic and environmental aspects of OCCUS supply chains?
4. What is the synthesis of a model that evaluates transport mode flexibility in OCCUS supply chains under uncertain CO_2 supply?
5. How can the impact of transport mode switching flexibility on economic and environmental feasibility of OCCUS supply chains be demonstrated through a case study?

1.3. Report Structure

The structure of this report is as follows. First, a background is provided regarding the required steps and technologies of OCCUS supply chains in chapter 2, focusing on research question 1. Chapter 3 answers research question 2 by presenting a comprehensive literature review to address modelling approaches used to model OCCUS supply chains incorporating uncertainty in CO_2 supply. Chapter 4 provides a detailed description of the developed model and addresses sub-research questions 3 and 4. This is followed by Chapter 5, which outlines the input parameters and describes the case study setup, contributing to the evaluation of sub-research questions 3 and 5. Chapter 6 presents the results of the model application and case study, with a particular focus on sub-research question 5. Chapter 7 offers a reflection on the modelling assumptions and discusses the limitations and implications of the approach. Finally, Chapter 8 summarizes the main findings and provides answers to the research questions.

2

Background on OCCUS Supply chains

This chapter focuses on the steps and technology required to operate the full OCCUS supply chain. The OCCUS supply chain is a comprehensive system designed to mitigate CO_2 emissions from the shipping industry. In section 2.1, OCC systems will be elaborated. After this, temporary storage methods are explained in section 2.2. In section 2.3, different offloading strategies are provided. After this, the different CO_2 transport methods are explained in section 2.4. The different outlet options are defined in section 2.5.

Figure 2.1 provides a global visualization of the conventional supply chain. It commences with the capture of CO_2 from ship exhaust gases using advanced technologies. The captured CO_2 is temporarily stored onboard until offloading is possible. Subsequently, the CO_2 is transported to designated outlet locations. At these locations, the CO_2 can either be utilized or stored permanently to prevent it from being released into the atmosphere.

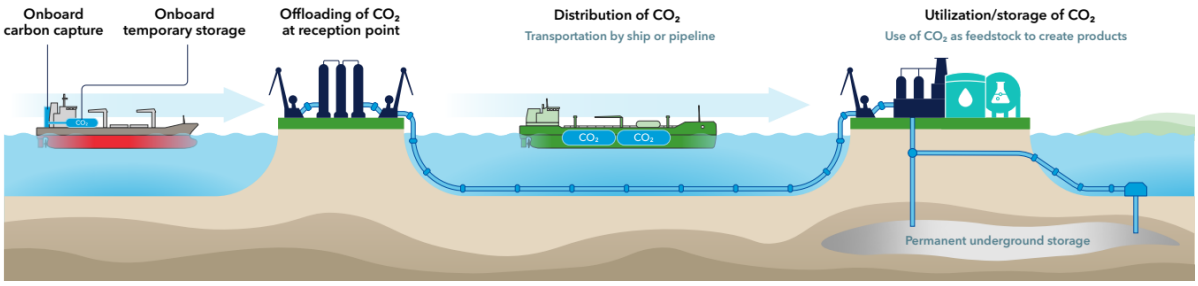

Figure 2.1: Global OCC supply chain visualization (DNV, 2024)

As highlighted in the chapter 1, the Value Maritime system differs from the conventional methodology. To provide background on the differences, similarities, and need for a supply chain model, an overview of the required steps is provided in this chapter.

2.1. Onboard Carbon Capture Systems

OCC represents the first step in the OCCUS chain, but its implementation onboard ships raises some important questions such as, how is carbon captured at sea, and what systems are required? While less mature than land-based applications, research indicates that OCC could be technically and economically viable for maritime use (BV, 2024; DNV, 2024; Luo & Wang, 2017; Zhao et al., 2025). Carbon capture technologies are typically grouped into three main categories: pre-combustion, oxy-fuel combustion and post-combustion.

Pre-combustion carbon capture, in which CO_2 is separated before combustion via syngas reforming, is currently not applied onboard ships due to high retrofitting costs, limited maturity, and compatibility issues with marine engines (Law et al., 2024; Thaler et al., 2022). Oxy-fuel combustion burns fossil fuels in pure oxygen instead of air, producing flue gas mainly composed of CO_2 and H_2O (Wilberforce et al., 2019). Onboard Oxy-fuel concepts are not competitive due to reduced engine efficiencies and high energy demand for onboard oxygen supply (Wohlthan et al., 2024). As both technologies remain underdeveloped for onboard application, they are excluded from the scope of this research.

Post-combustion carbon capture represents the most developed carbon capture technology (Bui et al., 2018). It typically relies on chemical absorption, where exhaust gas passes through an absorber column and contacts a lean solvent that captures CO_2 (MacDowell et al., 2010). The cleaned exhaust gas is vented, and the CO_2-rich solvent is sent to a regenerator column, where heat releases the captured CO_2 and regenerates the solvent. The solvent is reused, and the released CO_2 is compressed and liquefied for transport or storage (Madejski et al., 2022).

The concept of OCC was first researched by Luo and Wang (2017), who introduced a solvent-based OCC system. A comprehensive Techno-Economic Assessment (TEA) was conducted for a cargo ship to evaluate the technical feasibility of the system. More recent research primarily assesses techno-economic viability through dedicated case studies. These studies span a wide range of vessel types, engine power levels, and fuel variations.

Across these studies, several common challenges have been highlighted. These include solvent selection, height restrictions for absorber and regenerating equipment, vessel operational schedules, the fuel penalty and onboard storage capacity(Feenstra et al., 2019; Long et al., 2021; Luo & Wang, 2017; Stec et al., 2021; Tavakoli et al., 2024). Among these, the fuel penalty and storage requirements are highlighted as the most challenging.

The fuel penalty is caused by the additional energy required for operating equipment such as compressors, pumps, and solvent regeneration. This results in increased fuel consumption, which varies based on capture system efficiency, fuel type, engine configuration, and use of waste heat recovery (Luo & Wang, 2017; Visonà et al., 2024). For example, Einbu et al. (2022) conducted an energy assessment including flue gas heat integration and concluded that available exhaust heat is not sufficient, resulting in a 6–9% fuel increase for LNG and 8–12% for diesel. This contrasts with Feenstra et al. (2019), who assumed sufficient high-temperature waste heat was available, and with Tavakoli et al. (2024), who reported much higher fuel penalties of 70–100%. These wide variations highlight the influence of multiple factors and the lack of consensus on a reliable range. This underscores the need for further research or alternative capture methods.

In addition to the energy penalty, storing the captured CO_2 onboard poses significant design and operational challenges. To optimize storage capacity, most studies propose liquefying CO_2. While Luo and Wang (2017) assumed a high storage pressure of 100 bar, more recent work suggests pressures in the range of 15–22 bar (Feenstra et al., 2019; Long et al., 2021; Tavakoli et al., 2024; Visonà et al., 2024). Although lower pressures ease technical demands, they still necessitate additional equipment and energy input, adding to the system's complexity and cost.

To address the challenges related to the fuel penalty, as indicated in the previous section, Value Maritime employs a different system. Unlike typical methods described in the literature, where CO_2 is regenerated using the heat from exhaust gases and subsequently liquefied for onboard storage, Value Maritime employs a method where CO_2 is regenerated on land using renewable energy sources if possible. Figure 2.2 shows schematically how the OCC system operates. In this system, lean solvent is stored in dedicated tanks or ISO tank containers onboard the vessel. During operation, a pump continuously circulates a solvent from the storage tanks to an absorption tower, where it is sprayed over the exhaust gases to capture CO_2 molecules. This cyclical process continues until the solvent becomes saturated with CO_2. Once saturation is achieved, the CO_2-rich solvent is offloaded to shore facilities, where it is replaced with fresh lean solvent.

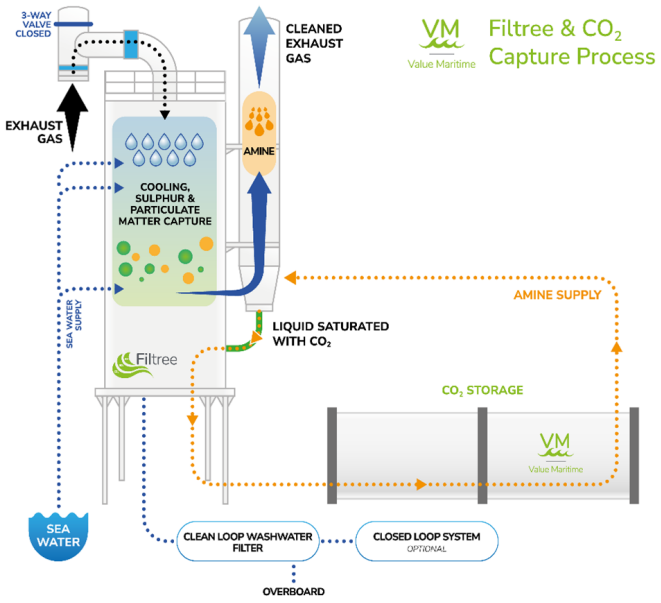

Figure 2.2: The Value Maritime onboard carbon capture process

This approach offers several advantages over conventional post-capture systems. The primary benefit is the reduced onboard energy requirement, as no additional heat is needed for CO_2 regeneration and less power is required for liquefaction equipment such as compressors. These factors contribute to a lower fuel penalty since less additional fuel is consumed. Furthermore, onboard storage requirements are less demanding, as the rich solvent can be stored in regular tanks, unlike LCO_2.

However, this approach also introduces several operational disadvantages. Most notably, the storage capacity for CO_2 is lower compared to liquefied systems since saturated solvent holds less CO_2 per unit volume. Furthermore, the high density of the solvent adds considerable weight, especially at larger volumes. Operating the system also requires a greater total volume of solvent, which must be regularly exchanged once saturation is reached, leading to more frequent transport cycles. Since solvent regeneration and CO_2 liquefaction occur on land, rich solvent must be transported efficiently to the conditioning facility. Table 2.1 provides a summarized comparison of key advantages and disadvantages. These factors underline the importance of designing a flexible solvent transport system.

Table 2.1: Comparison of Value Maritime and conventional carbon capture systems

	Advantages	Disadvantages
VM	Low fuel penalty Less onboard equipment Less stringent storage requirements Less expensive	Lower absolute storage capacity High mass of saturated solvent Extra transport steps on land
LCO_2	More storage capacity Fewer transport steps on land	More equipment required High fuel penalty Strict storage requirements More expensive

2.2. Temporary (onboard) Storage

The second step in the chain is temporary onboard storage, which is an important aspect of the system. It depends on various parameters specific to each vessel, such as operational profile, offloading intervals, and storage capacity. LCO_2 Storage is typically categorized into low-pressure (LP, 5.7–10 bara, -54.3°C to -40.1°C) and medium-pressure (MP, 14–19 bara, -30.5°C to -21.1°C) systems. There are two different solutions for onboard LCO_2 storage, either insulated vessels or ISO tank containers (Buirma et al., 2022). The best solution may vary depending on the vessel type (Skagestad et al., 2024). In addition to onboard storage, temporary storage on land is carried out in the same manner.

Saturated solvent storage requires no insulation or pressurized tanks, making it easier to operate and retrofit. It can be stored in ISO containers or dedicated tanks, although it stores less CO_2 compared to LCO_2. Since Value Maritime's process is used, onboard storage of liquefied CO_2 is excluded from this study. Instead, the saturated solvent is chosen as the temporary onboard storage method. The same applies to temporary storage before the regeneration and liquefaction process. Up until this stage, it is possible to store the CO_2 in the solvent. Hereafter, the CO_2 is liquefied, and the same conditions described above apply.

2.3. Offloading of CO_2

The third step in the OCCUS chain is offloading captured CO_2, either for temporary buffer storage or direct transfer to transport. Research on offloading options is limited, but GCMD (2024) outlines four main concepts:

- Ship-to-Liquid Bulk Terminal
- Ship-to-Floating CO_2 Storage via an intermediate receiving vessel
- Ship-to-Liquid Bulk Terminal with an intermediate receiving vessel
- Ship-to-Terminal with ISO Tank Containers

For the Value Maritime process, Ship-to-Terminal with ISO containers or Ship-to-Chemical Barge is used.

2.4. Transportation of CO_2

The next step is to transport the received CO_2 from the port to the conditioning plant or the selected outlet. The most common CO_2 transport modes include pipelines, ships, trucks, trains, and barges (Al Baroudi et al., 2021; Dziejarski et al., 2023; Gür, 2022). Understanding the requirements for transporting CO_2 and the factors influencing the choice of transport mode is critical for designing a reliable and cost-effective OCCUS infrastructure.

2.4.1. Pipeline transport

Pipelines are considered the most efficient method for transporting large volumes of CO_2 (Wilberforce et al., 2019). Extensive research has been conducted to develop pipeline networks. Even open-source pipeline design tools such as SimCCS are available (Middleton et al., 2020). The decision to use pipelines depends on various factors. One key factor is the transport distance. Pipelines are generally considered viable for distances up to 1500 km (Bui et al., 2018). Another important factor is the required flow rate of CO_2, which directly influences the pipeline diameter and, consequently, the investment cost (Solomon et al., 2024).

Although pipelines are considered the most cost-effective way of transporting large volumes of CO_2, it has some minor disadvantages. Constructing a pipeline network requires significant capital and development time. An optimal design considers flow rates, pressure drops, and the potential for future expansion. Integrating CO_2 transport infrastructure with capture and storage systems is essential to enhance the overall efficiency of the CCUS chain (Bui et al., 2018). A network is likely to be established only if both the storage capacity and the volume of captured CO_2 are assured at a sufficient scale. At the same time, emitters will capture CO_2 only if there is guaranteed transportation to a storage site. This mutual dependence could potentially slow down its development (Oeuvray et al., 2024).

Although solvent could theoretically be transported via pipelines, this has not been studied in the literature. Moreover, long-distance transportation of solvent is generally not expected, so the use of pipelines for solvent transport is excluded from the scope of this study.

2.4.2. Ship and barge transport

Ship and barges are often considered for CO_2 transport for longer distances and relatively lower quantities compared to pipelines (Al Baroudi et al., 2021). Although CO_2 transport by ships or barges has been used for decades in the food and beverage industry, the quantities required in this sector are much smaller, with capacities ranging from 800 m^3 to 1000 m^3. For CCUS chains, volumes up to 10,000 m^3 are required (Hua et al., 2023).

The preferred operating pressure for CO_2 shipping is generally considered to be near 7 barg, which is widely considered optimal due to its cost-effectiveness and technical feasibility (Roussanaly et al., 2021b). This specification is also comparable to the conditions typically used for onboard CO_2 storage. However, due to operational constraints, reconditioning could be required (d'Amore et al., 2024).

Various studies have examined the transport of CO_2 by ships and barges, often comparing their application to pipelines. Generally, there is consensus that shipping provides notable advantages under specific conditions, primarily due to its flexibility. Ships can connect multiple capture sites, reroute easily to alternative storage sites, and adjust capacities when necessary, reducing financial risks and uncertainties (Kjärstad et al., 2016; Neele et al., 2017).

The Capital Expenditure (CAPEX) of ships are lower compared to a pipeline network, but Operational Expenses (OPEX) are significantly higher, reflecting a distinct difference in cost structure (Kjärstad et al., 2016). Besides, ships emit more GHG emissions than pipelines during operation, as they still primarily rely on fossil fuels. A major source of emissions during CO_2 transport by ship is the electricity consumption of the CO_2 liquefaction plant. Additionally, some CO_2 is lost through vaporization during transport. To control the pressure inside the storage tanks, a fraction of the LCO_2 is released as boil-off gas, typically around 0.15% (Al Baroudi et al., 2021; Jayarathna et al., 2021).

The transport of saturated solvent by ships or barges has not been thoroughly researched in literature. The saturated solvent is classified as chemical. Therefore, it can be transported by regular chemical ships or barges. According to transport companies, the use of stainless steel classified tanks is preferred. Ocean-going transport of saturated solvent is unlikely to be required. Therefore, these vessels will be excluded from this research. Barges may be used for collecting and delivering saturated solvent to ocean-going vessels equipped with OCC systems.

2.4.3. Truck and train transport

CO_2 transport by truck or train has received less attention compared to pipeline, ship, or barge transport. However, interest in truck or train transport has increased in recent years, as pipeline infrastructure and large-scale shipping often require years to develop and implement, which slows down CCUS deployment (Oeuvray et al., 2024). Generally, for short distances, shorter project lifetimes, and smaller quantities, trucks or trains may be more suitable according to presented overviews (Myers et al., 2024).

CO_2 transport by truck or train is carried out under similar conditions to that of ships and barges. Two main transport options exist: container-based and dedicated. Container-based transport uses 20-foot ISO tank containers ($\approx$ 20 tonnes capacity), while dedicated transport involves fixed tanks with higher capacity but requires filling and discharging steps, potentially leading to LCO_2 reconditioning (Oeuvray et al., 2024). For saturated solvent, the same options apply, but the fluid is transported at ambient conditions.

Container-based transport is preferable for early deployment due to its existing infrastructure, whereas dedicated transport offers greater long-term advantages in terms of capacity, cost-efficiency, and environmental performance. Trucks provide high flexibility but at the cost of higher emissions, expenses, and congestion. Trains are more reliable but lack cost-efficiency due to limited economies of scale (Oeuvray et al., 2024).

2.5. Storage and Utilization

The outlet or sink of captured CO_2 is generally divided into two different possibilities, either permanent storage or utilization.

2.5.1. Permanent Storage

Storage of CO_2 is the process of injecting CO_2 in a suitable deep underground storage site (IEA, 2020). This process relies on established technologies that have been available for decades (Rubin et al., 2005). CO_2 is commonly used in Enhanced Oil Recovery (EOR), where it is injected into reservoirs to boost oil production (Bui et al., 2018). Experience from EOR demonstrates the feasibility of geological CO_2 storage, with studies suggesting that 99% of the CO_2 can be retained for at least 1000 years (Metz et al., 2005). Storage sites for CO_2 are available worldwide, both onshore and offshore. Onshore projects often face societal resistance and legal restrictions, such as in the Netherlands (Arning et al., 2019). Offshore storage avoids these concerns but involves higher costs, introducing uncertainty in global and local storage capacity estimates. In general, three different storage options are distinguished: depleted oil& natural gas reservoirs, (unmineable) coal seams and saline aquifers.

Currently, only a few storage facilities are commercially operational or expected to open in the near future (Global CCS Institute, 2024b). Examples include Aramis, Northern Lights, and Porthos. However, the shipping industry is not the only sector capturing CO_2 and seeking access to these storage sites. Raising the critical question how much capacity will be available for CO_2 captured by maritime vessels. Although large quantities of CO_2 can be stored, some have already been fully booked, such as Porthos.

Permanent underground storage is an interesting option for shipping. Starting January 2024, the EU ETS will require shipping companies to purchase allowances for their GHG emissions based on their emissions monitored according to Monitoring Reporting and Verification (MRV). To facilitate a phased transition, shipping companies will need to buy emission allowances incrementally:

- Covering 40% of verified emissions reported for 2024 in 2025.
- Increasing to 70% of emissions reported for 2025 in 2026.
- From 2027 onward, surrendering allowances for 100% of emissions reported annually.

According to Directive 2003/87/EC, emissions captured and stored under Directive 2009/31/EC (CCS Directive) allow shipping companies to subtract captured CO_2. Directive 2023/959, which was added later, allows for the reduction of GHG emissions if they are permanently chemically bound in a product, preventing their release into the atmosphere during normal use (BV, 2024; DNV, 2024).

In addition to this. At MEPC 83, a new chapter was added to MARPOL Annex VI, establishing a framework for the approval of a new GHG Fuel Intensity (GFI). This regulation will enter into force in 2027 and will apply to all ships above 5000 GT. The GFI is a well-to-wake metric GHG emissions per unit of energy used onboard. There are two targets: the base target and the direct compliance target. The base year is 2008. If the ships GFI is below the Direct Compliance target, it earns surplus units. If its GFI is higher, it incurs compliance deficits. A GFI between the two targets results in a Tier 1 deficit, while a GFI above the Base target results in both Tier 1 and Tier 2 deficits. Surplus units can be transferred to other ships or banked for up to two years. Tier 2 deficits can be covered with surplus units or Tier 2 remedial units at \$380 per tonne of CO_{2eq}. Tier 1 deficits must be offset with Tier 1 remedial units at \$100 per tonne (IMO, 2025). A graphical representation of the tiers and pricing mechanism is shown in figure 2.3.

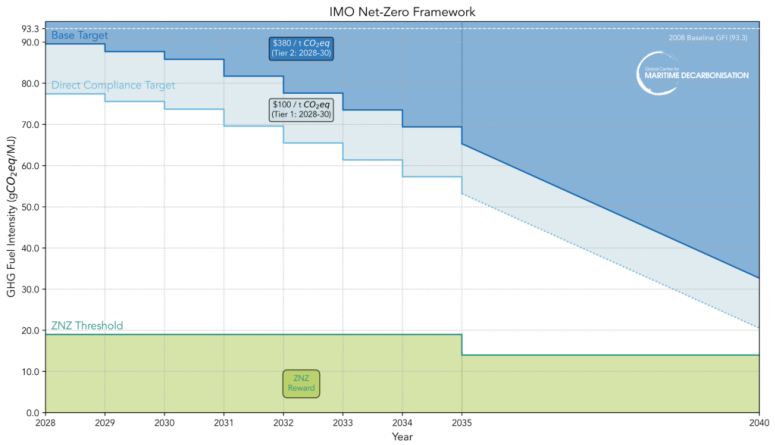

Figure 2.3: GFI pricing system (GCMD, 2025)

2.5.2. Utilization

An alternative to underground storage is CO_2 utilization, which (re)uses CO_2 as a raw material in various industrial processes (Osman et al., 2021). Numerous utilization pathways for CO_2 already exist or are being actively researched (Rafiee et al., 2018). Figure 2.4 provides a schematic process flow of possible utilization options, which shows that CO_2, in combination with (renewable) energy and other products, can be transformed to required materials such as synthetic fuels, chemicals or construction materials. Another option is to use captured CO_2 for growing crops or flowers in greenhouses. Utilization does not necessarily reduce emissions and does not necessarily deliver a net climate benefit (Hepburn et al., 2019). To assess the net reduction, a comprehensive Life Cycle Assessment (LCA) study is required.

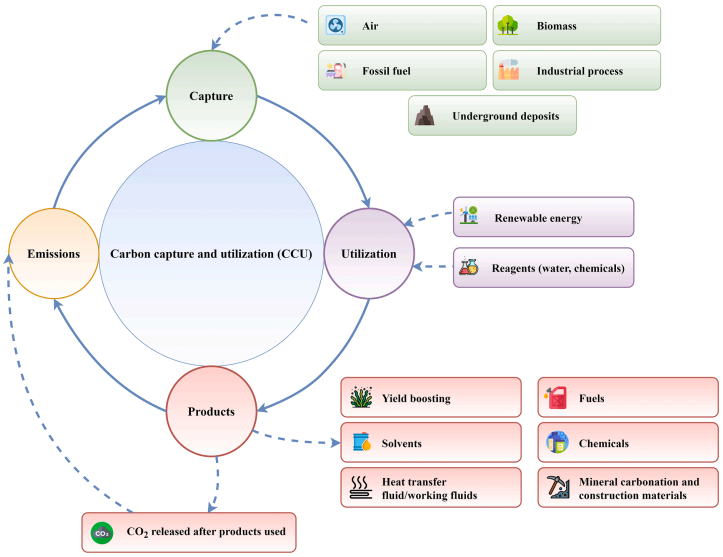

Figure 2.4: Overview of CCU process flow (Dziejarski et al., 2023)

In contrast to permanent CO_2 storage, emission allowances under the EU ETS cannot be deducted if the captured CO_2 is used for utilization purposes. However, economic incentives may arise from the sale of CO_2 to companies that use it in their processes. The price of CO_2 varies, ranging from $15 to $400 per ton CO_2 depending on purity requirements (IEA, 2019).

2.6. Conclusion supply chain steps

This section provides the final findings and scope related to this research.

2.6.1. Findings

Based on the available literature, industry reports and discussions with Value Maritime, the steps in the OCCUS supply chain are influenced by several factors, including the type of carbon capture system used and the method of temporary onboard CO_2 storage. These early choices significantly influence the required subsequent steps. For this study, conducted in collaboration with Value Maritime, the supply chain is defined as follows: The process begins with OCC using a post-combustion, solvent-based carbon capture system, in which CO_2 is absorbed and stored in the solvent under ambient conditions. Upon arrival at the port, the solvent is offloaded and transported by truck or barge to a conditioning facility. The switch decision model is focussed on this particular transport step. At the CO_2 hub, the solvent is regenerated, and the CO_2 is liquefied. In the final stage, the liquefied CO_2 LCO_2 is transported to an underground storage site for permanent sequestration. A schematic overview of these steps and scope is illustrated in figure 2.5.

Because the adoption of OCC is still in its early stages, the total volume of captured CO_2 arriving at ports is highly uncertain but expected to grow significantly over time. Combined with the need for additional solvent transport, as highlighted in section 2.1, this creates a strong demand for efficient and flexible solvent transport infrastructure to ensure economic and environmental feasibility during early deployment phases.

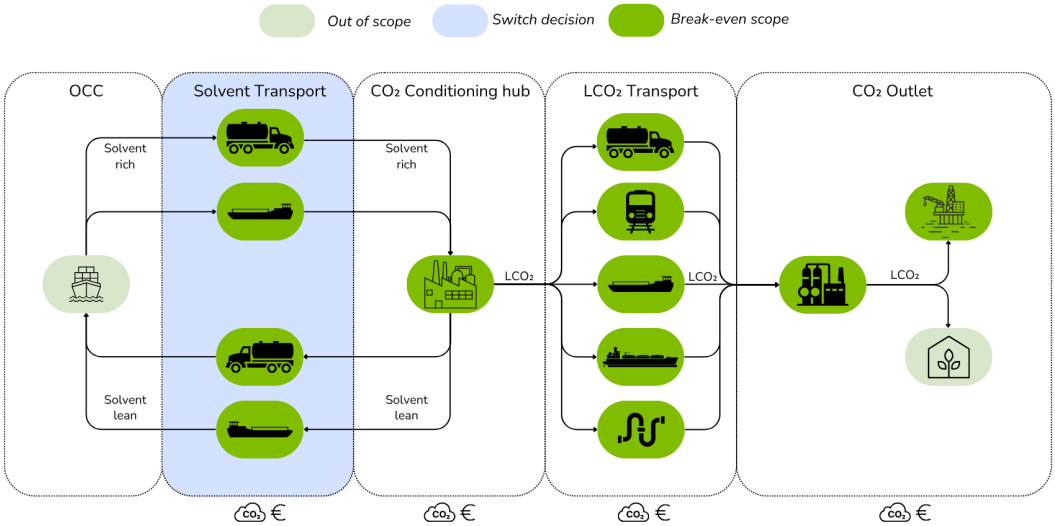

Figure 2.5: OCCUS supply chain steps

2.6.2. Scope

Due to the complexity and the large number of potential configurations within the overall OCCUS supply chain, as illustrated in the previous sections, scoping is necessary to ensure the research remains manageable within the constraints of the available time and accessible public data.

As discussed in section 2.5.2, a comprehensive LCA is typically required for a complete environmental assessment. However, this study considers only direct emissions (Scope 1 and 2). Scope 3 emissions are excluded.

As this study is conducted in collaboration with Value Maritime, the modelled OCCUS supply chain is based on their principles and system design, as illustrated in section 2.6.1. Given that their primary area of operation is within Europe, the geographical focus of this study is limited to the European region. The analysis concentrates on the start-up phase of the OCCUS supply chain, covering the period from 2025 to 2035. Further details are provided in chapter 5.

The study focuses on the land-based part of the supply chain. Therefore, costs and emissions due to the fuel penalty of the OCC systems are excluded from the scope of this research. Based on the Value Maritime OCC system with a lower fuel penalty, this is reasonable as the processes are transferred to land. In addition, the model is more focused on a broader fleet-wide scale. Therefore, technical parameters such as onboard storage capacity are excluded. Instead, a total aggregate CO_2 supply by a fleet is considered.

As described in section 2.2, depending on the type of onboard storage, it may be necessary to either pump solvent or handle storage containers. This step is excluded from the analysis in this study, as including it would result in an overly complex model. Additionally, temporary storage before and after the conditioning process is also excluded.

As elaborated in section 2.4, various transport modes are available for moving CO_2. However, this study is limited to truck and barge transport for the transport of saturated solvent, reflecting the early phase of deployment. For the transport of LCO_2, the transport modes are limited by the modes assessed by Oeuvray et al. (2024).

The sizing of equipment and the required capacity of the regeneration and liquefaction process are excluded from the scope of this study to limit complexity. It is assumed that the plant has sufficient capacity for the incoming CO_2 flows. While these factors do influence the required minimum CO_2 price to achieve break even, they do not affect the value of switching flexibility between transport modes.

The selection of promising CO_2 utilization routes and assessment of corresponding market demand are excluded from the scope of this study due to ongoing uncertainties regarding regulations and their actual emission reduction potential. As a result, the analysis focuses solely on underground storage as the outlet. Furthermore, the analysis excludes consideration of the available share of underground storage capacity that could be allocated to captured CO_2 from maritime vessels, as well as any assumptions regarding minimum required volumes for storage.

3

State of the Art Literature Review

In this chapter, an overview of the relevant literature with respect to OCCUS supply chains will be presented. The review aims to assess how current research models the OCCUS supply chain under uncertainty, with a particular focus on flexibility in transport deployment. Drawing from available literature, the main gaps in current research will be identified. Section 3.1 outlines the search plan and approach used to identify and select relevant literature. Section 3.2 provides an overview of the current modelling approaches of OCCUS supply chains. After this, land-based CCUS modelling approaches are discussed. Finally, section 3.4 summarizes the key findings of the literature review.

3.1. Search plan

This section describes the literature search plan to obtain relevant literature for this research. To gain a comprehensive understanding of the OCCUS supply chain, it is important to understand the process, including the technologies used, the steps involved, and the current state of academic research.

To achieve this, a comprehensive literature review is performed. The primary database used is *Scopus*. In addition, other databases such as *Semantic Scholar*, *Google Scholar*, and *Web of Science* are checked for relevant papers. To supplement scientific literature, industry reports and public research outputs are also included. For example, reports from classification societies such as Det Norske Veritas (DNV), organisations like the *Global Centre for Maritime Decarbonisation* and research projects like *EverLoNG* are included. To find more relevant research, the snowballing technique is applied.

To retrieve the relevant research papers focusing on the uncertainty in CO_2 supply by maritime vessels and the overall OCCUS supply chain, the following search terms and combinations are searched on Scopus.

- ship based OR onboard carbon capture AND supply chain AND uncertainty
- ship based OR onboard carbon capture AND supply chain AND flexibility
- ship based OR onboard carbon capture AND transport AND uncertainty
- ship based OR onboard carbon capture AND transport AND flexibility
- ship based OR onboard carbon capture AND transport AND supply uncertainty
- ship based OR onboard carbon capture AND transport AND CO_2 supply

After screening the titles and abstracts of the retrieved results, only a few studies were found that examined the full ship based carbon capture supply chain. This finding highlights the limited attention the topic has received in existing literature and the need for scientific research in this area. Other results mainly focus on the shipping of CO_2, rather than OCC.

3.2. OCCUS modeling methodologies

This section provides a state-of-the-art overview of modelling OCCUS supply chains.

The study by Buirma et al. (2022) is currently the only comprehensive published paper on Scopus addressing the complete OCCUS supply chain. It conducts a feasibility assessment of OCC for a specialized LNG-fueled offshore crane vessel, carried out as part of the DerisCO_2 project. This study adopts a systems engineering framework. Systems engineering is a structured methodology for developing, analysing, and comparing system concepts to ensure they meet technical and economic requirements throughout their entire life cycle. It involves three main stages—concept development, engineering development, and post-development—each aimed at transforming operational needs into viable, maintainable, and adaptable system solutions (Kossiakoff et al., 2011). As such, the study develops and compares different conceptual supply chain designs, estimates potential emissions reductions, and evaluates economic feasibility through a payback period analysis based on assumed revenues from both carbon taxation and CO_2 utilization.

The study addresses uncertainty in various parameters by developing multiple scenario sets in which parameters such as distances (off- and onshore), storage capacity, operational mode, and capture cost are varied. Due to variation in storage capacity, it could be argued that this represents the uncertainty in the supply of total CO_2 from the vessel. However, this is only a single vessel. An interesting discussion point is that a study of the disruptive nature of the CO_2 market is required. Adaption will increase marketed CO_2, which could entail a risk of market saturation (Buirma et al., 2022). This is an interesting point, especially if other sectors also capture want to store or sell CO_2.

Two critical limitations make this study unsuitable for addressing the objectives of this research. First, it distinguishes between two vessel types: Type 1 (cargo vessels with relatively constant operational profiles) and Type 2 (offshore vessels with more stochastic behaviour), but focuses solely on Type 2. The assumption that cargo vessels have constant operational profiles is questionable, and the model does not account for the variation across vessel types. As a result, it lacks general applicability to OCCUS supply chains. Second, the study considers only a single vessel and does not address fleet-level dynamics or multiple emitters. This limits its ability to capture uncertainties in aggregate CO_2 supply to ports. While the study offers valuable case-specific insights, its scope is too narrow to support informed strategic level decision-making.

Visonà et al. (2024) applied a comprehensive TEA to evaluate different OCC systems for an ultra large container ship. Unlike other OCC studies, this work includes the transport and storage costs. However, it assumes the presence of mature transport infrastructure at every port. In addition, the transport assumptions lack detail, particularly whether CO_2 is moved by ship or pipeline, making this approach questionable. TEA proves valuable for evaluating technical system design choices but is less suitable for addressing supply chain flexibility or uncertainty in transport infrastructure.

As part of the EverLoNG project, a report by Aas et al. (2024) presents eight full-chain OCCUS scenarios involving an LNG carrier and a semi-submersible crane vessel. Each scenario includes a specified storage and utilization pathway and is assessed using LCA and TEA. The report does not provide detailed methodological justification or criteria for the selected full-chain cases. Since the report is limited to these specific vessel types, uncertainty in varying CO_2 supply levels to the port is not addressed. As a result, the study does not offer the necessary insights for addressing uncertainty in the CO_2 supply to the port.

LCA is a standardized, quantitative method used to evaluate the environmental impacts of products or processes across their entire life cycle, from raw material extraction to disposal (ISO, 2024a, 2024b). It involves defining the scope, collecting inventory data, assessing environmental impacts through classification and characterization, and interpreting results with consideration of uncertainties (Leonzio, 2023).

For the same research project, Reitz et al. (2024) conducted a more comprehensive LCA assessing the Global Warning Potential (GWP) of complete OCC chains for specific case studies. Although the study followed ISO and MEPC guidelines, it does not provide GWP detailed outcomes and emphasises the need for further research, particularly when captured CO_2 is used for synthetic fuel production.

Although LCA is well-suited for comprehensive environmental assessments, including raw material extraction and end-of-life disposal, such a full-scale approach is too detailed for the scope of this study. Instead, only direct emissions from transport modes and energy-intensive processes such as regeneration and liquefaction will be required.

To date, no other reports or research papers addressing full-chain OCCUS supply chains and the associated uncertainties in total CO_2 supply to ports have been found in the searched databases. Therefore, the next section turns to land-based CCUS literature to evaluate established supply chain modelling approaches and techniques for managing uncertainty. The same search terms are used, but the terms "onboard" and "ship-based" are removed. This revised search strategy results in a substantially broader set of available literature.

3.3. Land-based CCUS modelling approaches

This subsection elaborates on the different modelling approaches applied in CCUS. Based on scanning the titles, abstracts, and snowballing from these papers, two different modelling approaches are found to include uncertainties Mixed Integer Linear Programming (MILP), and Real Options (RO).

3.3.1. MILP modelling

The majority of retrieved literature focuses on the optimization of CO_2 transport networks. A commonly applied optimization method is MILP, which involves selecting the best possible values for decision variables to maximize or minimize an objective function subject to a set of linear constraints. It is commonly used for optimizing resource allocation among competing activities (Hillier & Lieberman, 2010).

Several studies have developed MILP models to optimize transport and storage networks under various policy and infrastructure constraints. These models vary in complexity, with some adopting dynamic or multi-period formulations to model the development of CCUS networks. Majority of the studies focus on minimizing the total system or network costs (d'Amore & Bezzo, 2017; d'Amore et al., 2018; Hasan et al., 2015; Middleton et al., 2020; Ravi et al., 2017). Other models aim to maximize the overall GHG emissions by using LCA (Ostovari et al., 2022). In addition, several studies adopt multi-objective frameworks that incorporate both economic and social acceptance or environmental impacts (d'Amore et al., 2020; Zhang et al., 2020). Most existing models focus on pipeline network design, optimizing parameters such as pipe diameters and layouts, but often exclude other transport modes like trucks, trains and barges. This highlights a gap in the literature for flexible OCCUS transport systems.

While the objectives and structures of these models vary, a common challenge across all studies is the presence of uncertainty. This includes uncertainty in future CO_2 supply, policy developments, and infrastructure availability. To address this, studies typically rely either on scenario-based modelling or stochastic approaches, each offering different strengths and limitations.

The most common and straightforward approach to address uncertainty is scenario-based optimization, originally proposed by Mulvey et al. (1995). This method involves developing a set of discrete scenarios that serve as inputs for a computational model, such as varying reduction targets. These targets determine the total amount of CO_2 to be captured, which can be interpreted as the uncertainty in CO_2 supply. Changes in this supply directly influence the design and capacity requirements of the transport and storage network (d'Amore et al., 2021, 2024; Gabrielli et al., 2022). Bennæs et al. (2024) varied with fixed supply volumes of CO_2, ranging from 5, 20, 50, and 100 Mtpa by adding emissions sources.

An alternative approach is to extend the MILP model by incorporating scenarios with associated probability distributions, enabling the model to optimize decisions across a range of uncertain future outcomes. Several studies have applied stochastic and Monte Carlo methods to incorporate uncertainty in modelling. Lee et al. (2019) developed a two-phase, two-stage stochastic multi-objective optimization model. Strategic decisions, such as facility location and sizing, are determined in the first phase, while operational decisions, including production and transportation, are optimized in the second phase after uncertainties are introduced. The addressed uncertainties include CO_2 emissions, acidifying substances, energy use, and cost parameters, and are represented using probabilistic scenarios generated with Monte Carlo sampling. This method estimates outcome distributions by running numerous simulations with inputs drawn from assumed distributions, typically normal (Leonzio et al., 2020).

Similarly, Leonzio et al. (2019) used Monte Carlo simulation to account for uncertainty in the prices and demand of CO_2-derived products. Demand was assumed to be normally distributed and varied between -50% and +50% around a baseline value to evaluate impacts on the Net Present Value (NPV) and payback period of a pipeline network. Nie et al. (2023) used Monte Carlo simulation to model uncertainty in offshore storage capacity, injection costs, and emissions factors. Parameters were sampled from specified ranges and used as input for an optimization model, which was run 10000 times per emission reduction scenario to generate probabilistic performance distributions.

Based on the reviewed studies, MILP models are not the most suitable modelling approach for this research. They are primarily designed for static pipeline network optimization and typically exclude alternative modes such as trucks, barges, and trains, highlighting a key research gap. While stochastic extensions exist, they often result in complex and computationally intensive models. Furthermore, scenario-based and stochastic approaches rely on predefined scenarios or probability distributions, limiting their ability to represent how uncertainty unfolds over time. For these reasons, MILP is not considered appropriate for evaluating transport flexibility in an onboard CCUS context. The focus will now shift to exploring different modelling approaches.

3.3.2. Real Options

An alternative method applied in the context of CCUS modelling and investment decisions is RO analysis. This concept was first introduced by Myers (1977) originating from the financial sector. Financial options give the holder the right, but not the obligation, to buy or sell a financial asset at a predetermined price and date in the future (Myers, 1977). Similarly, firms with investment opportunities have the right, but not the obligation, to invest in and acquire real assets in the future, depending on whether the conditions are advantageous (Dixit & Pindyck, 1994).

In the context of transportation research, Zheng and Jiang (2023) provides an overview of research papers and applications. For example, Sødal et al. (2008) developed a real options model to assess the value of flexibility in shipping, specifically by valuing the option to switch between the dry bulk and wet bulk markets based on historical price differentials.

Pimentel et al. (2021) used a binomial lattice tree to assess the growth option value. Based on exogenous variables, the binomial process of the expected number of flights is determined. Oliveira et al. (2021) did something similar but focused on tons of cargo handled. They made use of historical data and expert opinions to determine the binomial parameters required to construct a binomial tree. These parameters include the volatility (σ) and growth rate (μ), from which the up factor, down factor and associated probability can be calculated. Based on a yearly timestep, the increase in flights or cargo is determined for a period of 10 years (Oliveira et al., 2021). Based on this approach, this method seems suitable to determine the total CO_2 supply to the port.

Wang and Qie (2018) applied RO to determine the investment threshold for a CCUS project, from a perspective of the supply chain. The study considers several uncertainties, including CO_2 price volatility, CO_2 capture rate, government subsidies, and technological advancements. To address these uncertainties, the study models CO_2 prices using Geometric Brownian Motion (GBM) and game theory to analyse strategic interactions between power producers and CCUS operators. The costs are scaled linearly as a function of the installed capacity of the power plant. The considered option is the timing option. To derive the minimum carbon price for the investment decisions, differential equations are deployed (Wang & Qie, 2018). Although the title suggests a supply chain perspective, the study assumes fixed costs for transportation and storage, thereby excluding flexibility in the transport component.

An overview of RO in CCUS applications is provided by Agaton (2021) and Lamberts-Van Assche and Compernolle (2022) focusing on CCS and CCU respectively. Both studies provide detailed overviews of the required steps and the current state of scientific research. They outline similar research frameworks consisting of the following key steps:

1. Identify the main source of uncertainty
2. Model how the uncertainty evolves over time
3. Define the applicable type of options
4. Select the most suitable valuation method

Based on the literature reviewed by Agaton (2021) and Lamberts-Van Assche and Compernolle (2022), the following main uncertainties have been identified and researched:

- CO_2 price
- Prices of coal, oil and natural gas
- Capital costs
- Operational costs
- Technology
- Subsidies
- Geological storage
- CO_2 supply
- Transport and network design

In the majority of the reviewed studies, the CO_2 price is identified as the primary source of uncertainty, as fluctuations in carbon pricing directly affect the economic viability of CCUS projects and influence the timing of investment decisions (Agaton, 2021). Only one study explicitly addresses transport network development, and just one includes uncertainty in CO_2 supply. This highlights a clear lack of studies applying real options to assess flexible transport within CCUS supply chains.

Different approaches are used to model the identified uncertainty over time, which are strongly related to the type of uncertainty. The most commonly applied method is the GBM, which is a continuous-time stochastic process in which uncertainty increases over time, following a lognormal path (Agaton, 2021). This is the most used method, as this is typically used for modelling the development of CO_2 or electricity prices. For technological processes, the most common method is the use of deterministic learning curves (Liu et al., 2022). Another applied method is the use of probability models, which are used to determine the likelihood of outcomes (Agaton, 2021).

Six types of options have been identified in the literature, each representing a different form of flexibility in decision making under uncertainty. The options are listed below, including a short description:

- Timing: Option to defer, delay or wait before applying CCUS depending on future conditions.
- Compound: A series of dependent investment decisions made in sequence.
- Abandon: The flexibility to exit a project if it becomes unprofitable.
- Shutdown: Flexibility to temporarily quit CCUS operations when conditions are unfavourable.
- Flexible design: Infrastructure designed with the ability to expand or adapt in the future.
- Switching: Switch to the lowest costs or most valuable future output.

The final step in the real options framework is selecting an appropriate valuation method. Several approaches have been applied in CCUS studies:

- Monte Carlo: Suitable for complex systems with multiple sources of uncertainty but increases complexity.
- Dynamic programming: Computationally intense but simpler and more intuitive. Commonly used to determine the optimal timing of investment decisions.
- Binomial lattices: Simplest method to value and interpret, used for timing or compound options.
- Differential equations (Black-Scholes): Requires complex mathematics, therefore not suitable for problems with many variables. Commonly used to evaluate timing options.

Having established the general methodologies and approaches of RO in transportation and CCUS research, we now turn our attention to specific studies that illustrate these applications in greater detail, focusing on supply chain or CO_2 networks as this may provide more insights.

Melese et al. (2015) applied a RO approach combined with graph theory and Monte Carlo simulation to evaluate CCUS network design under uncertainty. Two uncertainties were considered. The timing of new sources joining the network and the amount of CO_2 each source contributes. The initial CO_2 supply is modelled using normal distributions with predefined mean and standard deviation, but how the values are obtained is not elaborated. To model future CO_2 flows GBM is used. The study evaluates two options: the option to defer network expansion and the option to expand by designing redundant capacity. The minimal required CO_2 price is determined by solving the NPV for 0 (Melese et al., 2015). While methodologically interesting, the study is limited to pipeline transport and relies on predefined flow estimates and standard deviations, which may be difficult to predict in the early stages. Besides, no methodology is proposed for obtaining these values. As this study focuses on pipeline scaling, the flexibility to switch between transport modes is not addressed, making the approach less applicable to this specific research.

Knoope et al. (2015) used a real options approach to evaluate the optimal timing of investments for a CO_2 pipeline transport network, comparing it to a deterministic perfect foresight model using MILP. The study incorporates uncertainties in CO_2 price, tariffs, and source participation, modelled usingGBM and Monte Carlo simulation. Option values are calculated using a binomial lattice model in which the value goes up or down. The study evaluates several options, including immediate versus postponed CCUS investments or joining existing trunk lines versus constructing new ones (Knoope et al., 2015). Although this is an interesting approach, the options assessed are not relevant to this research. The combination of MILP, RO and Monte Carlo simulations is powerful. However, it requires sufficient time to develop and test, and much computational power is required. Due to the limited timeline of this study, this method is not feasible.

Fan et al. (2020) and Zhang et al. (2014) both applied trinomial lattice models to determine the optimal investment timing for retrofitting power plants with CCUS systems. Using a trinomial tree, the CO_2 price is allowed to increase, decrease, or stay constant. Elias et al. (2018) and Wang and Du (2016) went one step further, applying a quadrinomial tree to address both uncertainties in CO_2 and coal prices. All these studies use a similar cost modelling approach, where capital and operational costs are scaled based on the installed capacity of a power plant. Transport and storage costs are assumed to be fixed. While these models improve accuracy and allow for analysing multiple uncertainties, they come at the cost of increased complexity and computational requirements due to the exponential growth of nodes. As a result, such models are considered too complex and not suitable for the scope of this study.

3.4. Conclusions Literature Review

The reviewed literature indicates that currently, limited research is conducted on the modelling of OCCUS supply chains. Existing studies that evaluate full chain tend to be case-specific, lack a global perspective, and overlook uncertainty in the aggregate CO_2 supply delivered by the maritime fleet to ports. Highlighting a significant research gap. Due to limited OCCUS studies, modelling approaches from land-based CCUS systems were reviewed. Two main methodologies were identified for handling CCUS supply chain design under uncertainty: MILP and RO analysis. MILP is widely used for optimizing large-scale pipeline networks, often incorporating uncertainty through scenario-based or stochastic methods such as Monte Carlo simulation. However, it is not well suited for evaluating operational flexibility, such as transport switching or investment timing under uncertainty. Real options analysis captures decision making flexibility under uncertainty and has been applied to CCUS investment timing and market switching. Yet, its application to switching between transport modes in the context of OCCUS supply chains is missing.

Real options analysis is selected as the most appropriate method for assessing the value of flexibility in transport deployment, which aligns best with the goal and research questions defined in chapter 1. A binomial lattice tree is chosen as the valuation framework to facilitate structured and interpretable modelling of CO_2 supply development over time.

4

Model description

As discussed in the previous chapter, a Real Options model is developed to evaluate the value of flexibility of switching between transport modes under uncertainty of CO_2 supply by maritime vessels. The goal of this chapter is to clarify the assumptions and setup of the model. First, a general model description is provided in section 4.1. Section 4.2 describes the binomial model setup and parameters. After this section 4.3 provides the cash flow calculations followed by a breakdown for costs calculations in section 4.4 and emissions in section 4.5. After these are known, section 4.6 gives the option valuation. Lastly, section 4.7 outlines the method for calculating the break-even CO_2 price.

4.1. General model description

This section provides an overview of the modelling steps. Python is selected for its flexibility, scalability, and ease of adaptation, which allows for efficient updates and modifications as assumptions or input data change. Moreover, Python handles complex operations more effectively than tools like Excel, such as sensitivity analyses and iterative algorithms like bisection search. The built-in libraries also support advanced data analysis, visualization, and automation, making it a more robust and efficient choice for comprehensive modelling tasks.

The general steps are visualized in figure 4.1. The modelling process begins with the collection of input data. These input data are used to calculate the required binomial parameters to estimate how the CO_2 and rich solvent supply evolves over time. The next step involves calculating the total costs and emissions of the supply chain for both the base and switch transport options. Following this, the model calculates the respective cash flows and (expected) discounted cash flows for both transport scenarios. These outputs are then used to calculate the option value and total value. A bisection search algorithm is then employed to identify the break-even CO_2 price. Finally, the model evaluates and visualizes the results, producing key outputs: option value, total value, and break-even CO_2 price. If required, the model can also generate additional outputs, such as truck transport emissions or total supply chain emissions, providing a more detailed analysis when needed.

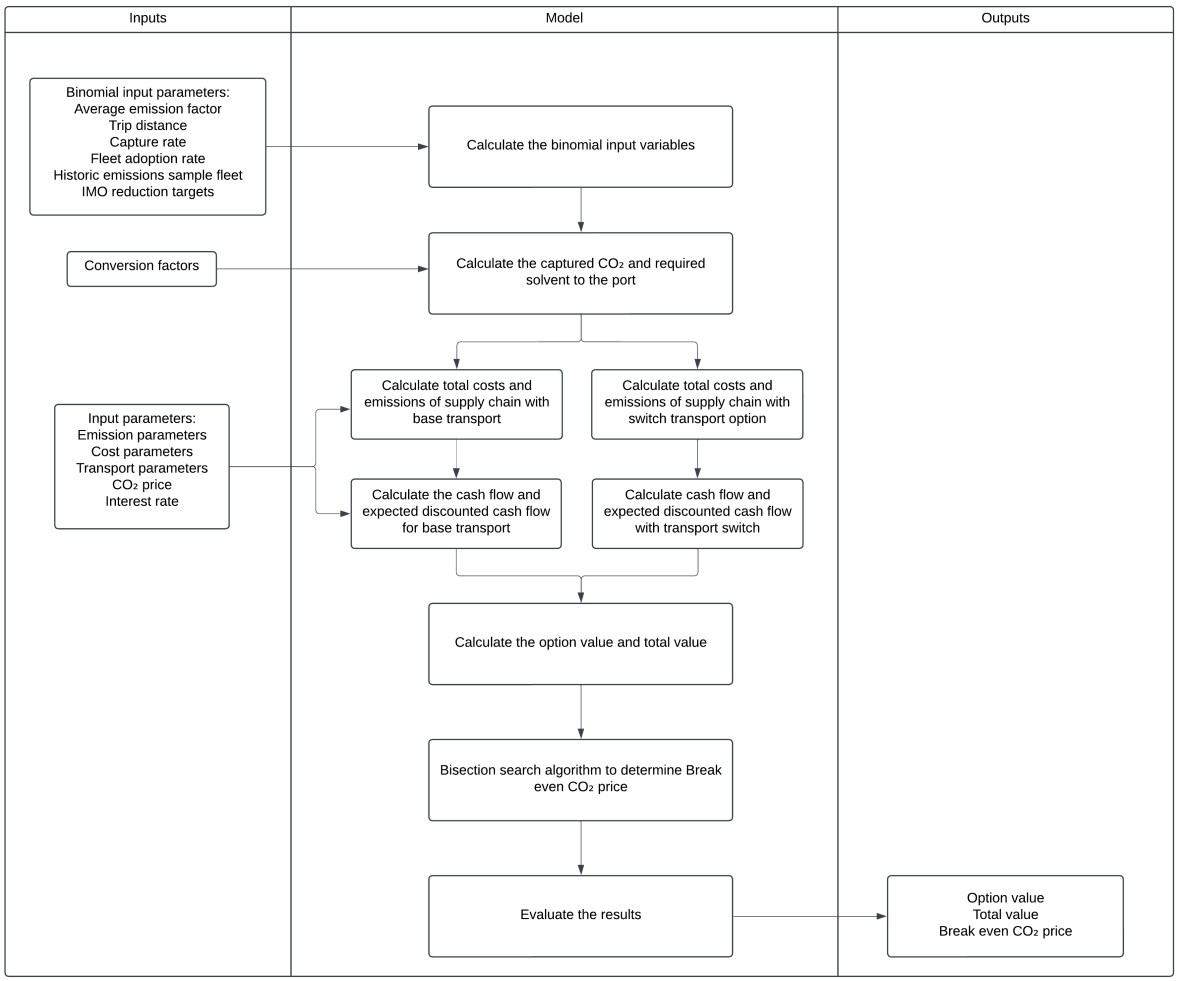

Figure 4.1: Simplified overview of the Real Options modelling steps

4.2. Binomial lattice tree

This section introduces the construction of the RO model, which deploys a binomial lattice tree to represent the incoming CO_2 supply at a port under uncertainty.

4.2.1. Binomial parameters

The first step in the RO approach is to construct a binomial lattice tree. As concluded in the previous chapter, the main source of uncertainty is the mass of CO_2 captured by maritime vessels entering a specific port. The initial incoming CO_2 supply at timestep $i = 0$ is denoted by S_0. At each subsequent timestep $i = 1, 2, \ldots, N$, the CO_2 supply can either increase by a multiplication factor u or decrease with d (Kim & Li, 2020). Each node in the lattice is indexed by (i, j), where i represents the time step and j is the number of possible states. In its current formulation, the model defines each timestep as one year. However, it can be adapted to any consistent time interval, provided that parameters such as u, d, σ, μ and interest rates are scaled accordingly. The choice of yearly intervals reflects the model's more strategic and long-term focus. Using shorter intervals would significantly increase the number of nodes in the binomial lattice, making the model more complex and computationally intensive without substantially improving decision quality at the strategic level. The CO_2 supply at any given node (i, j) is then defined as:

$$S_{i,j} = S_0 \cdot u^{i-j} \cdot d^j \tag{4.1}$$

$S_{i,j}$	CO_2 supply at node (i, j)	tCO_2/y
S_0	CO_2 supply at the root node (0,0)	tCO_2/y
u	Upward factor	-
d	Downward factor	-

The initial CO_2 supply, S_0 is determined by calculating the total emissions, E_{ships}, from a selection of vessels into a specified port. This is multiplied by the average capture rate η_{cap} and the fleet adaption rate F_0, which states the percentage of vessels operating a carbon capture system at the first time step.

$$S_0 = E_{ships} \cdot \eta_{cap} \cdot F_0 \tag{4.2}$$

E_{ships}	Total emissions by fleet into port	tCO_2/y
η_{cap}	OCC efficiency	-
F_0	Initial fleet adaption rate	-

At each time step, the model transitions to an upward state with probability p and up factor u or to a downward state with probability $(1 - p)$ and down factor d. The up and down factors are assumed to remain constant over time, which leads to a recombining tree, which significantly reduces computational time (Deutsch & Beinker, 2019). Due to this property, the CO_2 supply at a specific node is path-independent. The sequence of up and down movements does not influence the outcome of the supply level. This recombination property holds only if $u \cdot d = 1$, a standard assumption in real options modelling (Cox et al., 1979).

In this context, recombination is justified because the objective is to model the overall distribution of possible CO_2 supply levels over time rather than to capture individual supply pathways or their associated probabilities. The parameters u, d, and p are calculated using equations (4.3) to (4.5). An illustration of the initial steps of the binomial tree is provided in Figure 4.2.

$$u = e^{\sigma\sqrt{\Delta t}} \tag{4.3}$$

$$d = \frac{1}{u} = e^{-\sigma\sqrt{\Delta t}} \tag{4.4}$$

σ	CO_2 supply volatility	-
Δt	Time step	y

In these equations, σ is the volatility parameter. In classic binomial models, this is calculated based on historic coal, or CO_2 prices (Zhang et al., 2014). However, in this model, the volatility represents the yearly fluctuation in CO_2 supply to the port. A more detailed explanation is given in section 5.2.3. Δt is the time step, which is defined by the total time divided by the total steps (T/N).

$$p = \frac{e^{\mu\Delta t} - d}{u - d} \tag{4.5}$$

p	Upward probability	-
μ	average growth rate	-

μ is the yearly average growth rate of CO_2 supply to the port, more detailed information about this parameter will be given in section 5.2.2.

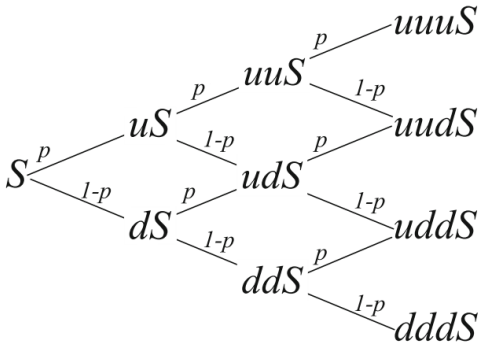

Figure 4.2: First steps of a binomial lattice tree (Deutsch & Beinker, 2019)

The next step involves multiplying the CO_2 supply at each node by factor κ. This factor represents the total amount of solvent needed to transport all captured CO_2 from the offloading location to the conditioning plant. It must be highlighted that this is not the total yearly required solvent, as the solvent can be reused if regenerated (Aas et al., 2024).

$$Sol_{i,j} = S_{i,j} \cdot \kappa \tag{4.6}$$

κ Conversion factor for required solvent -

4.2.2. Binomial probability

As mentioned, this is a recombining binomial tree with fixed u and d. Therefore, multiple pathways exist to reach the node (i, j). To obtain the total probability of reaching any node within the tree, this must be multiplied by the number of possible pathways to this node (Deutsch & Beinker, 2019). The total equation to calculate the probability of any given node in the lattice is given by Equation 4.7.

$$P(i,j) = \binom{i}{j} \cdot p^{(i-j)}(1-p)^j = \frac{i!}{j!(i-j)!} \cdot p^{(i-j)}(1-p)^j \tag{4.7}$$

4.3. Cash flow calculation

The operational cash flow of the OCCUS supply chain at each node is determined by subtracting the total costs from the total revenues. Revenue is calculated by multiplying the net amount of reduced CO_2 with the corresponding CO_2 price at each timestep. The methodology for calculating the net CO_2 reduction is elaborated in section 4.5. The mathematical formulation of the operational cash flow is provided in equation (4.8).

$$CF_{i,j} = TR_{i,j} - C_{OCCUS_{i,j}} \tag{4.8}$$

$CF_{i,j}$	Operational cash flow at node (i, j)	€/y
$TR_{i,j}$	Total revenue at node (i, j)	€/y
$C_{OCCUS_{i,j}}$	Total costs of OCCUS chain at node (i, j)	€/y

In the model, revenue is generated by one of the two following possibilities:

- Reduced expenditure on EU ETS carbon credits, due to the capture and removal of CO_2 emissions (European Commission. Joint Research Centre., 2024).
- Selling captured CO_2 to industries that utilize it in their production processes.

It is important to note that for the second case, current regulations only exempt CO_2 emissions from EU ETS obligations if they are either permanently stored or chemically bound. Although future regulatory frameworks might consider CCU applications, they require detailed LCA to demonstrate actual CO_2 avoidance.

As such, this study adopts a simplified approach proposed by Lamberts-Van Assche et al. (2023) considering only the short carbon cycle. Specifically, it assumes that the reduced emissions m_{red} are calculated by subtracting only the emissions associated with delivering CO_2 to the outlet. While this introduces certain limitations, current regulations do not yet offer clear guidance on how to account for these emissions in CCU applications (BV, 2024).

The total revenue is subsequently calculated according to Equation 4.9.

$$TR_{i,j} = (S_0 - E_{OCCUS_{i,j}}) \cdot P_{CO_{2i}} \tag{4.9}$$

E_{OCCUS}	Emissions for operating OCCUS supply chain at node (i,j)	tCO_2/y
$P_{CO_{2i}}$	Received CO_2 price at year i	€/tCO_2

4.4. Costs calculations

This section describes how the individual costs components within the supply chain are calculated. Each step is characterized by its own cost function, which will be elaborated further in the following sections. The overall costs equation is defined in equation (4.10).

$$C_{occus_{i,j}} = C^{sol}_{tr_{i,j}} + C_{reg_{i,j}} + C_{liq_{i,j}} + C^{LCO_2}_{tr_{i,j}} + C_{ps_{i,j}} \tag{4.10}$$

$C_{occus_{i,j}}$	Total costs of the OCCUS supply chain at node (i,j)	€/y
$C^{sol}_{tr_{i,j}}$	Solvent Transport costs at node (i,j)	€/y
$C_{reg_{i,j}}$	Costs for regeneration at node (i,j)	€/y
$C_{liq_{i,j}}$	Liquefaction costs at node (i,j)	€/y
$C^{LCO_2}_{tr_{i,j}}$	LCO_2 Transport costs at node (i,j)	€/y
$C_{ps_{i,j}}$	Permanent storage costs at node (i,j)	€/y

4.4.1. Solvent transport costs

The solvent transport costs depend on the type of transport mode used, which can either be $C_{truck_{i,j}}$ or $C_{barge_{i,j}}$. In the model, the unit transport costs are calculated as a function of both transport distance and mass flow based on quotes obtained from transport companies. These quotes typically reflect real-world pricing, meaning this will come closest to reality.

However, transport cost quotes are often provided only for specific combinations of distance and tonnage. Therefore, to estimate the unit transport costs for arbitrary combinations not explicitly quoted, linear interpolation is applied. This method allows the model to approximate costs within the range of available data by assuming a linear relationship between known points.

The total truck costs are calculated by multiplying the unit costs by the distance and the total mass to be transported, as described in equation (4.11)

$$C_{truck_{i,j}} = UC_{truck} \cdot x^{sol}_{tr} \cdot Sol_{i.j} \tag{4.11}$$

$C_{truck_{i,j}}$	Truck solvent transport costs at node (i,j)	€/y
UC_{truck}	Unit cost of truck solvent transport	€/tCO_2 km
x^{sol}_{truck}	Truck solvent transport distance	km

The costs for barge transport are calculated according to 4.12. Linear interpolation between known data points of costs for a certain distance and volume is applied. Therefore, at least two data points are required to obtain the costs for other distances and volumes. In this equation, x_{barge}^{low} and $C_{barge}(x_{barge}^{low})$ represent the data points for a low transport distance and costs respectively, while x_{barge}^{high} and $C_{barge}(x_{barge}^{high}$ represent the data point for the larger distance and costs. At first, the solvent supply may seem to have no impact on the costs, which is not true and will be discussed further in section 5.3.1.

$$C_{barge_{i,j}} = C_{barge}(x_{barge}^{low}) + \frac{x_{barge}^{sol} - x_{barge}^{low}}{x_{barge}^{high} - x_{barge}^{low}} \cdot \Big(C_{barge}(x_{barge}^{high}) - C_{barge}(x_{barge}^{low})\Big) \tag{4.12}$$

$C_{barge_{i,j}}$	Barge solvent transport costs at node (i,j)	€/y
$C_{barge}(x_{barge}^{low})$	Cost of solvent barge transport short	€/y
$C_{barge}(x_{barge}^{high})$	Cost of solvent barge transport long	€/y
x_{barge}^{low}	Barge transport distance short	km
x_{barge}^{high}	Barge transport distance long	km

4.4.2. Regeneration costs

In existing literature, the regeneration process is typically done at the point source of the carbon capture system (Roussanaly et al., 2021a). However, Roussanaly et al. (2021b) also suggests that centralized regeneration is feasible when multiple emitters are connected to a shared facility. For this model, this is assumed to be the case, as saturated solvent is transported to this central facility. Due to the limited availability of detailed studies on centralized regeneration facilities, both the CAPEX and fixed OPEX are assumed to follow the same cost trajectory as the liquefaction process, as described in section 4.4.3.

The main cost drivers for this process are the variable OPEX, especially electricity or gas costs, which are needed to supply the plant with sufficient heat for the regeneration process (Zhao et al., 2025). However, it is possible to reduce these costs through heat integration with other industrial processes using available waste heat (Becattini et al., 2024).

To account for potential heat integration with available waste heat, a correction factor $1-h$ is applied. If $h=1$, all the required energy is assumed to be supplied by waste heat, $h=0$ implies that no rest heat is available, and the full energy demand must be met by purchased electricity or gas. The overall cost equation for the regeneration process is described according to equation (4.13).

$$C_{reg_{i,j}} = \left((I_{reg,ref} + I_{reg,ref} \cdot OM_{reg}) \cdot \left(\frac{S_{i,j}}{S_{ref}^{liq}} \right)^{-N_{reg}} + (1-h) \cdot \frac{SEC_{reg} \cdot P_e}{\eta_{reg}} \right) \cdot S_{i,j} \cdot e^{-\beta i} \tag{4.13}$$

$I_{reg,ref}$	Reference investment costs for regeneration plant	€/tCO$_2$/y
OM_{reg}	Operational & Maintenance costs for regeneration plant	-
S_{ref}^{reg}	Reference yearly CO$_2$ flow	tCO$_2$/y
N_{reg}	Exponential factor for economies of scale	-
h	Percentage of available rest heat	-
SEC_{reg}	Specific energy consumption for regeneration	kWh/tCO$_2$
P_e	Electricity price	€/kWh
η_{reg}	Efficiency of the regeneration process	-
β	Learning factor for regeneration	-

4.4.3. Liquefaction costs

After the regeneration process, the CO_2 is liquefied to meet the pressure and purity requirements of the selected transport mode in the next step. The costs for liquefaction depend on the previously mentioned conditions, the process layout and the yearly flow rate (Seo et al., 2016). This model adopts the liquefaction process according to (Deng et al., 2019; Seo et al., 2016).

The cost for a liquefaction plant consists of CAPEX and OPEX. The aforementioned studies provide detailed cost analysis for a reference flow of 1 $MtCO_2$/y. To account for varying scales, the method from Roussanaly et al. (2021b) is adopted, which applies a scaling power law to adjust investment costs for different flow rates.

Fixed OPEX is assumed to be a fraction of the investment costs (Deng et al., 2019). The variable OPEX is dominated by the electricity costs. To calculate this, the specific energy consumption for liquefying 1 ton of CO_2 is multiplied by the electricity price, divided by technical efficiency.

It is assumed that the liquefaction process will be optimized and improved in the corresponding years. Therefore, a learning rate γ is assumed.

The total yearly costs for liquefaction are calculated by multiplying this with the yearly CO_2 flow as shown in equation (4.14).

$$C_{liq_{i,j}} = \left((I_{liq,ref} + I_{liq,ref} \cdot OM_{liq}) \cdot \left(\frac{S_{i,j}}{S_{ref}^{liq}} \right)^{-N_{liq}} + \frac{SEC_{liq} \cdot P_e}{\eta_{liq}} \right) \cdot S_{i,j} \cdot e^{-\gamma i} \tag{4.14}$$

$I_{liq,ref}$	Reference investment costs for liquefaction plant	€/tCO_2/y
OM_{liq}	Operational & Maintenance costs for liquefaction plant	-
S_{ref}^{liq}	Reference yearly liquefaction CO_2 flow	tCO_2/y
N_{liq}	Exponential factor for economies of scale	-
v	CO_2 Venting factor	-
SEC_{liq}	Specific energy consumption for liquefaction	kWh/tCO_2
η_{liq}	Efficiency of the liquefaction process	-
γ	Learning factor for liquefaction	-

4.4.4. Liquid CO_2 transport

To calculate the transport costs for LCO_2, the fitting curve equations proposed by Oeuvray et al. (2024) are used. The fitting curves are well-suited for this model because of two main reasons:

Firstly, the cost estimates for varying LCO_2 volumes are derived from quotes provided by logistic companies, while dedicated ships or pipelines are based on existing literature. These specifically refer to supply chains connecting inland industrial emitters with offshore permanent storage sites in Northwestern Europe (Oeuvray et al., 2024). Although the values are not direct one-to-one representations, they provide realistic and regionally relevant cost indications.

Secondly, the study focuses on early users of carbon capture, which requires readily available transport options to start CCUS projects quickly. As a result, the study includes a wide range of transport distances and annual CO_2 volumes, offering a solid basis for estimating transport costs across diverse scenarios (Oeuvray et al., 2024).

The corresponding fitting curve equations are provided in equations (4.15) to (4.17). The model uses these equations to calculate the unit costs for each applicable transport mode. It takes the fitted parameters α and computes total transport costs by multiplying the unit cost by the transport distance and the LCO_2 flow. The latter is corrected for venting losses during the liquefaction process. Please refer to section 4.5.3.

$$UC_{tr}^{LCO_2} = \alpha_1 + \frac{\alpha_2}{x_{tr}^{LCO_2}} \tag{4.15}$$

$$UC_{tr}^{LCO_2} = \alpha_1 + \frac{\alpha_2}{x_{tr}^{LCO_2}} + \frac{\alpha_3}{S_{i,j}} \tag{4.16}$$

$$UC_{tr}^{LCO_2} = \alpha_1 + \alpha_2 \cdot \left(\frac{x_{tr}^{LCO_2}}{x_{tr,ref}^{LCO_2}} \right)^{\alpha_3} \cdot \left(\frac{S_{i,j}}{S_{ref}} \right)^{\alpha_4} \tag{4.17}$$

$$C_{tr}^{LCO_2} = UC_{tr}^{LCO_2} \cdot x_{tr}^{LCO_2} \cdot S_{i,j} \cdot (1 - \nu) \tag{4.18}$$

$UC_{tr}^{LCO_2}$	Unit cost of LCO_2 transport	€/tCO_2 km
$x_{tr}^{LCO_2}$	LCO_2 transport distance	km
$x_{tr,ref}^{LCO_2}$	Reference LCO_2 transport distance	km

4.4.5. Permanent storage

In this model, CO_2 is permanently stored underground. The total storage cost is calculated using equation (4.19), unit storage costs are multiplied by the total volume of CO_2 injected. These unit costs depend on both the annual injection rate and the type of storage site. Typically, CO_2 storage sites are large-scale projects operated by consortia, where capacity is shared among multiple emitters (Roussanaly et al., 2021a). It is assumed that sufficient capacity is available to handle captured CO_2 from shipping, and costs are distributed equally among participants. Therefore, unlike other cost functions in this model, the unit storage cost is not calculated per tonne of captured CO_2 from shipping but is based on the total annual injection volume provided by the storage facility.

$$C_{ps_{i,j}} = UC_{ps} \cdot S_{i,j} \cdot (1 - \nu) \tag{4.19}$$

UC_{ps}	Unit costs for permanent underground storage	€/tCO_2

4.5. Emission calculations

This section describes how the emissions of each step in the supply chain are calculated. The total yearly emissions at each node of the chain are calculated by summing the emissions for each cost component.

$$E_{\text{occus}_{i,j}} = E_{tr_{i,j}}^{sol} + E_{reg_{i,j}} + E_{liq_{i,j}} + E_{tr_{i,j}}^{LCO_2} + E_{ps_{i,j}} \tag{4.20}$$

$E_{occus_{i,j}}$	Total emissions of the OCCUS supply chain at node (i,j)	tCO_2/y
$E_{tr_{i,j}}^{sol}$	Solvent transport emissions at node (i,j)	tCO_2/y
$E_{reg_{i,j}}$	Emissions from the regeneration process at node (i,j)	tCO_2/y
$E_{liq_{i,j}}$	Emissions from the liquefaction process at node (i,j)	tCO_2/y
$E_{tr_{i,j}}^{LCO_2}$	LCO_2 transport emissions at node (i,j)	tCO_2/y
$E_{ps_{i,j}}$	Emissions from permanent storage at node (i,j)	tCO_2/y

4.5.1. Solvent transport emissions

The solvent transport emissions are calculated according to the proposed standards by (VCS, 2024b). In the proposed standards, two options are provided for calculating emissions from transport, monitoring and using default emissions factors. This model adopts the use of default emission factors as monitoring is not suitable for predictive models (VCS, 2024b). The emissions factor for the selected transport mode is multiplied by the transport distance and the total mass of the CO_2. To convert from grams to tonnes, the factor 10^{-6} is applied.

$$E^{sol}_{tr_{i,j}} = EF_{tr} \cdot x^{sol}_{tr} \cdot Sol_{i,j} \cdot 10^{-6} \tag{4.21}$$

EF_{tr} Emission factor of transport mode gCO_2/tkm

4.5.2. Regeneration emissions

The emissions associated with the regeneration process are calculated using equation (4.22). These emissions originate from the type of energy used, represented by an emission factor. This factor is multiplied by the specific energy requirement and the total CO_2 flow. The heat integration factor is also integrated here, as less required energy leads to lower emissions.

$$E_{reg_{i,j}} = EF_{en} \cdot (1-h) \cdot SEC_{reg} \cdot S_{i,j} \cdot 10^{-6} \tag{4.22}$$

EF_{en} Emission factor of energy source gCO_2/kWh

4.5.3. Liquefaction emissions

The emissions associated with the liquefaction process are calculated in the same manner as the regeneration process. It is assumed that the same energy source is used, with the only difference being the specific energy requirement.

The factor ν represents the fraction of CO_2 vented to the atmosphere during liquefaction and purification. Venting is required to remove non-condensable components. However, the vented gas includes both impurities and CO_2 (Jensen et al., 2025). To account for this, the CO_2 emissions from venting must be added, calculated according to equation (4.23)

$$E_{liq_{i,j}} = (EF_{en} \cdot SEC_{liq} + \nu) \cdot S_{i,j} \cdot 10^{-6} \tag{4.23}$$

4.5.4. Liquid transport emissions

The LCO_2 transport emissions are calculated according to the same method as described in section 4.5.1. However, in this transport leg, LCO_2 is transported. Since a fraction of CO_2 is vented during the liquefaction process, not all of the captured CO_2 reaches the transport stage. Therefore, a correction is applied to account for the actual amount of CO_2 transported. The emissions factor for the selected transport mode is multiplied by the transport distance and the total mass of the CO_2. To convert from grams to tonnes, the factor 10^{-6} is applied.

$$E^{LCO_2}_{tr_{i,j}} = EF_{tr} \cdot x^{LCO_2}_{tr} \cdot S_{i,j} \cdot (1-\nu) \cdot 10^{-6} \tag{4.24}$$

4.5.5. Storage emissions

Emissions from permanent storage arise primarily from the energy required to operate equipment involved in the CO_2 storage process (VCS, 2024a). These energy requirements can be estimated by calculating the power needed for pumps and injection systems (Knoope et al., 2014). For simplification, this model applies a specific energy consumption factor, which represents the energy required to store one tonne of CO_2. To determine total emissions, this factor is multiplied by the emission intensity of the energy source and the total mass of CO_2 to be stored Zhang et al. (2020).

$$E_{ps_{i,j}} = SEC_{ps} \cdot EF_{en} \cdot S_{i,j} \cdot (1-v) \cdot 10^{-6} \tag{4.25}$$

SEC_{ps} Specific energy consumption for permanent storage kWh/tCO_2

4.6. Option valuation

Based on the binomial lattice tree and parameters described in section 4.2, combined with the cash flow calculation in section 4.3 and the costs and emissions from sections 4.4 and 4.5 the total Discounted Cash Flow (DCF) at each node is calculated. This process is applied to both the base transport mode and the considered alternative transport option.

The DCF for both base and alternative transport option is calculated using backward induction (Deutsch & Beinker, 2019). At the nodes of final time step I, the DCF is equal to the cash flow of that year, as no future cash flows remain to be considered, which results in $DCF_{I,j} = CF_{I,j}$.

For all preceding nodes $(i < I)$, the DCF is determined by summing the immediate cash flow at the current node and the expected value of the future DCF. The expected value is calculated as a probability-weighted average of the DCF in the upward and downward branches of the binomial tree, using the risk-neutral probability p. The result is then discounted back to the current time step, as shown in equation (4.26).

$$\begin{aligned} DCF_{i,j} &= CF_{i,j} + EDCF_{i,j} \\ EDCF_{i,j} &= \frac{p \cdot DCF_{i+1,j} + (1-p) \cdot DCF_{i+1,j+1}}{(1+r)^{dt}} \end{aligned} \tag{4.26}$$

$DCF_{i,j}$	Discounted cash flow at node (i,j)	€
$EDCF_{i,j}$	Expected discounted cash flow at node (i,j)	€
r	Interest rate	-

With the DCF values calculated for both transport options, the model evaluates at each node whether it is optimal to switch or continue using the base mode. This decision is based on the option value. At the final time step $i = I$, the decision involves either staying in the current state, which yields no additional value or switching and obtaining the value corresponding to the difference.

$$OV_{I,j} = max\left[DCF_{I,j}^{switch} - DCF_{I,j}^{base}\ ;\ 0\right] \tag{4.27}$$

$OV_{i,j}$	Option value at node (i,j)	€

At preceding time steps $(i < I)$, the decision incorporates the possibility of deferring the switch. The model compares the immediate gain from switching to the expected value of waiting. The expected future option value is computed as the discounted probability-weighted average of the option values from the next time step as shown in equation (4.28)

$$OV_{i,j} = max\left[DCF_{i,j}^{switch} - DCF_{i,j}^{base}\ ;\ \frac{p \cdot OV_{i+1,j} + (1-p) \cdot OV_{i+1,j+1}}{(1+r)^{dt}}\right] \tag{4.28}$$

In summary, if for any given node in the binomial tree, the following condition holds:

$$DCF_{i,j}^{switch} - DCF_{i,j}^{base} > \frac{p \cdot OV_{i+1,j} + (1-p) \cdot OV_{i+1,j+1}}{(1+r)^{dt}}$$

The optimal decision is to switch immediately. If the right-hand side of the inequality is larger, the value of the option to switch in the future exceeds the immediate benefit of switching, and the decision is deferred.

4.7. Break even price calculation

This section outlines the method and steps used to determine the break-even CO_2 price. The break-even price can be calculated for each node in the tree, representing the minimum average CO_2 price required from that point onward to ensure neither a loss nor a profit is made.

To assess the influence of switching flexibility on the minimum required CO_2 prices for the overall supply chain to break even, a comparison is made between the break-even CO_2 prices with and without the option to switch transport modes. As discussed in section 4.3, P_{CO_2} is a parameter within the cash flow calculation and consequently affects the DCF. Therefore, we need to find a value for the CO_2 price without considering the option value, where the following condition must hold:

$$DCF_{i,j} \approx 0$$

For the break-even price with the option value, the following condition needs to hold:

$$TV_{i,j} = DCF_{i,j} + OV_{i,j} \approx 0$$

To achieve this, a bisection search algorithm is used because this is the most straightforward and most robust method for finding the root of a function (McClarren, 2018). In this case, the root corresponds to the break-even CO_2 price. The algorithm iteratively reduces the interval between a predefined lower and upper bound for P_{CO_2} by evaluating whether the resulting value, either $DCF_{i,j}$ or $DCF_{i,j} + OV_{i,j}$ is above or below zero. Based on the sign of this outcome, the bound is updated, and the process continues until the interval becomes smaller than a specified tolerance. In this model, the lower bound is set to 0 and the upper bound to 500, a range that consistently returns a valid break-even CO_2 price. The tolerance, which defines the precision of the result, is set to 0.001 but can be adjusted to meet specific requirements or personal preferences.

5

Case study and input parameter values

To run and test the developed model as defined in chapter 4, a comprehensive set of parameters and input data is required. Many of these inputs depend on specific regional characteristics. This chapter outlines the selected case study, input parameters and details used for implementation and testing of the model. Section 5.1 introduces the case of the Port of Rotterdam, including relevant logistical and infrastructural considerations. The derivation of binomial model parameters under uncertainty is described in section 5.2. Subsequently, technical and economic data required for cost calculations are presented in section 5.3, followed by emissions-related inputs in section 5.4.

5.1. Case study description

The Port of Rotterdam is selected for this case study based on a combination of strategic and logistical factors. As one of the largest ports in the world, the Port of Rotterdam aims to position itself as a front-runner in the decarbonization of port infrastructure and the maritime sector (Port of Rotterdam, 2024). According to 2022 AIS data, it ranks as the second highest port in terms of annual CO_2 emissions from ship voyages arriving at the port (DNV, 2024). In addition, the port is actively positioning itself as a leading hub for CO_2 handling and storage. This ambition is supported by the development of two major offshore carbon storage projects, Porthos and Aramis, which are currently under construction in close proximity and cooperation with the port (Global CCS Institute, 2024a). Lastly, the Port of Rotterdam offers excellent multimodal transport infrastructure and connectivity to the hinterland. This ensures the availability of a diverse range of transport providers for transporting solvents and LCO_2.

With the case study area defined, the location-specific parameters can be introduced. The simulation period is set to 10 years, with annual intervals. This time frame is appropriate for a strategic level model while extending the horizon further would introduce significant uncertainty.

At each node of the binomial tree, the annual rich solvent supply is calculated. However, it is important to note that the solvent does not arrive at the port in a single shipment. For instance, if the yearly solvent supply is 10000 tons, this would require only four barges with a loading capacity of 3000 tons each. While this may appear efficient, such an approach would always favour barge transport, leading to an unfair comparison between truck and barge transport. Moreover, it would implicitly require temporary storage at the offloading location to accumulate sufficient volume for each shipment. The goal of this study is to support strategic decision-making on when to switch from truck to barge transport-based supply volumes. Including temporary storage or optimizing shipment timing would shift the focus to the operational side, which is outside the scope of this study. To avoid biased results in the analysis, the total annual solvent supply is instead divided by 52 to derive an average weekly solvent flow. Based on this weekly flow, the costs associated with deploying trucks or barges are calculated.

In this case study, it is assumed that all captured CO_2 and solvent are offloaded at the Maasvlakte, a designated site within the Port of Rotterdam. From this offloading location, the rich solvent is transported to the CO_2 hub for regeneration and liquefaction. The conditioning hub is assumed to be located at the EVOS Rotterdam terminal. While this facility does not currently exist, it is considered operational and scaled sufficiently to handle all supply levels originating from the supply tree.

During the start-up phase of the OCCUS supply chain, containerized truck transport is assumed to be the mode of transportation. This method offers operational simplicity and flexibility, making it particularly suitable for the early stages of supply chain deployment (Oeuvray et al., 2024). As supply increases, a transition to inland waterway transport is considered, potentially operating CEMT-IVa, CEMT-Va inland chemical barges, or a combination of both. The decision to consider barge transport is based on the findings of Oeuvray et al. (2024), which suggest that as supply volumes increase, transitioning to barge transport becomes a more viable and efficient option.

The estimated transport distance between the Maasvlakte terminal and the EVOS Rotterdam site is approximately 27 km for truck transport via the roadway network. But as the truck also needs to return a container of rich solvent, the distance is set to $x^{sol}_{truck} = 57$ km. The barge distance is set $x^{sol}_{barge} = 40$ km, which is a round trip from the EVOS site to Maasvlakte via the waterway network. An overview of the locations is shown in figure 5.1.

Figure 5.1: Visualization of the offloading and CO_2 conditioning hub locations

At the EVOS site, the CO_2 is regenerated from the solvent and subsequently liquefied. The liquefied CO_2 is then transported via containerized truck transport to the collection point of the Aramis offshore storage site at the Maasvlakte. The transport distance for this leg is set to $x^{LCO_2}_{truck} = 27$ km. It is chosen to deploy truck transport as the mass flow for LCO_2 is only a third of the solvent flow. In addition, the truck provides more flexibility (Oeuvray et al., 2024).

The electricity price is set at €0.1545/kWh, based on the 2024 average for non-household consumers in the Netherlands (Eurostat, 2024). The current grid emissions factor is approximately 270 gCO_2/kWh, but this is expected to gradually decline in line with the Netherlands' national decarbonization goals. To account for the partial use of renewable energy at the plant itself, a reduced average emissions factor of 135 gCO_2/kWh is assumed for simplicity.

Two approaches are considered for incorporating the CO_2 price into the model. In the first approach, a fixed average price is used for simplicity and setting a base case. The current EU ETS price is approximately €73 per tonne of CO_2, while a study by Bloomberg (2024) projects a potential rise to €194 per tonne by 2035 due to the progressive reduction in emission allowances. Taking the average of the current and projected maximum prices, the CO_2 price is set at €136 per tonne.

The second approach allows for a variable CO_2 price over time. According to Bloomberg (2024), the EU ETS price is expected to reach around €158 per tonne by 2030, with a maximum of €194 per tonne in 2035. Using the known values for the current year 2030, and 2035, linear interpolation is applied to estimate the prices for the intermediate years. The projected yearly CO_2 prices are shown in table 5.1.

Table 5.1: Projected CO_2 prices from 2025 to 2035

Year	2025	2026	2027	2028	2029	2030	2031	2032	2033	2034	2035
CO_2 price (€/tCO_2)	65	82	99	116	133	150	158.8	167.6	176.4	185.2	194

All the general parameters dependent on the timeline and location of the case study are summarized in table 5.2.

Table 5.2: General parameters for the case study

Parameter	Unit	Value	Description	Comment/Source
T	y	10	Total years	User input
N	y	10	Total intermediate steps	User input
P_e	€/kWh	0.1545	Average price non-households NL	(Eurostat, 2024)
EF_{en}	gCO_2/kWh	135	Dependent on energy source	(Statista, 2023)
P_{CO_2}	€/tCO_2	136	Average of 2035 prediction and current price	(Bloomberg, 2024)
x_{truck}^{sol}	km	54	Transport distance solvent truck	Maps
x_{barge}^{sol}	km	40	Transport distance solvent barge	Euris
$x_{tr}^{LCO_2}$	km	27	Transport distance LCO_2	Maps

5.2. Binomial parameters

The approximation of the initial parameters S_0, σ, and μ is essential for constructing the CO_2 supply lattice. These parameters represent the initial supply level, volatility, and expected growth rate, forming the basis for simulating future CO_2 inflow to the port. However, accurately estimating them is challenging due to the limited availability of historical data and the inherent uncertainties in operational conditions (Lewis & Spurlock, 2004). Classical lattice models typically rely on historical data of the uncertain parameter or a combination of data and expert judgment to provide more reliable estimations (Lewis & Spurlock, 2004).

5.2.1. Initial supply

For this study, port call and vessel data are available from a representative part of the fleet. These databases consist of both port calls and info about large deep-sea ocean-going vessels, which were used to simulate an ammonia-powered shipping network (Boersma, 2024). Although these vessels are not the primary vessel types which are likely to operate OCC systems, they provide a good indication of emissions from a sample fleet to the port.

The port call data was imported from an Excel dataset containing timestamped entries of vessel arrivals and departures. The dataset is chronologically sorted by vessel IMO number to reconstruct the sequence of port visits for each ship. An additional column is added to include the previous port name, which is done by shifting the Port Name column downward. If a switch of vessels is detected, the previous port name remains blank and is filtered out later.

Since the case study focuses on the Port of Rotterdam, a filter was applied to only include vessel arrivals to Rotterdam and its sub-regions: Botlek, Maasvlakte, and Waalhaven. Anchorage movements and internal port calls are excluded, as it is assumed that CO_2 is only offloaded at the main port terminal after a seagoing voyage.

From the remaining port calls, the vessel IMO names are extracted and coupled with a ship database containing all the required info for each vessel in the port calls dataset. To operate OCC systems, vessels must have SO_x free exhaust gases to minimize solvent degradation (Feenstra et al., 2019).

Therefore, vessels without SO_x abatement systems installed or pending are filtered out. Figure 5.2 provides a graphical representation of the number of vessels per fleet type which visit Rotterdam at least once.

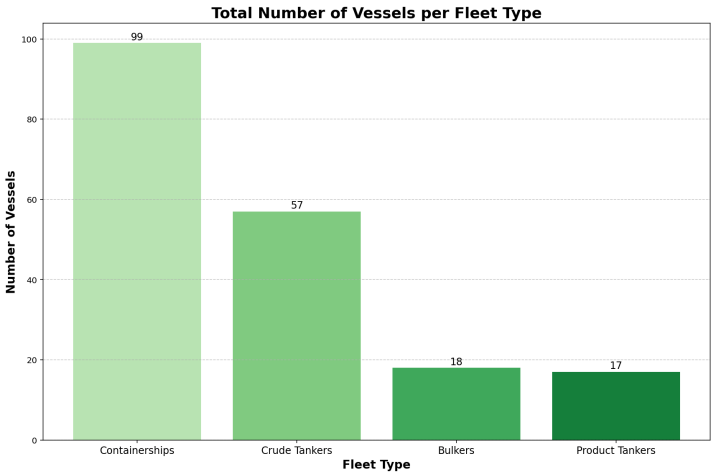

Figure 5.2: Total number of vessels fitted with SO_x scrubber fitted visiting the Port of Rotterdam at least once.

The remaining vessels are matched with the THETIS-MRV database, a publicly available dataset that reports CO_2 emissions from vessels operating in European waters. This dataset also provides the average CO_2 emissions in kilograms per nautical mile for each vessel for the corresponding reporting year (EMSA, 2025).

To estimate the total average emissions for a single trip from a previous port to Rotterdam, the sailing distance in nautical miles must be determined. For this purpose, the searoute Python tool is used, which calculates realistic sea routes between two ports based on their coordinates (Halili, 2025). Port coordinates are sourced from the World Port Index database (WPI, 2025). However, not all ports listed in the port call logs are available in this database. In such cases, missing ports are manually added, including the coordinates of specific offshore facilities such as Floating Production, Storage and Offloadings (FPSOs). Additionally, when vessels are recorded as departing from anchorages near a port, it is assumed that they depart from the nearest recognized port. The total emissions to the port of Rotterdam are calculated by summing the individual trip emissions. Figure 5.3 provides a representation of the trip routes to the port of Rotterdam by the sample fleet.

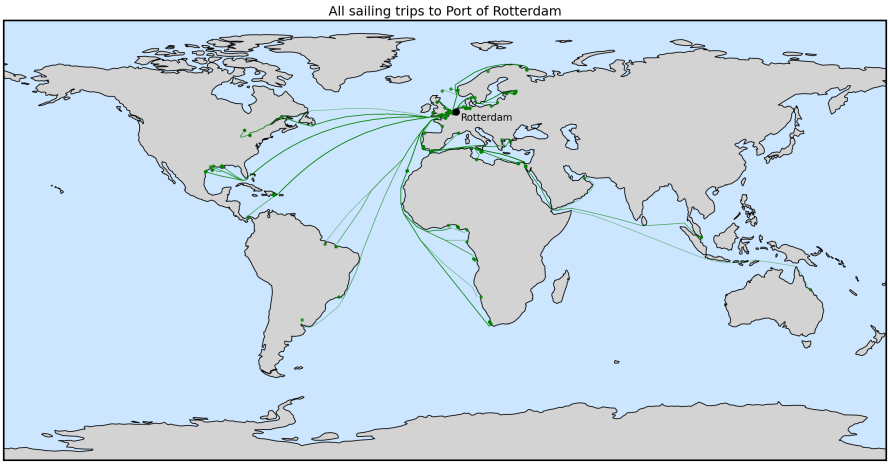

Figure 5.3: Overview of all the vessel trips sailing to the Port of Rotterdam

Using equation (5.1), the total CO_2 emissions by the sample fleet to the port of Rotterdam at time step 0 are calculated to be 627075 tCO_2/y. The total emissions per fleet type are presented in figure 5.4. At the initial time step, the fleet adaptation rate, F_0, is assumed to be 4%, and the capture efficiency, η_{cap}, is set at 40% (Zhao et al., 2025). Substituting these values into equation (4.2) results in an initial CO_2 supply to the port of 10033 tCO_2/y, which corresponds to 30100 t solvent per year by multiplying with the factor κ.

$$E_{ships} = \sum_{n_{trip}}^{N_{trip}} x_{ship} \cdot EF_{ship} \tag{5.1}$$

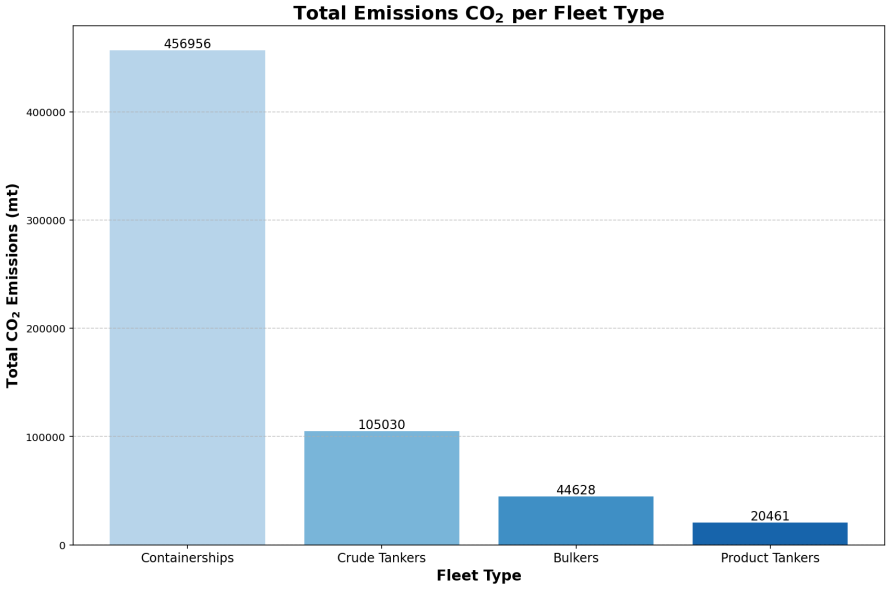

Figure 5.4: Total emissions per fleet type

All the required input parameters for calculating the total fleet emissions to the port are summarized in table 5.3.

Table 5.3: Required parameters from the different data sets to obtain the total emissions

Parameter	Unit	Description	Source
IMO	-	IMO number	AIS data
t	UTC	Timestamp	AIS data
H_a	-	Port name	AIS data
H_d	-	Previous port name	AIS data
Move type	-	Arrival	AIS data
SO_x	-	SO_x Fitted or Pending	Clarkson Research WFR
Lat	°	Latitude coordinate of port	WPI
Long	°	Longitude coordinate of port	WPI
x_{ship}	nm	Trip distance	Calculated with searoute
EF_{ship}	$kgCO_2/nm$	Yearly average vessel emission factor	THETIS-MRV
η_{cap}	-	Carbon capture efficiency	(Zhao et al., 2025)
F_0	-	Fleet adoption rate at first time step	Assumed

5.2.2. Average growth rate

Typically, historical data is used to determine the average drift or growth rate. However, since OCC is not yet widely implemented, such data is unavailable. Based on publicly available data, three alternative approaches are considered.

The first approach assumes that the average growth rate follows the same trend as ship arrivals. The data is obtained from the annual yearly reports of the Port of Rotterdam (Port of Rotterdam, 2025). However, after reviewing the data from 2016 onward, it is observed that total ship arrivals declined by 1.2%. This trend is not aligned with projections indicating that CO_2 supply to the port will increase (DNV, 2024). Therefore, this method is not feasible.

A second approach is to link the average growth rate with the reported total yearly emissions of the sample fleet. It must be highlighted that this is not the same value as S_0, which was calculated based on port calls data from one year only. Estimating the growth rate requires more data points. Therefore, a different approach is required. To calculate the total yearly emissions by the same sample fleet, the THETIS-MRV datasets from 2018 to 2023 are collected. For each reporting year, the total annual emissions were obtained by summing the emissions reported by each individual vessel in the sample fleet. The resulting total emissions are shown in figure 5.5. Based on this data, the annual start-to-end growth rate is calculated using equation (5.2), which is 3.1 %

Although this approach provides a more realistic growth rate compared to vessel arrivals, it is debatable whether this strategy is the most accurate for predicting the average growth rate of CO_2 supply. Since it does not account for emission reduction targets, it is expected that reported emissions will eventually decline due to the implementation of such targets.

$$\mu(\%) = \left(\frac{E_{reported,2018}}{E_{reported,2023}} \right)^{\frac{1}{\Delta t}} - 1 \tag{5.2}$$

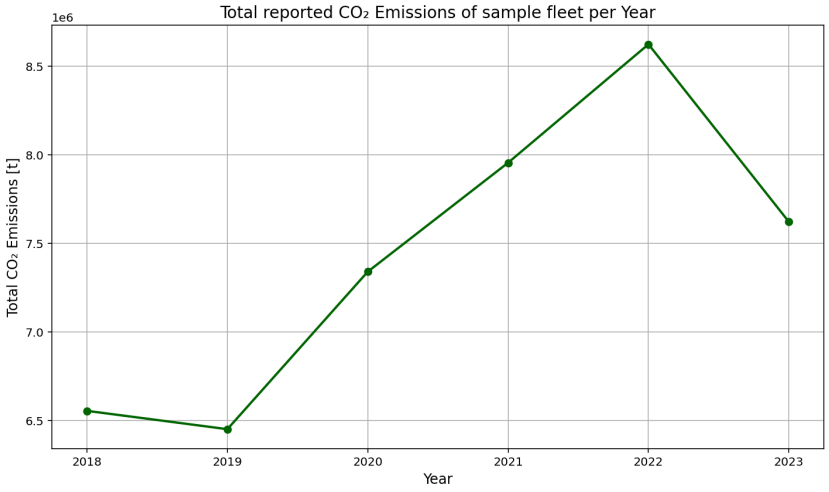

Figure 5.5: Total reported CO_2 emissions of the sample fleet calculated based on THETIS-MRV database

The third approach assumes that the average growth rate of incoming CO_2 follows an inverse trend to the emissions reduction pathway outlined by the IMO at the MEPC 83 meeting. The reduction targets are illustrated in figure 5.6, which apply to all maritime seagoing vessels above 5000 GT (IMO, 2025). It is reasonable to expect that the overall emissions reduction of the global maritime fleet will follow a similar trajectory, and the sample fleet will do so as well. Although OCC is only one of several decarbonization strategies available to the maritime industry, it is assumed in this study that the volume of CO_2 captured via OCC will increase in proportion to the overall reduction in fleet emissions. Based on the assumed inverse relationship with the emission reduction trajectory proposed by the IMO, the corresponding average growth rate is calculated according to equation (5.3) and set to 3.71%.

$$\mu = \frac{Target_{2035} - Target_{2028}}{\Delta t} = \frac{0.3 - 0.04}{7} = 0.0371 \tag{5.3}$$

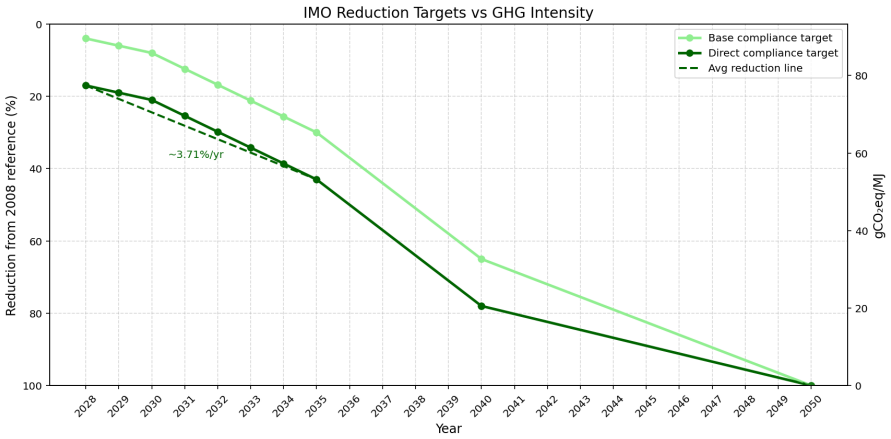

Figure 5.6: Average Well-to-Wake (WTW) reduction targets

The last approach, which assumes the average growth rate to follow the opposite trend of the reduction targets, is the best fit for this case study because this approach reflects expected developments and incorporates global emission reduction targets set by the IMO. While it is difficult to predict what fraction of the total emission reductions will be achieved using OCC systems, this uncertainty is addressed through the incorporation of volatility in the model. Additionally, a sensitivity analysis will be performed to assess the impact of different growth rate assumptions on the outcomes. However, the base growth rate as input for the model is set to 3.71%.

5.2.3. Volatility

Since historical data of captured CO_2 from maritime vessels to the Port of Rotterdam is unavailable, the volatility must be determined using an alternative method. In the first approach, the volatility was assessed based on the annual variation in ship arrivals, under the assumption that captured CO_2 volumes could follow a similar trend. This approach resulted in a calculated volatility of only 3.71%. Given the structure of the RO model, it is necessary that the volatility exceeds the average growth rate. Lower volatility would result in unrealistically small fluctuations and lead to probabilities above 1 for up-states and negative probabilities for down-states. Therefore, this method is deemed unsuitable for estimating the volatility in this model.

As the cargo turnover indirectly reflects ship movements, it was tested whether calculating the volatility based on cargo turnover could provide a better estimation. However, similar to the ship arrivals, the resulting volatility was determined to be only 3.19%, even lower compared to ship arrivals. Therefore, the same problem arises as described earlier, making this approach infeasible as well.

Furthermore, the emission reduction targets set during the MEPC 83 meeting (IMO, 2025) provide projections for average CO_2 reduction but do not specify anything regarding the expected volatility of CO_2 supply. Therefore, this data can not be used in this case.

Consequently, it has been decided to base the volatility estimation on the total reported CO_2 emissions of the sample fleet, consistent with the second approach used for determining the growth rate. The data is derived from the THETIS-MRV datasets covering the years 2018 to 2023, as shown in figure 5.5. This approach allows for year-by-year variability of the sample fleet, making it the most suitable approach. To calculate the volatility as a percentage of the average, the yearly average emissions are first calculated using equation (5.4).

$$\bar{x} = \frac{1}{N} \sum_{i=1}^{N} x_i \tag{5.4}$$

Then, the volatility σ is determined as the standard deviation of the yearly emissions around the mean, as shown in equation (5.5).

$$\sigma = \sqrt{\frac{1}{N-1}\sum_{i=1}^{N}(x_i - \bar{x})^2} \tag{5.5}$$

Since the data represents only a sample of the fleet, the denominator $N-1$ is used instead of N to correct this and avoid underestimating the true variability. Based on this approach, and using equation (5.5), the volatility of CO_2 supply to the port is calculated to be 11.22%.

5.3. Cost input parameters

This section provides all the input parameters required to evaluate the costs of each step in the supply chain. The same order of the required steps is followed for clarity.

5.3.1. Solvent transport costs

As described in section 5.1, the OCCUS supply chain initially relies on container truck transport for moving saturated solvent. As transport volumes increase, a switch to chemical barge transport might become economically more favourable. This subsection outlines the cost structures of both transport modes, starting with truck transport followed by barge transport.

Truck transport

Truck transport costs have been derived from quotations provided by a commercial transport company. For various distances, the cost of transporting a single container is obtained and visualized in Table 5.4. The trucking company shared a discount could be given, which is referred to as the bulk trip price if at least 400 containers would need to be transported annually. This corresponds to an average of at least eight containers per week. With the maximum capacity of 28.5t, this could already be achieved if the solvent supply is 11400 tons per year (220 t per week).

Table 5.4: Costs for transporting one container

Distance [km]	Price [€]	Bulk trip price [€]
19.3	305	255
19.4	305	255
22.2	330	280
30.1	380	330

Based on the quotations listed in table 5.4, the corresponding total transport costs for both the regular and bulk prices are plotted in figure 5.7. For each data point, unit costs are calculated by dividing the total cost by the transport distance and the mass of a fully loaded container. To estimate costs for different distances, it is assumed that total transport costs scale linearly with distance. As a result, the unit cost in €/tkm follows a function of the form $a + \frac{b}{x_{tr}^{sol}}$ consistent with the containerized transport cost formulation proposed by Oeuvray et al. (2024). The resulting unit cost functions are illustrated in figure 5.8 and mathematically defined in equation (5.6).

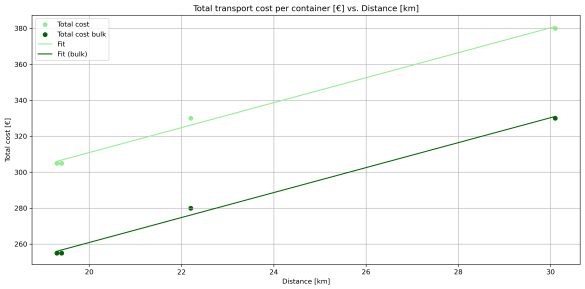

Figure 5.7: Total truck transport cost as a function of distance.

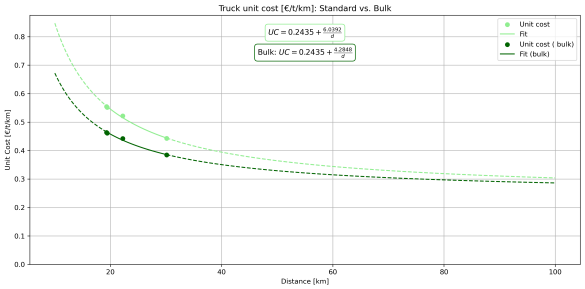

Figure 5.8: Unit truck transport cost [€/tkm] as a function of distance.

$$UC_{truck} = \begin{cases} 0.2453 + \frac{6.0392}{x_{tr}^{sol}} & \text{if } n_{\text{cont}} < 400 \\ 0.2453 + \frac{4.2435}{x_{tr}^{sol}} & \text{if } n_{\text{cont}} > 400 \end{cases} \tag{5.6}$$

Due to the specific transport quotes and the need to charter tank containers, the cost function for truck transport has been slightly adjusted for this case study, as shown in equation (5.7). Transport costs are calculated on a weekly basis and then scaled to annual costs by multiplying by 52 weeks. The reason for using weekly calculations is elaborated in section 5.1.

The unit cost obtained from transport quotes represents the cost of transporting a single container per kilometre. To calculate the cost per container per trip, this unit cost is multiplied by both the maximum container mass and the transport distance.

To determine the total weekly transport cost, this single container transport cost is multiplied by the number of containers required each week. The number of containers is calculated by dividing the weekly solvent flow with the maximum capacity (M_{cont}) of a container, which is 28.5t, as shown in equation (5.8). Since partial containers are not possible, the resulting value is rounded up to the nearest whole number.

$$C_{truck_{i,j}} = (UC_{truck} \cdot M_{cont} \cdot x_{tr}^{sol} \cdot n_{cont} + C_{cont} \cdot n_{cont}) \cdot 52 \tag{5.7}$$

$$n_{cont} = \frac{\frac{Sol_{i,j}}{52}}{M_{cont}} \tag{5.8}$$

Table 5.5: Container parameters

Parameter	Unit	Value	Description	Comment/Source
C_{cont}	€	55	Container rental price per week	Quote
M_{cont}	t	28.5	Maximum container capacity	Datasheet

To provide insight into the total weekly transport costs as a function of both the weekly solvent supply and transport distance, figure 5.9 is presented. Figure 5.10 shows the corresponding unit transport costs [€/t/km]. Notably, a significant cost reduction occurs at approximately 220 tonnes of solvent per week, where the bulk discount becomes applicable. Furthermore, the figure illustrates that unit costs remain constant across varying mass flows, which is expected given the transport is containerized.

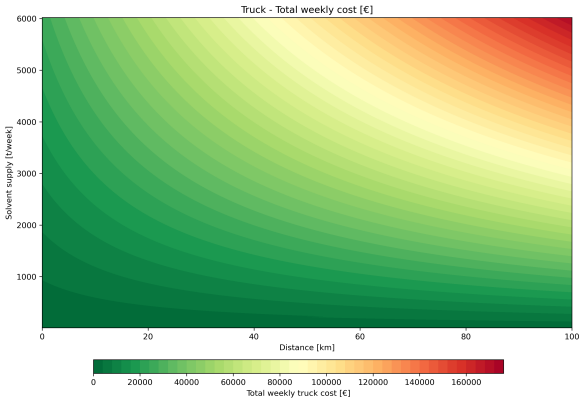

Figure 5.9: Total weekly transport cost for truck transport.

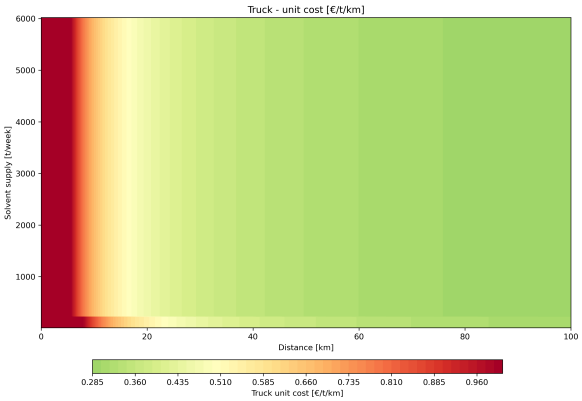

Figure 5.10: Unit transport cost [€/t/km] for truck transport.

Barge transport costs

To obtain representative cost estimates for barge transport, quotations were obtained from a barge company specializing in transporting chemicals. Based on data provided by the operators, the loading and discharging times for 500 t of solvent each take approximately 12 hours. It was noted that the difference in time between handling 500 t and 1000 t is constrained by lower pumping capacities at lower volumes and significantly higher capacities at higher volumes. On average, the pumping capacity at full load is 350 (m^3/h). For the transportation of solvent, it is recommended to use barges equipped with stainless steel tanks. There are two types of barge classes recommended for this purpose. Their specifications are detailed in table 5.6.

Table 5.6: Barge parameters

CEMT-class	L [m]	B [m]	Load Capacity [t]	Load volume [m^3]
Iva	85	10.95	1639	1650
Va	110	11.40	3448	3761

The received cost data for transporting varying amounts of solvent with the corresponding barge types is shown in table 5.7.

Table 5.7: Received quotes for barge transport

CEMT-class	Distance [km]	Solvent [t]	Price [€]
	40	500	12000
Iva	40	1639	16000
	140	500	14500
	140	1639	18500
	40	1000	18000
Va	40	3448	26000
	140	1000	20500
	140	3448	28500

Based on the obtained quotations, the total costs for various weekly solvent supply volumes are calculated. Intermediate and partial load costs are assumed to scale linearly and are estimated through interpolation or extrapolation. It is further assumed that if the maximum capacity of a barge is exceeded, an additional barge can be deployed at a cost equivalent to transporting one ton in the initial barge. Consequently, the total cost function exhibits a discontinuous, stepwise pattern resembling a staircase, as illustrated in figures 5.11 and 5.12. By dividing the total cost by the product of distance and solvent

supply, unit costs are derived. Due to the stepwise nature of the total cost function, the resulting unit cost profile displays a sawtooth-like behaviour, as shown in figures 5.13 and 5.14.

In the graphs, three distinct lines are presented. The dashed line, labelled *Combined*, represents the operational flexibility of deploying both CEMT-Iva and CEMT-Va class vessels. This approach allows for dynamic allocation. Once the smaller barge reaches its maximum capacity, the larger barge can be used. Conversely, if the larger barge is at full capacity, an additional smaller barge can be deployed instead of introducing another large vessel.

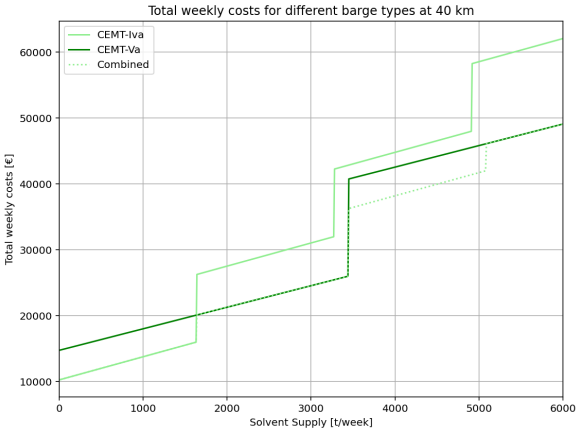

Figure 5.11: Weekly barge costs for 40 km transport distance for different weekly solvent supplies

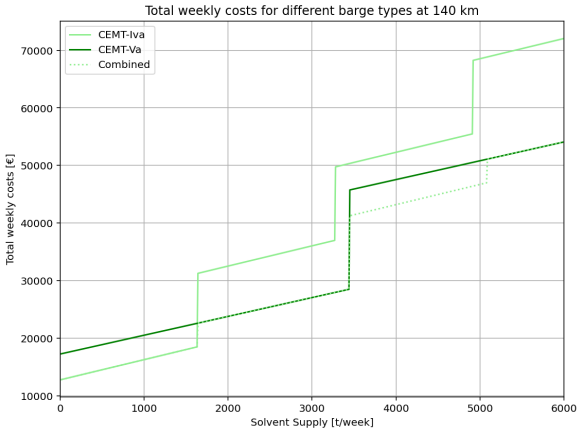

Figure 5.12: Weekly barge costs for 140 km transport distance for different weekly solvent supplies

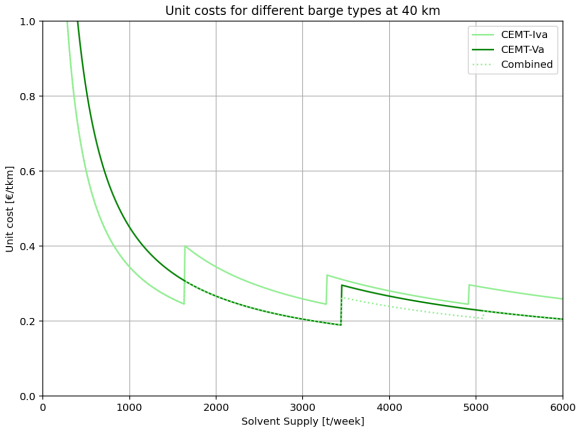

Figure 5.13: Unit costs for 40 km barge transport distance for different weekly solvent supplies

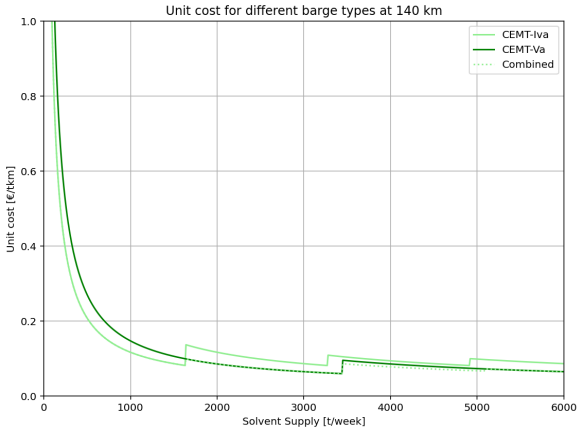

Figure 5.14: Unit costs for 140 km barge transport distance for different weekly solvent supplies

To enable cost estimation for varying transport distances, it is assumed that total transport costs scale linearly with distance. However, due to the stepwise discontinuities in the cost function arising from the discrete nature of barge deployment, it is not feasible to formulate a continuous unit cost function that simultaneously depends on both distance and solvent supply. Instead, the total cost for a given solvent supply at a new distance is determined through linear interpolation between known data points, which is visualised in section 4.4.1. It must be noted that the number of available data points is limited. However, since the distance intervals between these points are relatively small compared to typical barge operating ranges, the interpolated cost estimates in the range of these values are considered reliable.

5.3.2. Regeneration

The input parameters required to calculate the unit and total costs for regeneration are summarized in table 5.8. Based on equation equation (4.13), the unit- and total costs are plotted in figures 5.15 and 5.16 respectively. Initially, unit costs decrease with increasing mass flow at lower volumes. However, this decrease is limited as unit costs quickly stabilize. This is primarily caused by the high energy requirements for solvent regeneration, which demands large quantities of steam from either gas combustion or electric boilers (Gür, 2022). Therefore, the costs are mainly driven by the price of electricity. A waste heat factor of 70% is assumed to reduce the heat requirement. Furthermore, a learning rate of 2% per year is applied to reflect potential cost reductions from technological advancements (Liu et al., 2021).

Table 5.8: Regeneration parameters

Parameter	Unit	Value	Description	Comment/Source
$I_{reg,ref}$	€/tCO_2/y	3.5	Reference investment costs for regeneration plant	80% of liquefaction
OM_{reg}	%	0.06	Operational & Maintenance costs for regeneration plant	Equal to liquefaction
SEC_{reg}	kWh/tCO_2	972	Specific energy consumption for regeneration per ton of CO_2	(Moser et al., 2020)
S_{ref}^{reg}	tCO_2/y	10^6	Reference yearly CO_2 flow	(Deng et al., 2019)
γ	%	0.02	Learning rate factor for regeneration	(Liu et al., 2021)
N_{reg}	-	0.3	Exponential factor for economies of scale	(Deng et al., 2019)
h	%	0.7	Percentage of available rest heat	Depending on lay out

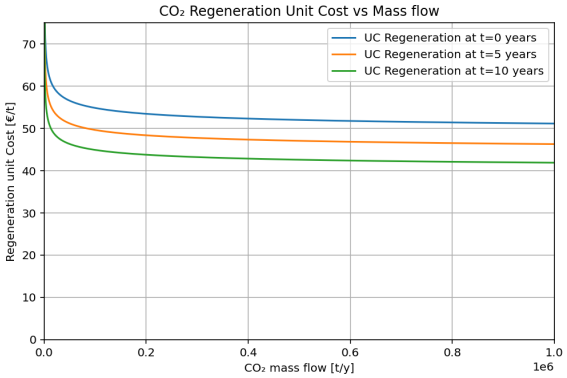

Figure 5.15: Unit costs for regeneration as a function of the mass flow

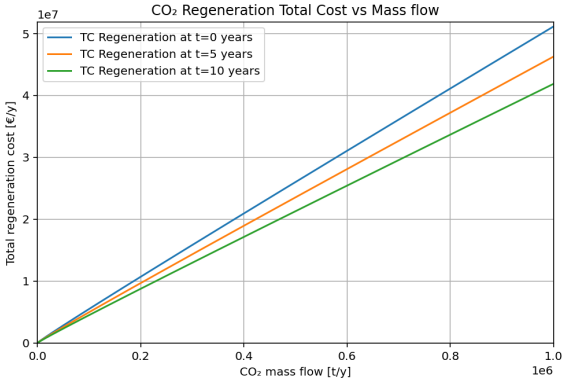

Figure 5.16: Total costs for regeneration as a function of the mass flow

5.3.3. Liquefaction

The input parameters to determine the liquefaction process are summarized in table 5.9. Based on equation equation (4.14), the unit- and total costs are plotted in figures 5.17 and 5.18 respectively. Compared to regeneration, the unit costs for liquefaction become constant at higher volumes. This process is less energy intensive because it does not require heat. Instead, it requires electricity for rotating equipment, such as pumps and compressors (Jensen et al., 2025). As a result of these differences, the unit costs stabilize at larger volumes as (Jensen et al., 2025). Additionally, it is clear that the costs for liquefaction are nearly two and a half times lower compared to regeneration, also caused by the lower energy requirement. Furthermore, a learning rate of 2% per year is applied to reflect potential cost reductions from technological advancements (Liu et al., 2021).

Table 5.9: Liquefaction parameters

Parameter	Unit	Value	Description	Comment/Source
$I_{liq,ref}$	€/tCO_2/y	4.3	Reference investment costs for liquefaction plant	(Deng et al., 2019)
OM_{liq}	%	0.06	Operational and Maintenance costs for liquefaction plant	(Deng et al., 2019)
SEC_{liq}	kWh/tCO_2	104.3	Specific energy consumption for liquefaction of 1 ton CO_2	(Deng et al., 2019)
S_{ref}^{liq}	t/CO_2/y	10^6	Reference yearly CO_2 flow	(Deng et al., 2019)
β	%	0.02	Learning rate factor for liquefaction	(Liu et al., 2022)
N_{liq}	-	0.3	Exponential factor for economies of scale	(Roussanaly et al., 2021b)
ν	%	0.05	Venting factor CO_2	(Jensen et al., 2025)

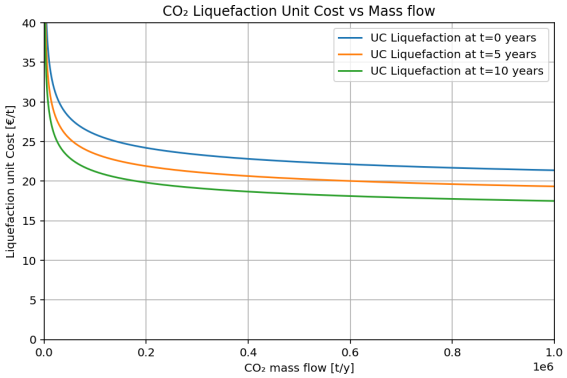

Figure 5.17: Unit costs for liquefaction as a function of the mass flow

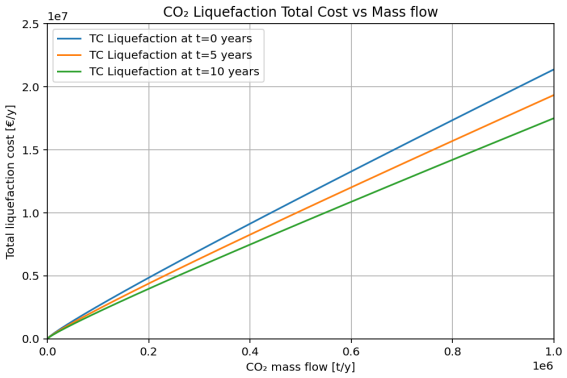

Figure 5.18: Total costs for liquefaction as a function of the mass flow

5.3.4. Liquid CO_2 transport costs

As mentioned in section 5.1, it is assumed all transport of LCO_2 from the conditioning facility to the underground storage site is carried out using containerized truck transport. According to the study by Oeuvray et al. (2024), equation (4.15) is applied for containerized truck transport. The total cost as a function of transported LCO_2 is shown in figure 5.19. These costs are significantly lower compared to solvent transport costs. This is caused by three reasons.

First, the transport distance is only half of the distance compared to solvent transport. Second, the total volume to be transported is lower due to the solvent conversion factor of 3, meaning that only one-third of the solvent volume needs to be transported as LCO_2. Lastly, as discussed in section 4.5.3 about, 5% of CO_2 is lost in the liquefaction process, reducing the overall total mass to be transported.

Table 5.10: LCO_2 constants as proposed by (Oeuvray et al., 2024)

Parameter	Unit	Value	Description	Comment/Source
α_1	€/tkm	0.15	Constant	(Oeuvray et al., 2024)
α_2	€/t	5.58	Constant	(Oeuvray et al., 2024)

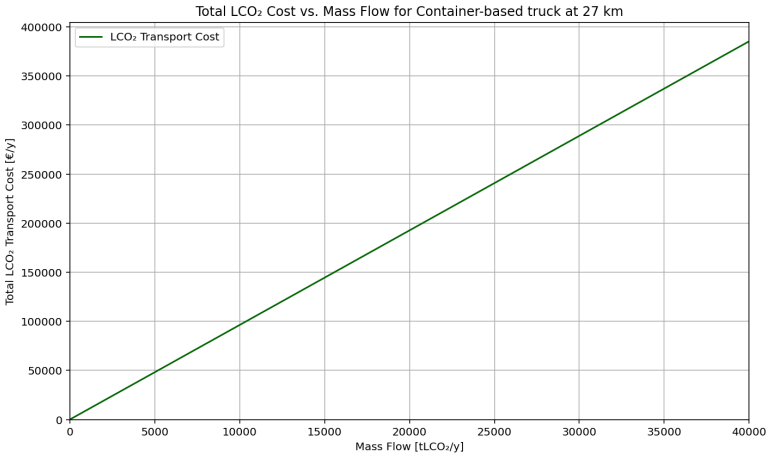

Figure 5.19: Total LCO_2 truck transport costs

5.3.5. Permanent underground storage

As explained in section 5.1, for this case study, all CO_2 is stored permanently underground at the Aramis offshore Depleted Oil&Gas Field (DOGF) (Global CCS Institute, 2024a). Based on the unit costs provided by Roussanaly et al. (2021b) for an offshore DOGF with reusable wells and a reference flow of 2.5 million tonnes annually, the unit costs are set at 7.5 €/tCO_2. These costs include all steps required, from offloading at the storage site to the actual underground storage part. The input parameters are provided in table 5.11. Using these parameters and equation (4.19), the total costs are plotted in figure 5.20.

Table 5.11: Parameters for permanent underground storage

Parameter	Unit	Value	Description	Comment/Source
UC_{ps}	€/tCO_2	7.5	Unit costs per ton of storage	(Roussanaly et al., 2021b)
SEC_{ps}	kWh/tCO_2	7	Specific energy requirement for underground storage	(Knoope et al., 2014)

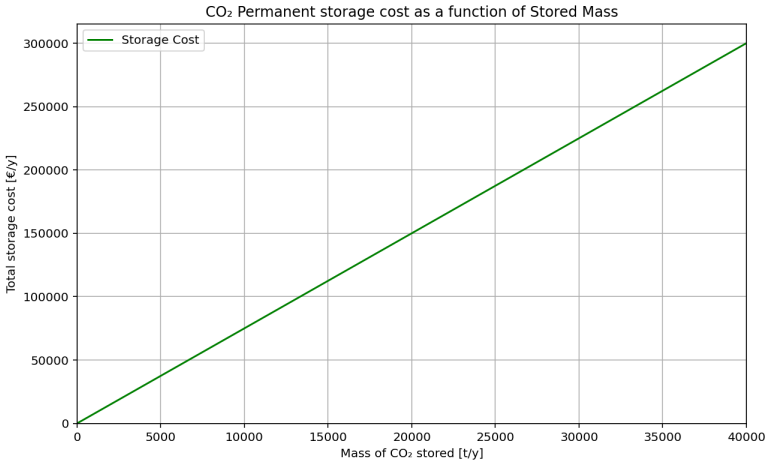

Figure 5.20: Total yearly costs of storage as a function of the mass flow

5.4. Emissions input parameters

This section provides all the input parameters required to evaluate the emissions of each step in the supply chain. The same order of the required steps is followed for clarity.

5.4.1. Transport emission parameters

The emissions factors used for truck and barge transport are reported in table 5.12. Based on these emissions factors and the predefined distances from section 5.1, the total emissions as a function of the yearly mass flow is shown in figure 5.21.

Table 5.12: Transport emissions factors.

Parameter	Unit	Value	Description	Comment/Source
EF_{truck}	gCO_2/tkm	62	Truck transport emission factor	(McKinnon & Piecyk, 2010)
EF_{barge}	gCO_2/tkm	31	Barge transport emission factor	(McKinnon & Piecyk, 2010)

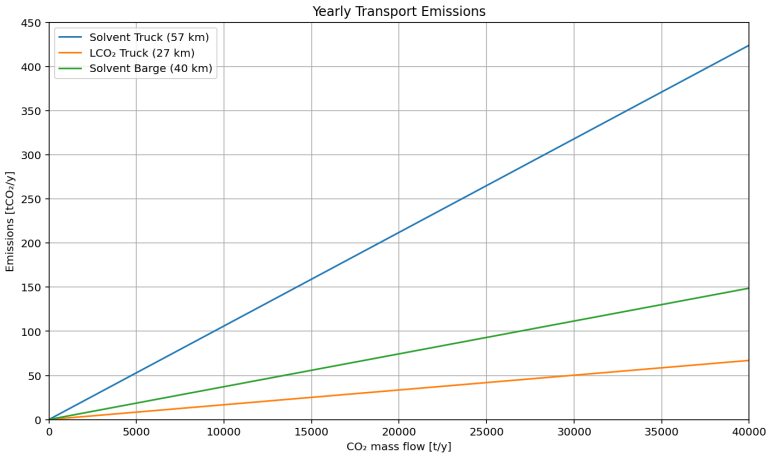

Figure 5.21: Total transport emissions as a function of the mass flow for the defined distances.

5.4.2. Regeneration and liquefaction emissions

The regeneration and liquefaction emission are calculated using equations equations (4.22) and (4.23), and the input parameters for the specific energy requirements given in the previous section. In figure 5.22, it is visible that the liquefaction process produces more emissions. At first, this seems contradictory as the regeneration process is more energy-intensive. However, rest heat integration is set at 70%, which lowers the overall emissions for this process. Besides, 5% of captured CO_2 is lost due to venting, as elaborated earlier. Due to these reasons, the emissions for liquefaction are significantly higher.

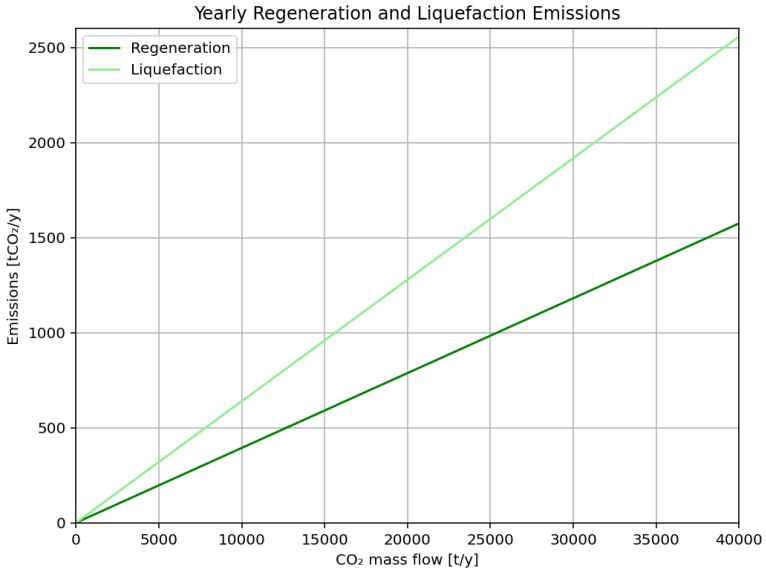

Figure 5.22: Yearly total emissions for the regeneration and liquefaction process

5.4.3. Permanent storage emissions

The permanent storage emissions are calculated according to equation (4.19), the input parameters are given in tables 5.2 and 5.11 as the specific energy requirements and the local emission factors are required. The total emissions as a function of the total CO_2 stored annually is shown in figure 5.23.

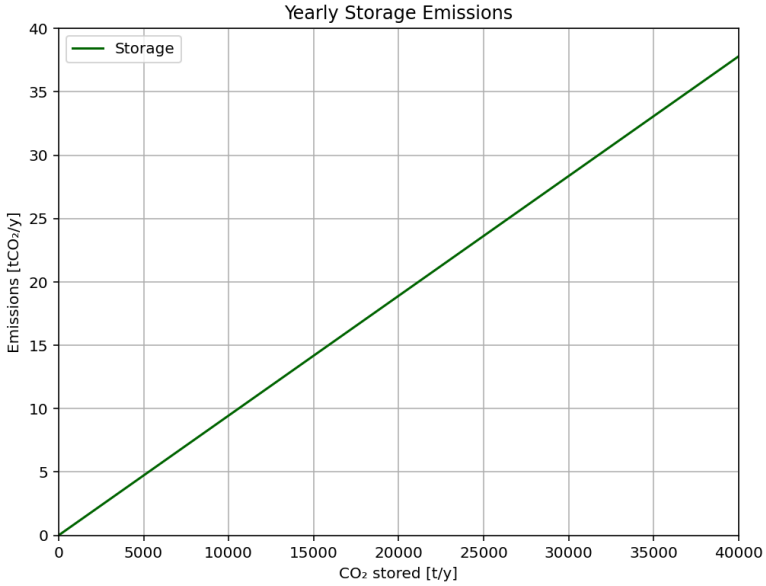

Figure 5.23: Total yearly storage emissions

6

Results

In this chapter, the results of the model developed in chapter 4, applied to the case study introduced in chapter 5 are presented. Each section begins with the truck-only case as a baseline, followed by a comparison of different barge transport configurations. Section 6.1 presents the outcomes of the binomial process, detailing the volumes of captured CO_2 and the corresponding required solvent. These represent the supply to the port and form the foundation for all subsequent results. Next, the results are divided into two main scenarios. The constant average CO_2 price case, discussed in section 6.2, and the variable CO_2 price case, covered in section 6.3. Finally, the chapter concludes with the presentation of the break-even CO_2 prices necessary for the economic viability of the OCCUS supply chain.

Additional results, such as the costs and emissions for the common supply chain steps regeneration, liquefaction, LCO_2 transport and permanent storage, have no direct influence on the switch decision. However, they are required to calculate the overall break-even price of the supply chain. Therefore, these results are presented in appendix A for reference.

6.1. Binomial process of the solvent supply

This section presents the results of the binomial process, which is fundamental for this analysis, as the quantities of captured CO_2 and required solvent form the basis for all subsequent calculations. Based on the input parameters outlined in chapter 5, the calculated binomial values are summarized in table 6.1. At each node, the supply is multiplied by 1.12, with an associated probability of 0.64 to transition to the upward state, and by 0.89, with a probability of 0.36 to the downward state.

Table 6.1: Binomial values

Variable	Description	Value
u	Upward factor	1.12
d	Downward factor	0.89
p	Upward probability	0.64

As calculated in section 5.2, the initial supply at time step 0 is set at 10033t of CO_2, requiring 30100t of solvent. From the starting node, the supply evolves over the ten-year period to multiple scenarios, ranging from a minimum of 3262t of CO_2 to a maximum of 30812t of CO_2 as shown in figure 6.1. This means a maximum of three times compared to the initial supply.

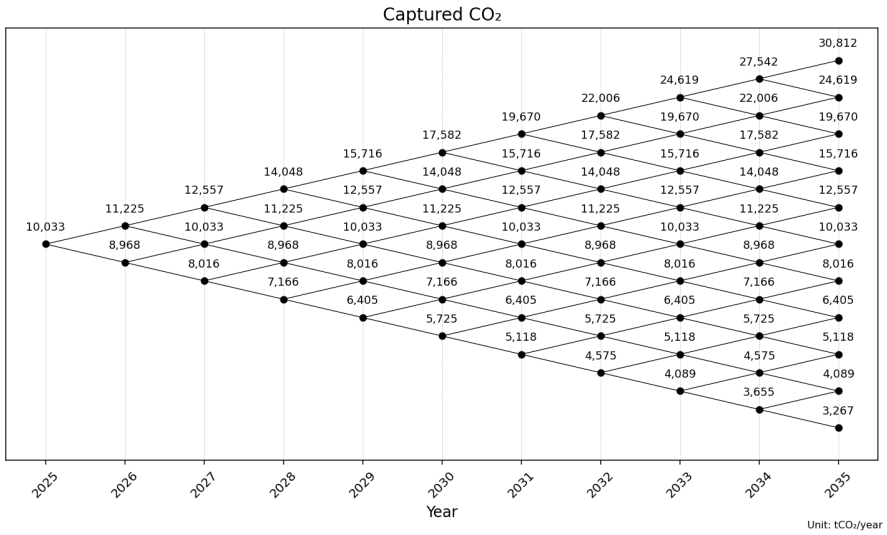

Figure 6.1: Calculated CO_2 supply based on the binomial process

The required solvent is visualised in figure 6.2, which shows the CO_2 supply multiplied by the conversion factor κ. Based on the minimum and maximum values, this corresponds to 9801 t and 92436 t of solvent, respectively.

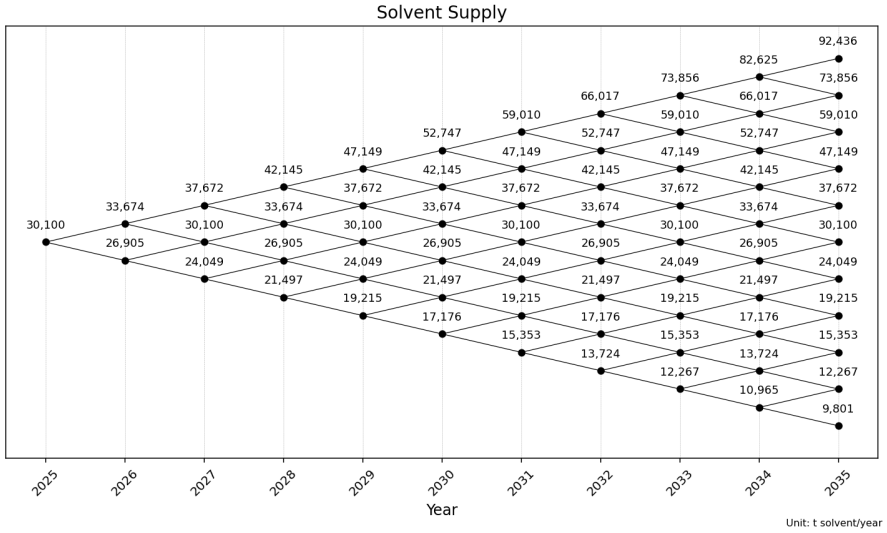

Figure 6.2: Yearly incoming solvent supply based on the captured CO_2

The probability of reaching each possible scenario (node) is calculated using equation (4.7). The results are visualised in figure 6.3. The figure shows that the probability of reaching a threefold increase in CO_2 supply is only 1.15%, while the probability of reaching the minimum supply level is nearly zero. These results were discussed with experts from Value Maritime, who noted that such a threefold increase in CO_2 supply is a plausible scenario. However, they believe that the model underestimates the likelihood of this outcome.

In addition, it can be observed that the likelihood of scenarios with a lower CO_2 supply is minimal, which aligns with expectations of increasing CO_2 supply to the port in the future. The most probable outcomes indicate a CO_2 supply growth between 12 and 20 tonnes, corresponding to approximately 36 to 60 tonnes of rich solvent over a ten-year period. These values are considered low by the experts of Value Maritime, which anticipate higher CO_2 supply levels in the most probable scenarios. These

results, when compared with the expectations of Value Maritime experts, suggest that this modelling approach or the method used to determine the binomial parameters may not be the most suitable approach for predicting future CO_2 supply volumes.

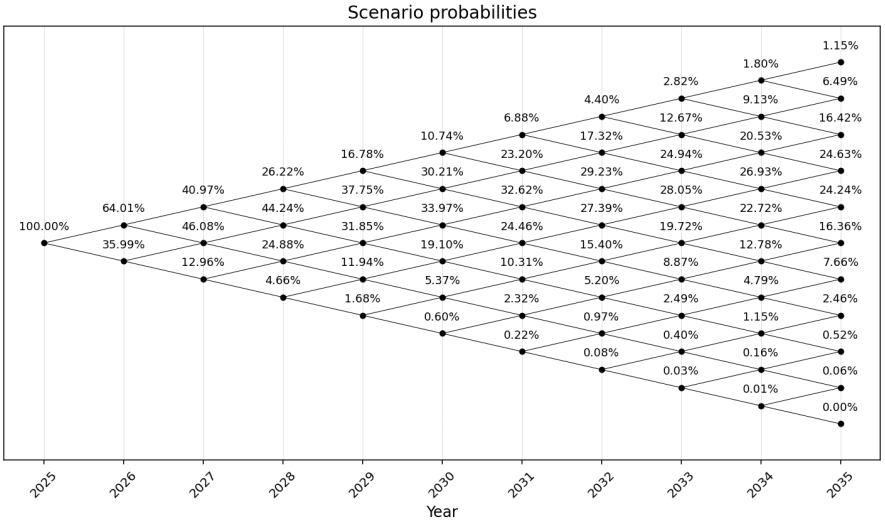

Figure 6.3: Probabilities of possible future scenarios

6.2. Average CO_2 price

The case study is first evaluated under the assumption of a constant average CO_2 price, as introduced in section 5.1. This section presents the results for the different transport switching strategies.

6.2.1. Truck transport

To create a baseline, the model is first run without the option to switch between transport modes. This means it is assumed that solvent is transported exclusively by trucks. This approach allows for a baseline evaluation of the supply chain performance under a fixed transport strategy. The resulting costs and DCF serve as references for further evaluation, where the option to switch from truck to barge transport will be introduced.

The total yearly transport costs for different supply levels are shown in figure 6.4. Similar to the solvent supply, the costs are also tripled, which aligns with expectations, as the total transport costs were assumed to be independent of the mass flow, resulting in a linear increase in the costs.

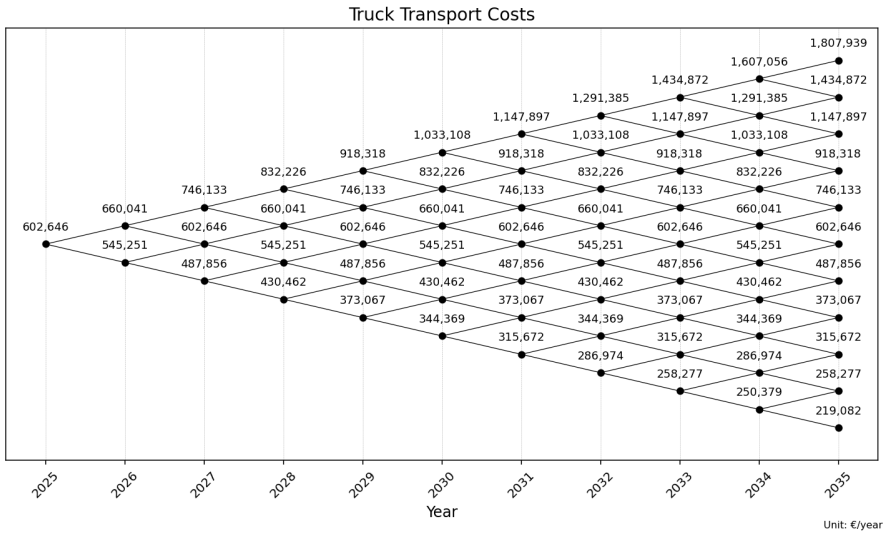

Figure 6.4: Total costs for using trucks for solvent transportation.

The total discounted cash flow (total value) accounts for all costs and revenues associated with operating the supply chain, discounted back to their corresponding year. As shown in figure 6.5, the discounted cash flow remains significantly negative across the assessed timeline. The total value at the root node is -€3884806, indicating that operating the supply chain is not economically viable. Even at the end nodes, for both the minimum and maximum supply scenarios, no positive value is achieved. This highlights that, under all scenarios, the price of CO_2 is insufficient to cover the costs of operating the supply chain. Notably, the results show that lower supply volumes lead to less negative total values compared to higher volumes. This suggests that the unit cost of operating the supply chain exceeds the average CO_2 price of €138/tCO_2, which leads to better (albeit still negative) performance at lower volumes. This observation is further supported by the minimum CO_2 price calculation, as discussed in section 6.4, which shows that a price of at least 184.21 €/tCO_2 would be required to achieve a DCF of approximately zero at the starting node.

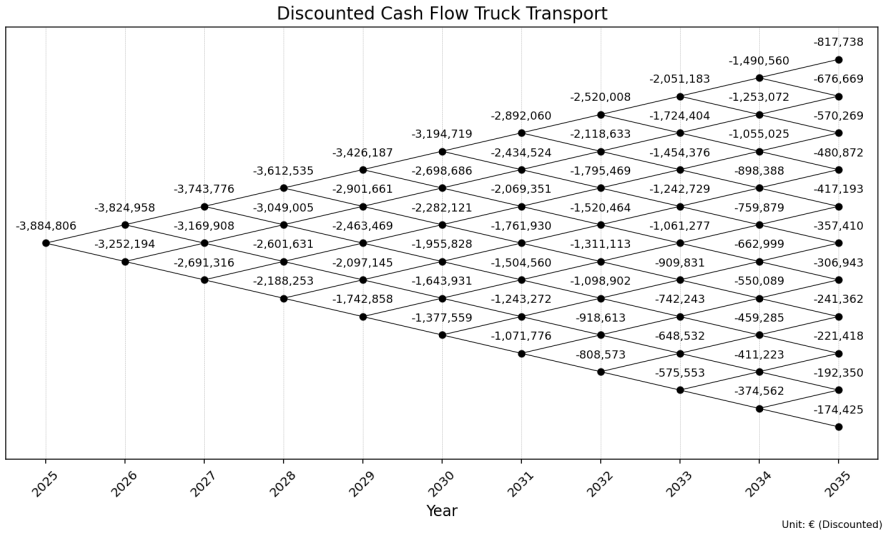

Figure 6.5: Discounted Cash Flow for operating the OCCUS supply chain using trucks for solvent transportation.

Based on the findings discussed above, the potential of switching to barge transport is now assessed to determine whether it can improve the DCF and result in a positive outcome.

6.2.2. Option to switch to CEMT-IVa

This section presents the total costs, option value, and total value, with the possibility of switching to the smaller CEMT-IVa barge available. Based on these results, the switch decision lattice is constructed, along with the corresponding yearly switch probabilities.

The associated total yearly transport costs are presented in figure 6.6. It can be observed that along the upward supply paths, costs increase according to the underlying cost function, whereas along the downward supply paths, costs decrease similarly. A notable jump in transport costs occurs at the highest supply node. This discontinuity is caused by the solvent supply exceeding the capacity of a single CEMT-IVa barge, necessitating the deployment of an additional barge to meet the transport demand.

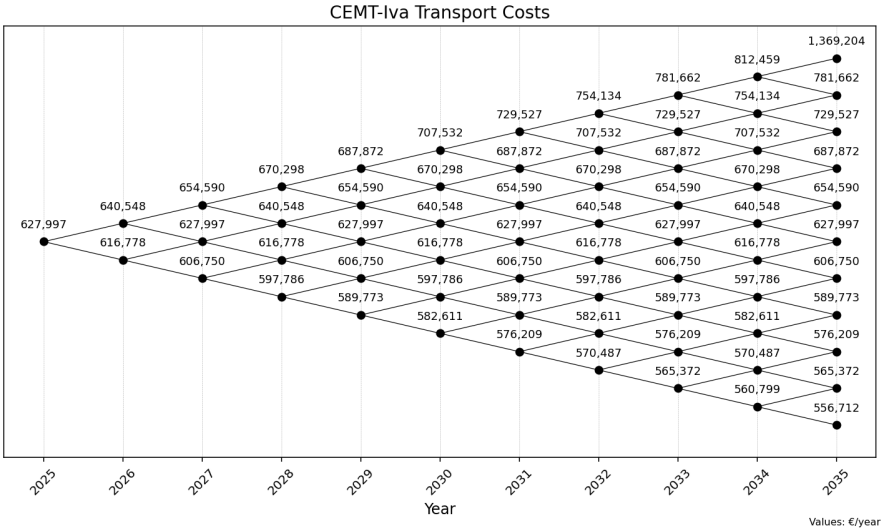

Figure 6.6: Total transport costs for using CEMT-IVa barge.

The option value lattice is shown in figure 6.7. It can be observed that the option value is relatively high. At the root node the option value is €630345, which is the value added by the option if in this year an decision must be made. For the upward nodes, the option value increases significantly, indicating that the barge is more favourable compared to truck transport. This is primarily due to the cost structure. No upfront investment costs or contract termination penalties are incurred. As a result, the option value increases over time as more information becomes available, generally favouring a switch more quickly. In addition, at the end nodes, the option values are relatively low compared to the preceding nodes, which is caused by the so-called end effect. In reality, this would not be the final year in which a decision to switch or stay is forced (Melese et al., 2015). To overcome this, a longer simulation timeline could be employed. However, it would significantly increase computational time.

Another notable observation is that, despite the higher costs associated with deploying an additional CEMT-IVa barge at the top-end node, switching remains beneficial at this supply level. However, the incremental option value gained is significantly lower compared to earlier nodes.

At lower supply nodes, the option value is zero, indicating that expected supply volumes are insufficient to justify switching, as barge costs exceed those of truck transport.

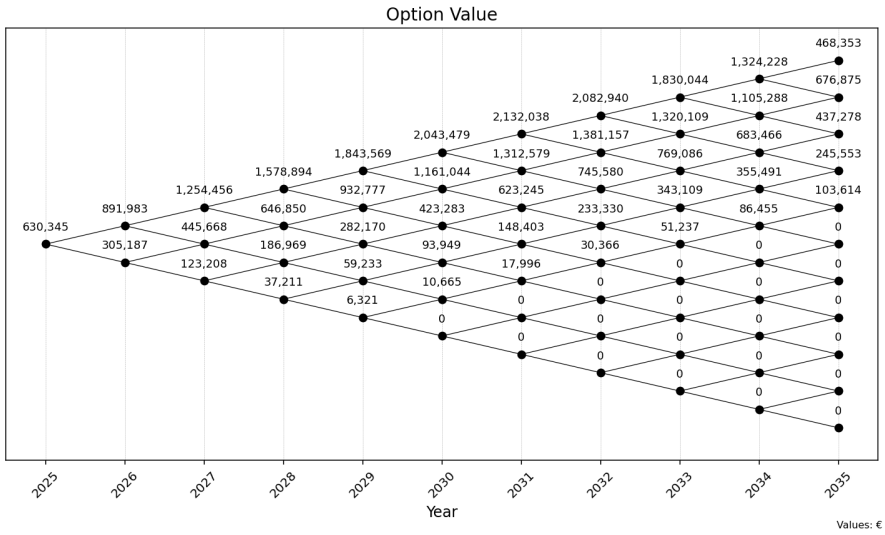

Figure 6.7: The option value lattice to switch to the CEMT-IVa barge.

The total value is the sum of the DCF for truck transport and the additional option value associated with switching to barge transport. Figure 6.8 shows the resulting total value lattice. It is visible that, for the majority of nodes, the total value has increased compared to the case without switching options. Except for the nodes in which the option value is calculated to be zero, the total value remains the same, as the option adds no value. Nevertheless, the total value remains negative at nearly all nodes, indicating that with the added value of the option, the CO_2 price is still insufficient.

One exception is found at one of the end nodes, where a small positive value is obtained. At the end of the decision tree, the option value reflects the immediate gain from switching if it is beneficial. This indicates that, at the final decision point for this particular path, switching from truck to CEMT-IVa barge would allow the supply chain to break even. Consequently, for this specific case, the required CO_2 price is estimated to be around 138 €/t. However, to obtain break-even at the start node, a minimum price of €176.19/t is required, which is only 4.4% lower compared to the price with no option, as will be elaborated further in section 6.4.

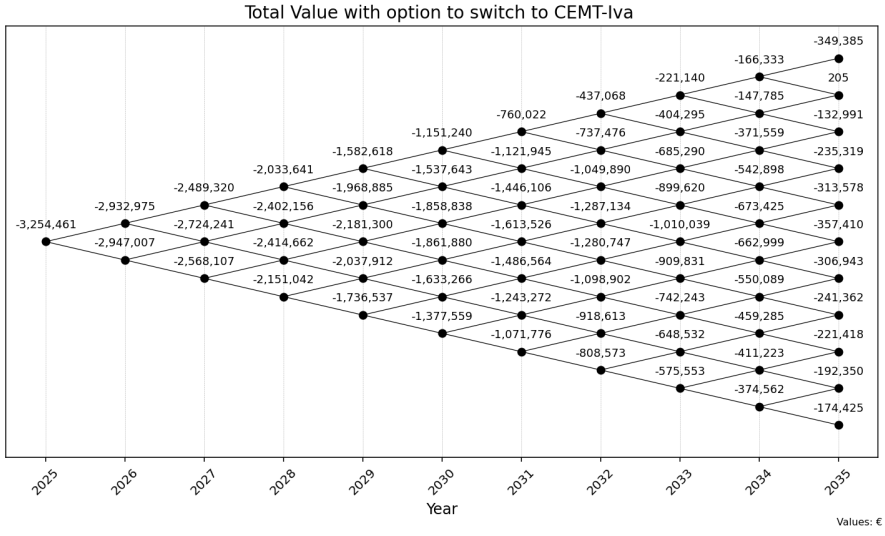

Figure 6.8: Total value of operating the OCCUS supply chain with the option to switch to CEMT-IVa barge.

The switch decision lattice is shown in figure 6.9. Based on the probability function, the likelihood of making a switch in each year is summarized in table 6.2. The first switch decision, with a probability of 41%, is already visible in 2027. However, it drops significantly to only 26% in the following year. This decline occurs because switching is only favourable if supply conditions are expected to improve in the next time step. If supply is expected to decrease, it is better to defer the option. As mentioned earlier, no contract penalties or investment costs are required for this switch option, meaning it can become favourable quickly if future conditions are expected to improve. This pattern continues in the subsequent years. The highest probability of switching occurs in 2034, reaching 81%. This high value indicates that switching to the CEMT-IVa barge is very likely at that point. However, switching too early can have negative consequences, which must be carefully considered.

Table 6.2: The yearly probability of switching to CEMT-IVa barge

	2025	2026	2027	2028	2029	2030	2031	2032	2033	2034	2035
Switch probability	0.00	0.00	0.41	0.26	0.55	0.75	0.63	0.78	0.68	0.81	0.73

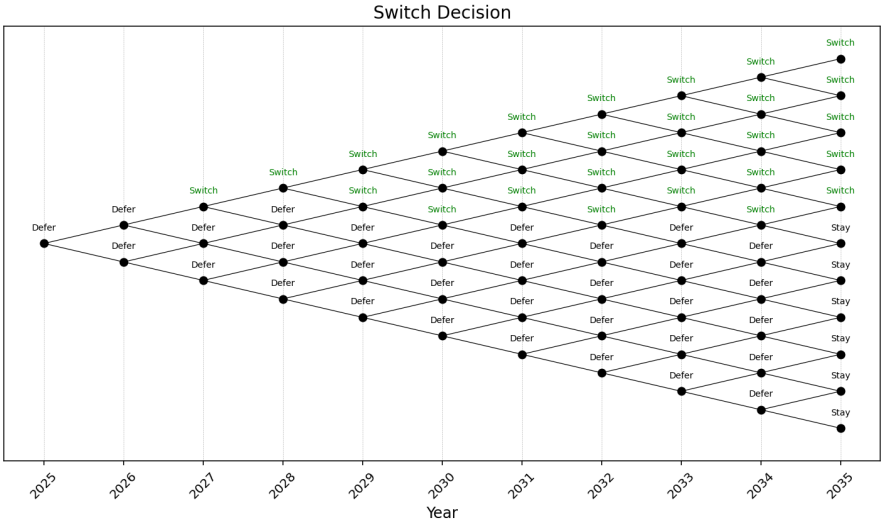

Figure 6.9: Decision lattice for switching to CEMT-IVa.

6.2.3. Option to switch to CEMT-Va

This section presents the total costs, option value, and total value when the possibility of switching to the large CEMT-Va barge is available. Based on these results, the switch decision lattice is constructed, along with the corresponding yearly switch probabilities.

The transport costs are displayed in figure 6.10. From this lattice, it can be observed that the costs for deploying this barge are indeed higher compared to the smaller CEMT-IVa barge. The costs gradually increase for all upward nodes and decrease for the downward nodes. Two key points must be highlighted. First, unlike the smaller barge, no jumps in cost are observed at any node, indicating that no extra-large barge is required. Because even at the highest supply level, the weekly supply is 1778 tonnes, representing only 52% of the maximum barge capacity. Second, when comparing these costs to the total costs of truck transport shown in figure 6.4, at a solvent supply of 47149 tonnes (roughly 906 tonnes per week), it becomes clear that operating this barge at just 25% of its maximum capacity already results in lower transport costs compared to truck transport, highlighting that in the case of even higher supply levels, a switch would become even more attractive.

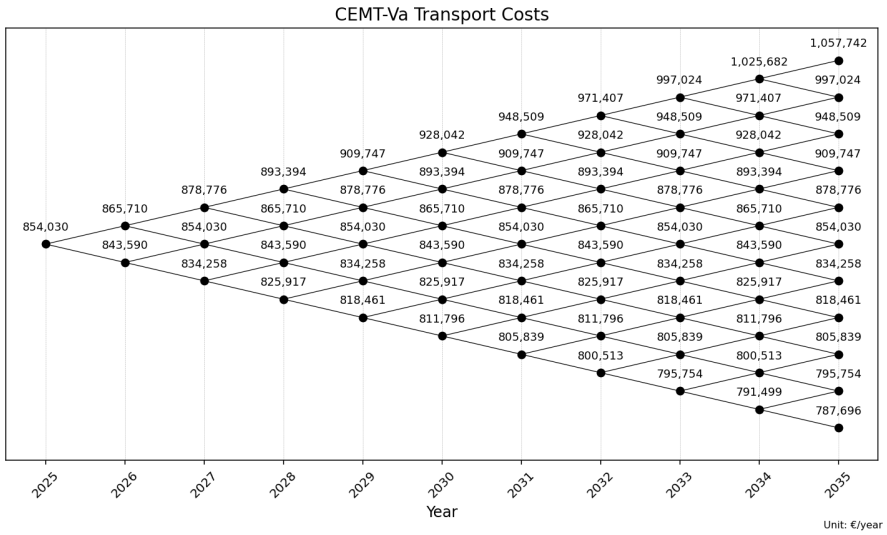

Figure 6.10: Total transport costs for using CEMT-Va barge.

The option values are shown in figure 6.11. In the early years, the option value is relatively low but increases steadily until 2032. Particularly between 2030 and 2033, the high option values indicate that switching will become beneficial if solvent supply continues to rise. However, if the decision is postponed too long, the option value gradually declines, reflecting the outcomes where supply is insufficient to justify the use of barges. Due to the same end effect, the option values at the terminal nodes are lower compared to the preceding nodes, as no future effects are considered.

A comparison of the option values for the larger and smaller barges indicates that, at these supply levels, the smaller barge is more attractive. The option values for the larger barge are significantly lower, reflecting its reduced economic viability under these conditions compared to the smaller barge. Additionally, the option value is zero at more nodes.

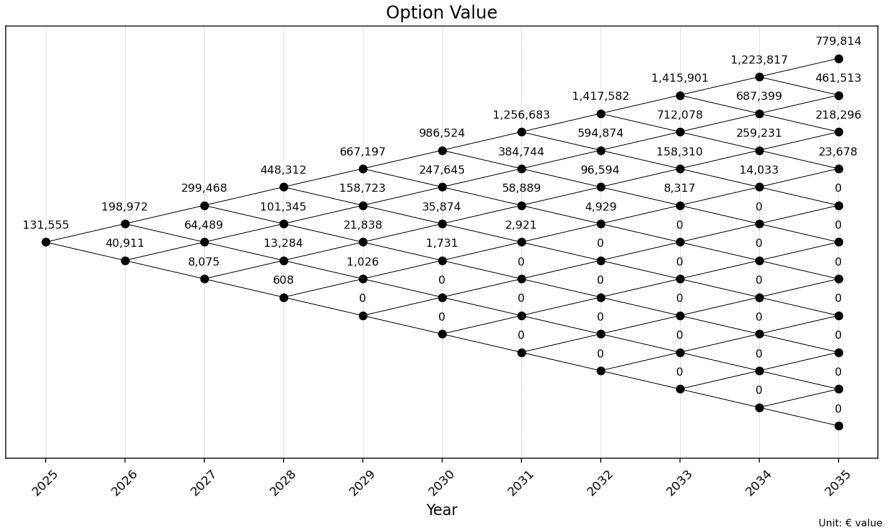

Figure 6.11: The option value lattice to switch to the CEMT-Va barge.

The total value remains negative for all the possible outcomes, which is in line with the expectations, as the option values are lower compared to the smaller CEMT-IVa barge. At the start node, the total value is significantly negative but decreases gradually over the year. This has two causes. First, the DCF for truck transport is decreasing as well. Secondly, the option value is increasing. Except for the

downward nodes. For which the total value remains equal. The CO_2 price is still insufficient to cover the costs to break even over the complete timeline. The minimum price calculation indicates that a price of at least €182.52/t is necessary to break even at the starting node, which is only a marginal reduction compared to the truck-only case.

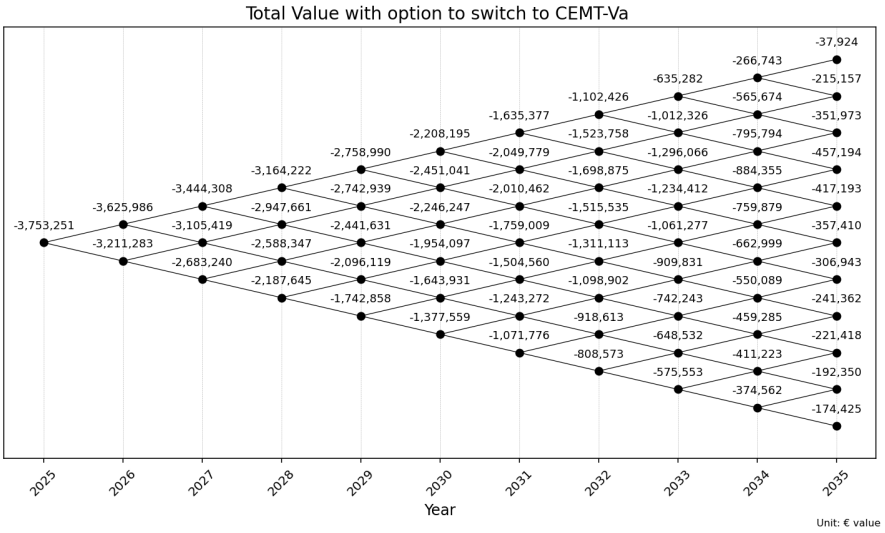

Figure 6.12: Total value of operating the OCCUS supply chain with the option to switch to CEMT-Va barge.

The yearly switch probabilities, as shown in figure 6.13, indicate that switching is not beneficial during the initial years up to 2029. In 2030, switching becomes favourable for the first time, but only under the condition that solvent supply has increased in each preceding year, an outcome with a probability of only 11%. In 2031, the probability declines to 7%, as switching is again only advantageous if supply continues to rise. Caused by the same reasons as mentioned in section 6.2.2. This pattern continues until 2035 when the probability of switching reaches 49%. A summary of the yearly switch decisions is provided in table 6.3. Compared to the smaller barge, the switching decision for the larger barge becomes favourable two years later and with a lower probability. This further highlights the higher efficiency of the smaller barge under the given supply conditions.

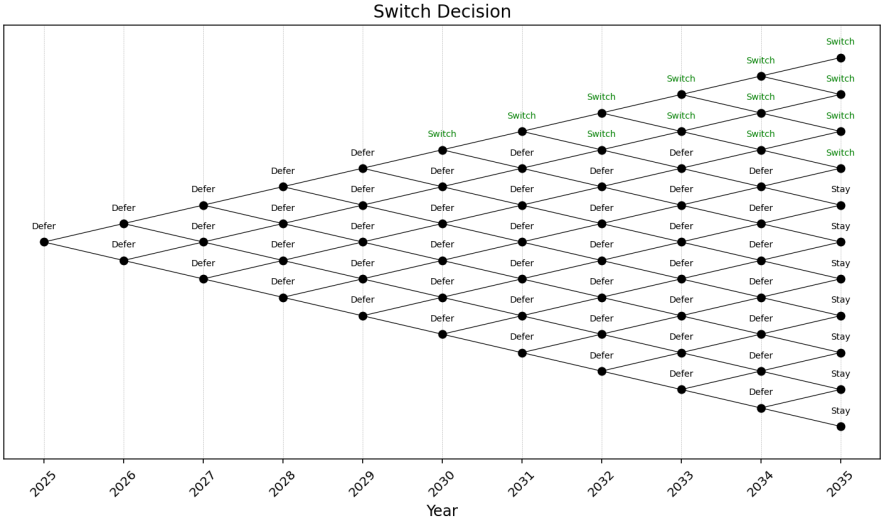

Figure 6.13: Decision lattice for switching to CEMT-Va.

Table 6.3: The yearly probability of switching to CEMT-Va barge

	2025	2026	2027	2028	2029	2030	2031	2032	2033	2034	2035
Switch probability	0.00	0.00	0.00	0.00	0.00	0.11	0.07	0.22	0.15	0.31	0.49

6.2.4. Option to switch to combined strategy

The final switching option considered is the use of a combined deployment of both barge types. Based on the previous results, it is already known that a second CEMT-IVa barge is only required in the case of the highest solvent supply. With this particular option, instead of deploying a second smaller barge, a large barge will be deployed at this specific node, as the model selects the most cost-effective barge based on the solvent volume.

The total costs are presented in figure 6.14. As expected, these are almost identical to the CEMT-IVa case. The only difference is observed at the maximum supply terminating node. Due to the deployment of the larger barge, the costs are reduced by approximately €300000/y in this node.

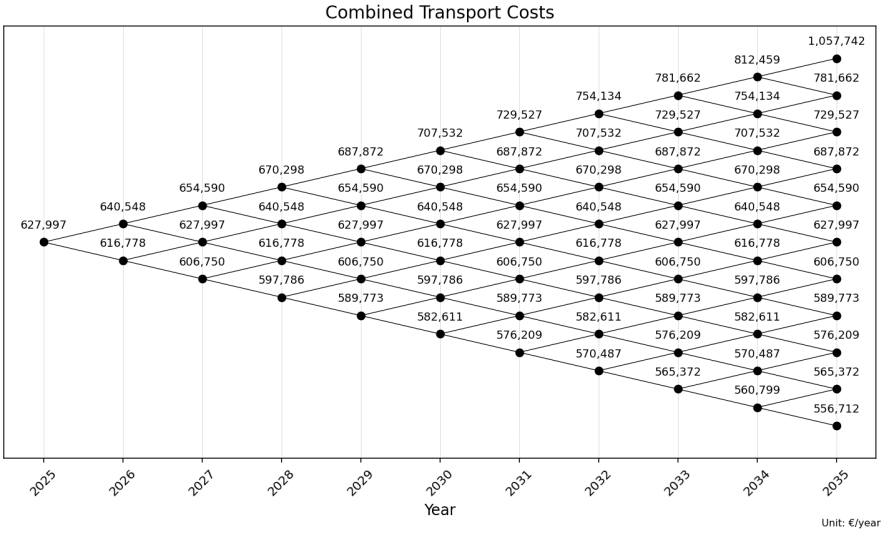

Figure 6.14: Total transport costs for combined barge strategy.

The option values of this switching option are presented in figure 6.15. Due to the findings presented above, the option values are very similar as well. Only at the highest supply node does the option value increase to €1057742. However, due to the limited probability of reaching this node, the option value increases by only around €2000, thereby limiting its overall impact on the total option value at the root node.

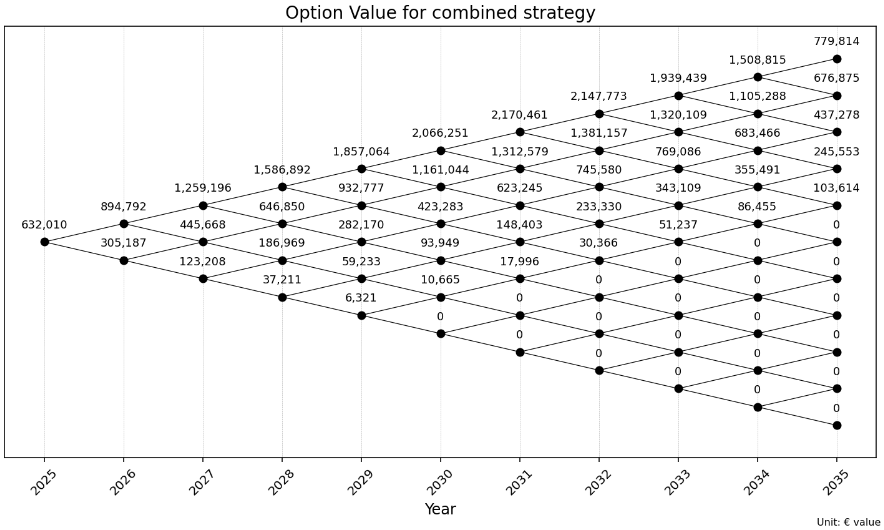

Figure 6.15: The option value lattice to switch to the combined strategy.

Figure 6.16 presents the total value for the combined barge deployment scenario. Similar trends are observed for the single barge type scenarios, with the total value remaining negative for the majority of the nodes. However, in the highest supply scenario in 2034, a positive value of €18255 is achieved. This indicates that, under this option, a modest profit can be generated in at least one scenario, although the probability of this outcome is only 1.8%.

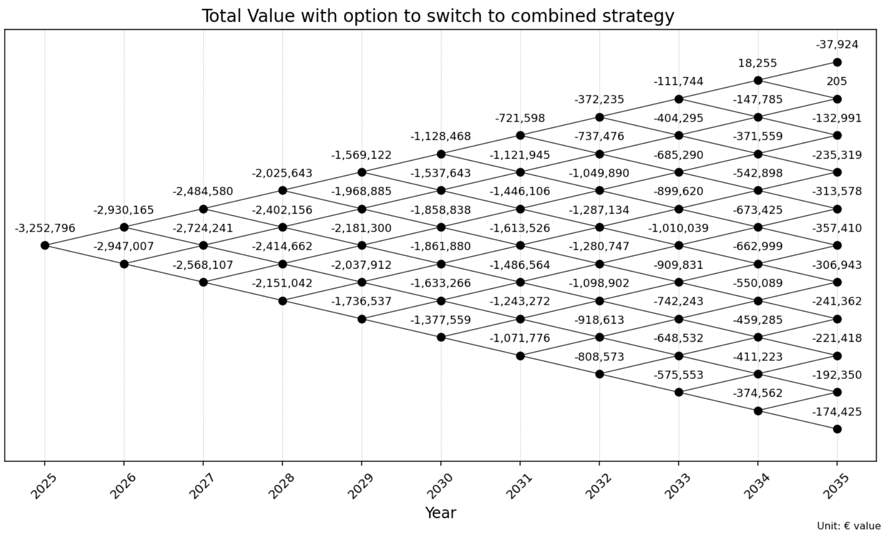

Figure 6.16: Total value of operating the OCCUS supply chain with the option to switch to combined strategy.

At the top node in 2035, where the larger CEMT-Va barge would be deployed, the switch decision would also have been made if a second small barge had been used instead. As a result, the switching decisions remain unchanged in this case, as shown in figure 6.17 and table 6.4.

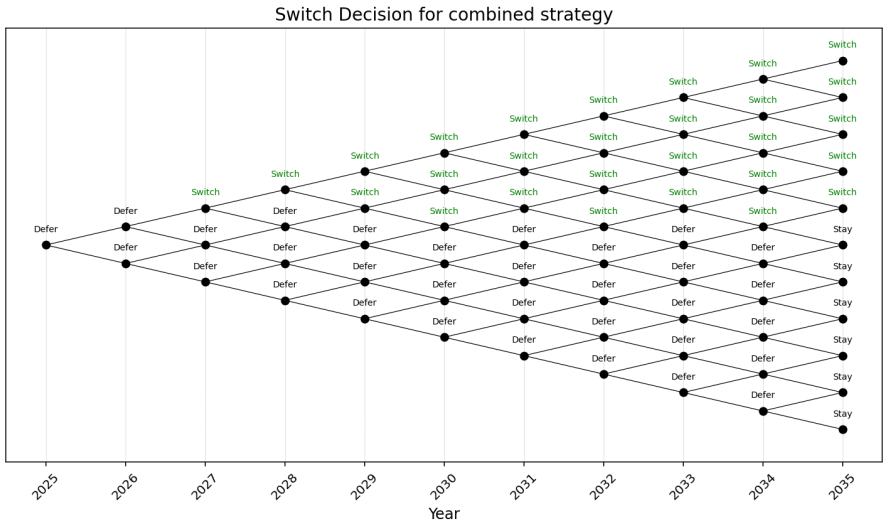

Figure 6.17: Decision lattice for switching to combined strategy.

Table 6.4: The yearly probability of switching for combined strategy.

	2025	2026	2027	2028	2029	2030	2031	2032	2033	2034	2035
Switch probability	0.00	0.00	0.41	0.26	0.55	0.75	0.63	0.78	0.68	0.81	0.73

As previously stated, the outcomes are nearly identical to those obtained for the scenario involving a switch to the CEMT-IVa barge only. For reference, the minimum required CO_2 price to achieve break-even decreases by just €0.02, to €176.17/t.

6.2.5. Sensitivity

As discussed in section 5.2, the binomial parameters used in the real options model are subject to considerable uncertainty due to limited historical data, evolving regulations and technical uncertainties. To assess how input parameters influence the output of the model, a sensitivity analysis is conducted (Van Der Spek et al., 2020). It is essential to note that the sensitivity analysis considers only one parameter at a time and is conducted for the root node only, as this assesses the entire time horizon and saves computational time.

The sensitivity analysis focuses on the mixed transport strategy, as it was shown to generate the highest value in the case study. In addition to the binomial parameters, other factors that may influence the switching decision, such as truck and barge costs, emission factors, and transport distances, are also included in the analysis. The mentioned parameters are varied by ±30% in 5% increments to assess their influence on the total value, option value and the required break-even CO_2 price.

In figure 6.18, the sensitivity of the selected parameters with respect to the option value is shown. It becomes clear that the costs for truck and barge transport, the fleet adoption rate, and the distance of truck transport have the most significant influence on the option value.

The strong influence of transport costs on the option value is intuitive. Truck and barge costs exhibit opposite trends. As barge costs increase, the option value declines and eventually tends to stabilize to -100%, which is expected, as the option value cannot fall below zero. A similar effect is observed when truck costs are decreased. As truck transport becomes significantly cheaper than barge transport, the flexibility to switch becomes redundant, and the option loses its value.

The strong influence of truck transport distance stems from the steep increase in costs associated with longer distances, as explained in section 5.3.1. As a result, higher distances make barge transport relatively more attractive, increasing the value of the switching option. Interestingly, the influence of

barge distance is significantly lower, which is due to the cost structure. Moreover, the absolute cost changes for truck transport are also higher, as the base distance is somewhat greater.

Another factor with considerable impact is the fleet adoption rate. This is reasonable, as a higher initial CO_2 supply results in larger absolute volumes over time. Since supply is multiplied at each time step in the binomial model, this effect compounds, increasing the financial scale and impact of switching decisions. At higher values, the option value increases more steeply, partly due to the ability to switch to larger, more cost-efficient barges.

The growth rate also shows a moderate influence, as it shifts the probabilities in the binomial tree. A higher growth rate increases the probability of moving to the up-states, which tend to add more value as switching becomes more attractive. The other parameters all have minimal influence on the option value, with the emission factors having the lowest impact.

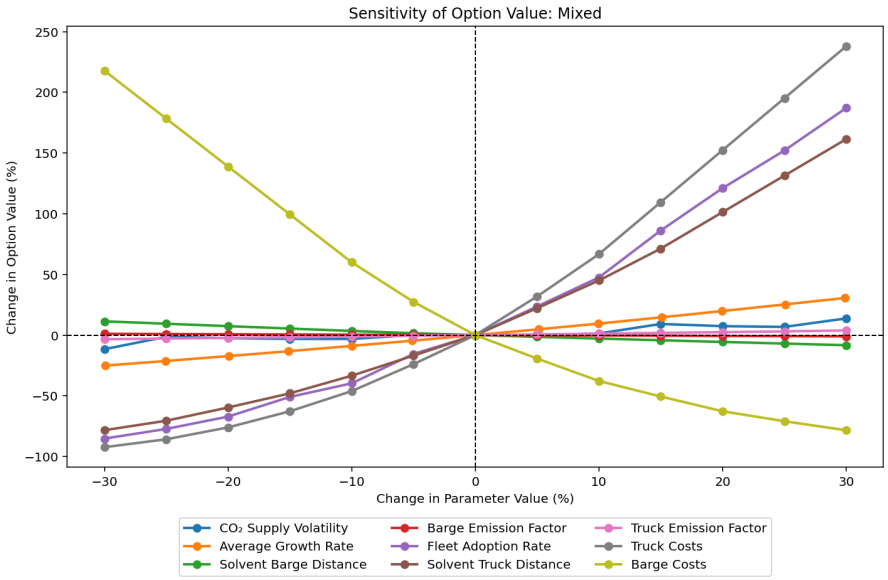

Figure 6.18: Sensitivity analysis with respect to the option value.

The sensitivity analysis for the total value is shown in figure 6.19. An important clarification must be made. As discussed in section 6.2.4, the CO_2 price is insufficient to cover the costs of operating the supply chain. Consequently, the total value remains significantly negative, even when accounting for the added value of the switching option. This situation introduces a complication. Calculating relative changes based on a negative baseline can lead to counterintuitive results in the graphs, as the values may appear inverted. Therefore, the baseline is set as an absolute value.

For the majority of the parameters, the total values do not follow the same trajectory as the option value. This is because changes in parameters also affect the DCF. For example, it cannot be said that if the option value increases 10%, the total value increases 10% as well. As concluded in the previous section, the current CO_2 price is insufficient to cover the costs of the supply chain. Therefore, in some cases, even though the option value increases, the total value decreases.

Among all variables, barge costs have the most significant influence, similar to their effect on the option value. A reduction in barge costs leads to an increase in the total value. Conversely, an increase in barge costs results in a gradual decline in total value. However, this decline is limited. If barge costs rise substantially relative to truck costs, the economic advantage of switching to barge transport diminishes.

The truck-related parameters, costs and solvent transport distances also affect the value but to a lesser extent. The total value also rises if the truck costs decrease, which is logical as the cash flow will increase. The same applies to truck transport distance, as this parameter significantly influences the cost of truck transport. If they increase, the loss in total value is limited to roughly 4%.

This effect is the result of having the option to switch. As truck costs or distances increase, the value of having the option to switch becomes larger. At a certain point, this increase in option value cancels out the additional losses in total value. Further cost increases no longer affect the total value, as the model has already switched. That is why the curve starts to flatten.

A particularly interesting observation is the influence of the fleet adoption rate on the total value. At lower adoption rates, the total value increases. Similarly, when the adoption rate increases with respect to the reference value of 4%, the total value also rises. This seemingly contradictory effect arises because lower adoption levels incur fewer costs. As concluded in section 6.2.4, the CO_2 price is insufficient to cover the full operating costs per ton. As a result, the system appears to perform better in terms of total value, even though this does not reflect actual operational effectiveness. Conversely, at higher adoption rates, the total value also improves, driven by the significant contribution of the option value, as shown in figure 6.18, which helps offset a larger share of the expenses.

The other values have limited influence on the total value and follow the expected trajectories.

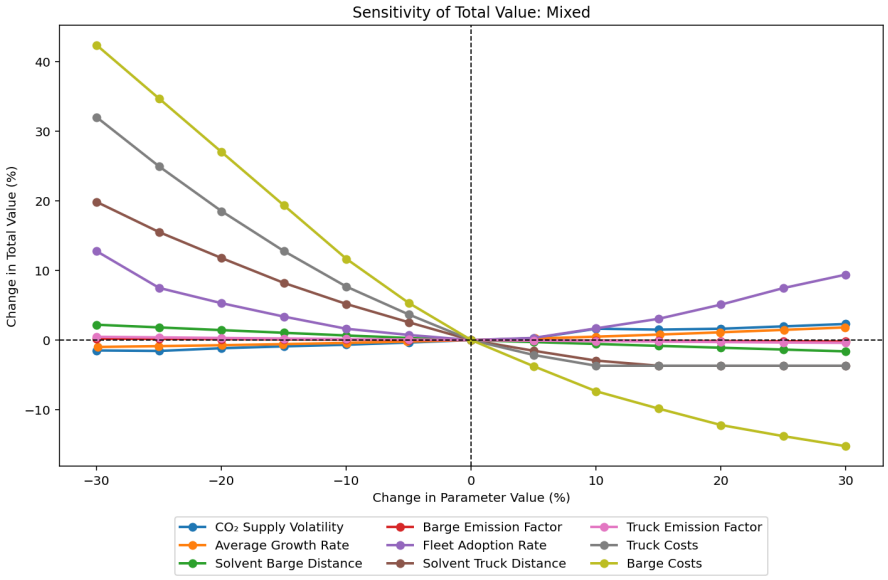

Figure 6.19: Sensitivity analysis with respect to the total value.

Figure 6.20 illustrates how the tested parameters influence the required CO_2 price for achieving break-even at the root node. The reference point is the break-even CO_2 price for the scenario where switching to both barges is possible, which was €176.16 per ton.

Similar to the results for the option value and total value, the fleet adoption rate and transport costs for both truck and barge have the most significant impact on the break-even CO_2 price. Reductions in transport costs and shorter distances lead to lower overall supply chain costs, which in turn reduce the required CO_2 price.

A comparable effect is seen with emission values. As emission factors decrease, the net CO_2 reduction increases, allowing a greater amount to be deducted under the EU ETS, improving the economic feasibility of the system and lowering the required price.

Conversely, a reduction in volatility and growth rate leads to a slight increase in the required CO_2 price. This is attributed to a shift in the probability distribution toward more pessimistic (downward) scenarios. The fleet adoption rate is an influential factor. At first glance, this may appear to contradict the trend observed in figure 6.19. However, this discrepancy can be explained by the fact that lower fleet adoption rates reduce total costs, potentially enhancing overall value. Nevertheless, they also result in a smaller net CO_2 reduction, thereby decreasing the revenue generated from emissions savings. As a result, a higher CO_2 price per ton is required to cover the costs.

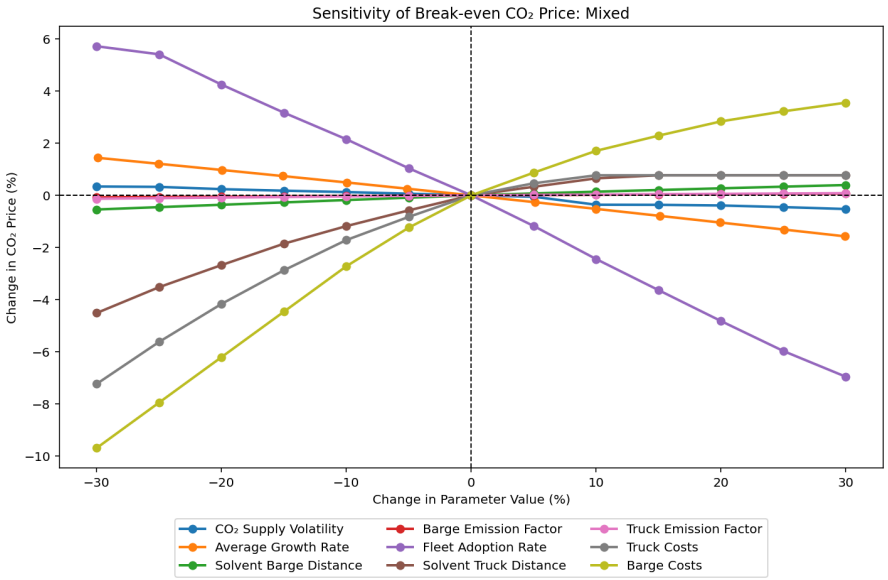

Figure 6.20: Sensitivity analysis with respect to the break-even CO_2 price

6.3. Variable CO_2 price

This section presents the results obtained under a scenario with a variable CO_2 price. As discussed in section 6.2, the average CO_2 price is insufficient to cover the operational costs of the OCCUS supply chain over the entire timeline. Therefore, an alternative, more realistic approach is explored in which the CO_2 price increases over time. The projected trajectory of the CO_2 price is based on the predictions provided by (Bloomberg, 2024). All cost structures will not be discussed further in this section because they remain unchanged.

6.3.1. Truck transport

The DCF for the truck-only transport scenario with increasing CO_2 prices is shown in figure 6.21. Compared to the results in section 6.2.1, it is evident that the DCF turns positive in later years. This shift is primarily driven by the projected rise in P_{CO_2}. The first year a positive DCF is observed is 2031, with a probability of 30%. In this year, the CO_2 price reaches €158.8 €/tCO_2. Although this is still insufficient to fully cover the costs for that year, the expected future prices and transport volumes result in a positive total value. A summary of the annual probability of achieving a positive total value for the truck-only scenario is provided in table 6.5. Additional results, including annual cash flow, transport emissions, and total chain costs, can be found in appendix B.

Table 6.5: The yearly probability of obtaining a positive total value with no option

	2025	2026	2027	2028	2029	2030	2031	2032	2033	2034	2035
Probability Positive total value	0,00	0,00	0,00	0,00	0,00	0,00	0,30	0,94	1,00	1,00	1,00

In many of these future scenarios, a switch to barge transport would already be the preferred option, as will be elaborated further in section 6.3.2. Interestingly, in scenarios with relatively lower supply, some nodes show a small positive DCF, while for the lowest supply scenarios, the DCF remains negative each year. This suggests that a minimum supply threshold may be required for profitability, even under increasing CO_2 prices. Consequently, this implies that volume could influence the overall economic viability. However, when compared to CO_2 flow rates reported in the literature, the volumes considered in this study are relatively small. As a result, the influence of volume on profitability is expected to be limited within the evaluated range of supply.

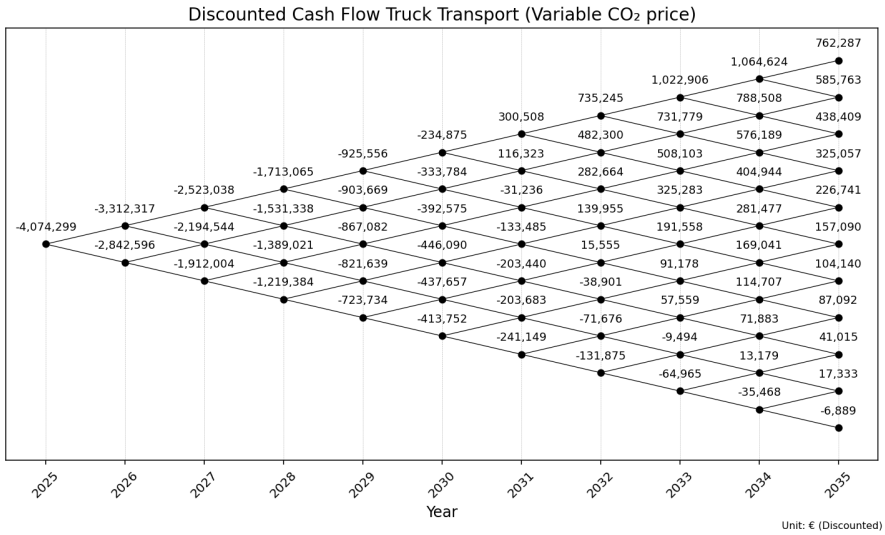

Figure 6.21: Discounted cash flow for truck transport with variable CO_2 price

6.3.2. Option to switch to CEMT-IVa

For the option to switch to the smaller barge, under the variable CO_2 price, the option value at the root node is slightly higher, but only €8000, which is only a very small fraction. For the increased supply volumes, the option values are increased, caused by the combination of higher CO_2 prices and lower relative transport costs increasing the margins. However, it can be seen that variable CO_2 prices, compared to the average value, have limited effect on the option values. As a result, the switching decision at each node is unaffected and remains identical to the results shown in figure 6.9.

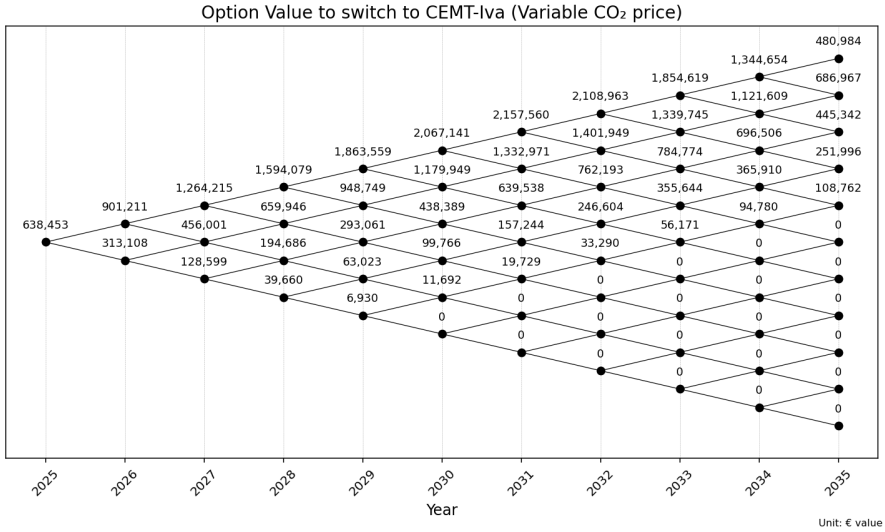

Figure 6.22: Option value with option to switch to CEMT-IVa barge under increasing CO_2 price

The DCF for the strategy with the option to switch to CEMT-IVa under variable CO_2 prices is shown in figure 6.23. Compared to the results with an average CO_2 price, some minor differences are visible. Although increasing future CO_2 prices indicate that supply chain operations become economically viable in later years, the total value at the root node is €180000 lower compared to the average price scenario. This is primarily attributed to the substantially lower CO_2 prices in the initial years, which results in significant losses. Moreover, these early years have a greater influence on the root node value due to the weighted average of different outcomes. Consequently, while the switching option provides strategic flexibility, the early losses significantly reduce the overall value.

Comparing the results to the truck-only case presented in section 6.3.1, analysis reveals significant improvements. Incorporating the option to switch to smaller CEMT-IVa barges accelerates the achievement of economic viability by two years, with a positive expected total value first occurring in 2029. In this year, two economically viable scenarios emerge with a combined probability of 55%. By 2031, the probability of achieving positive total value exhibits substantial improvement, increasing from 30% in the truck-only scenario to 87% with the switching option. In subsequent years, CO_2 prices reach sufficient levels to exceed the economic threshold for truck transport operations. Consequently, the probability of attaining a positive total value stabilizes and becomes independent of transport mode selection. The overall probabilities of achieving positive values with the option to switch to CEMT-IVa barge are summarized in table 6.6. Additional results, including annual cash flow, transport emissions, and total chain costs, can be found in appendix C.

Table 6.6: The yearly probability of obtaining a positive total value with option to switch to CEMT-IVa

	2025	2026	2027	2028	2029	2030	2031	2032	2033	2034	2035
Probability Positive total value	0.00	0.00	0.00	0.00	0.55	0.75	0.87	0.94	1.00	1.00	1.00

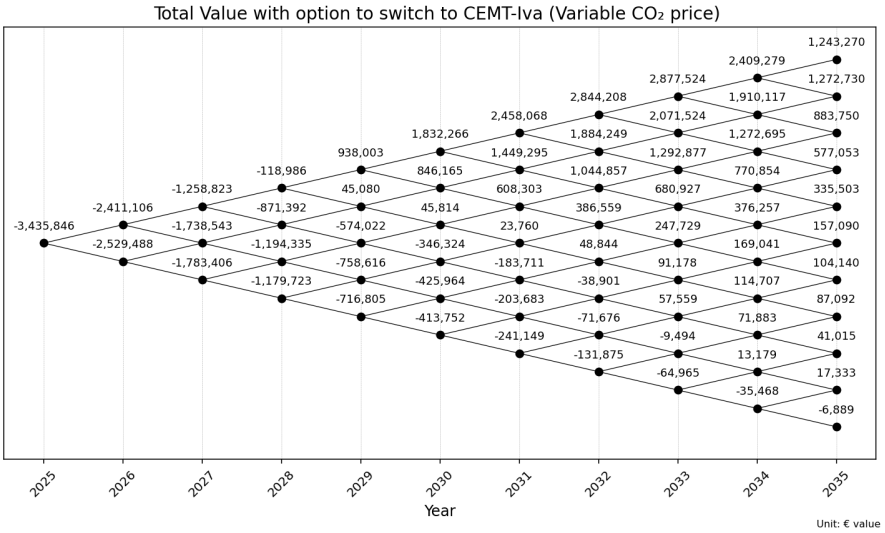

Figure 6.23: Total value with option to switch to CEMT-IVa barge under variable CO_2 price

6.3.3. Option to switch to CEMT-Va

The option values under variable CO_2 pricing with the possibility to switch to the larger CEMT-Va barge are presented in figure 6.24. The findings are consistent with those observed in the CEMT-IVa barge analysis presented in section 6.3.2. Overall, the option values exhibit a modest increase due to cost reductions achieved through CEMT-Va barge deployment at larger volumes, which generates increased revenue and profitability under elevated CO_2 price scenarios. Given the marginal differences in option values, the switching decision lattice remains unchanged.

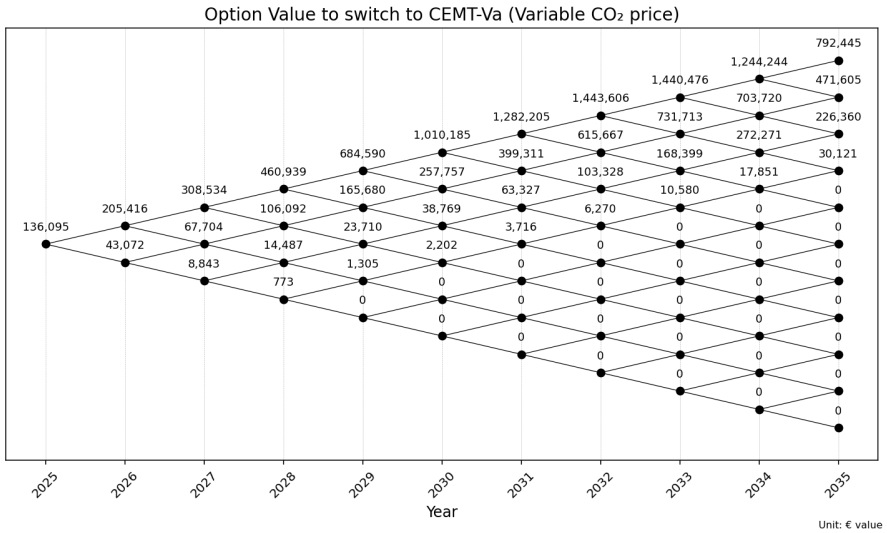

Figure 6.24: Option value with option to switch to CEMT-Va barge under variable CO_2 price

The total values of switching to the larger barge are presented in figure 6.25. These results show similar trends to those observed for the smaller CEMT-IVa barge under the increasing CO_2 price scenario. In this scenario, the total value at the root node is €185000 lower compared to the average CO_2 price case. The difference is slightly higher compared to the smaller CEMT-IVa cases. The larger difference is primarily due to lower option values, as the potential gains from deploying the larger barge are less. Furthermore, the lower total value relative to the average price scenario is also influenced by reduced CO_2 prices in the early years, which lead to increased negative cash flows and, consequently, a lower overall value.

The first year in which a positive total value can be achieved is 2030, with a modest probability of 11%. A positive value is reached one year later compared to the smaller barge case but one year earlier than in the truck-only scenario, although the probability remains lower than in both other cases. In the following year, the probability of attaining a positive value increases to 63%, which is almost double compared to the truck-only scenario. However, it remains lower compared to the smaller barge scenario. In the final years, the probability of attaining positive values reaches 100%, which aligns with the previous cases caused by the high CO_2 price levels. The overall probabilities of achieving positive values with the option to switch to CEMT-Va barge are summarized in table 6.7. Additional results, including annual cash flow, transport emissions, and total chain costs, can be found in appendix D.

Table 6.7: The yearly probability of obtaining a positive total value with option to switch to CEMT-Va

	2025	2026	2027	2028	2029	2030	2031	2032	2033	2034	2035
Probability Positive total value	0.00	0.00	0.00	0.00	0.00	0.11	0.63	0.94	1.00	1.00	1.00

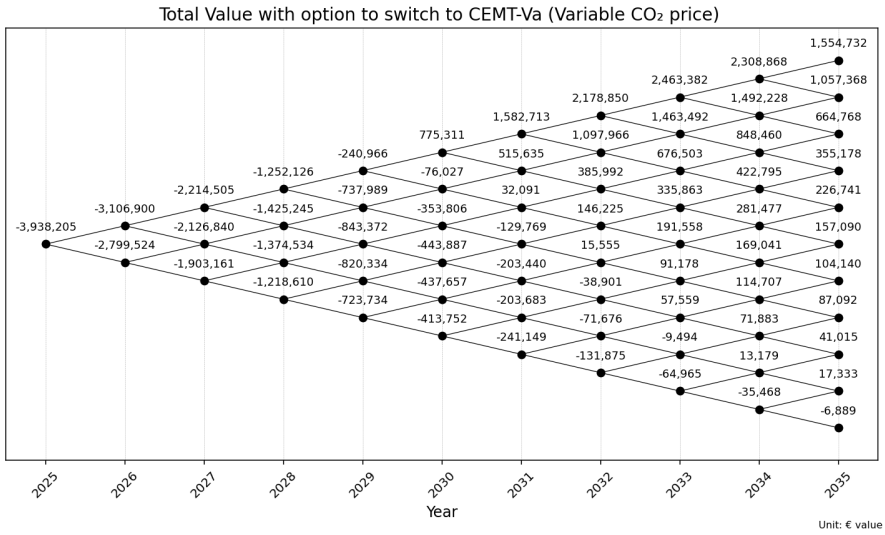

Figure 6.25: Total value with option to switch to CEMT-Va barge under variable CO_2 price

6.3.4. Option to switch to combined strategy

The results for deploying the combined strategy under the variable CO_2 price scenario are presented in this subsection. As the results for this switch option were found to be almost identical to those for the CEMT-IVa barge in the average price scenario, they are expected to be the same in this case.

This is confirmed in figure 6.26, which shows the option values of the combined barge option under increased CO_2 pricing. In section 6.2.4, it was elaborated that only for the top node the larger barge would be deployed. Due to the low probability of reaching this scenario, the value added is limited. For the variable CO_2 price scenario, this remains unchanged. Therefore, the results follow a similar trend.

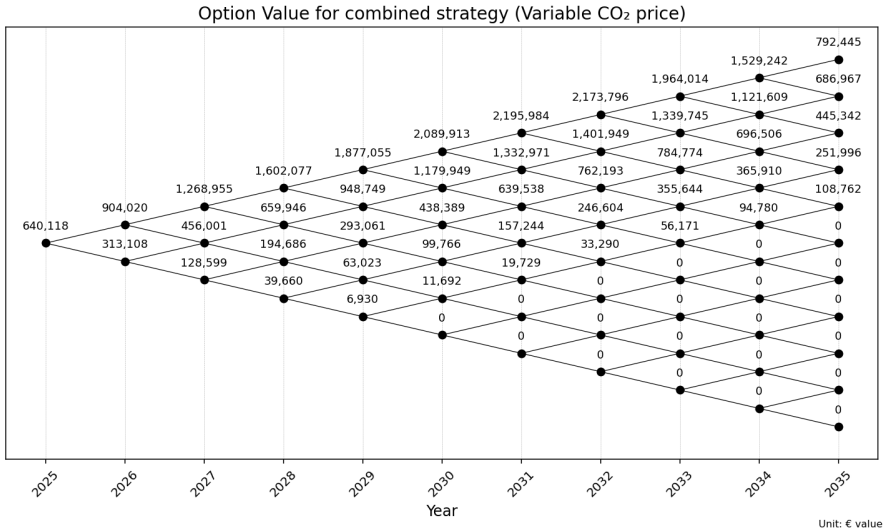

Figure 6.26: Option value with option to switch to combined strategy under variable CO_2 price

The total values are presented in figure 6.27. In this scenario, the results closely align with those of the CEMT-IVa option. Compared to the average price scenario, the total value at the root node is reduced due to the factors previously discussed. Nonetheless, the total value at the root node is marginally higher due to the deployment of a larger barge at the highest supply node, which leads to additional value. However, due to the low associated probability (p = 1.15%) this incremental value is very limited at the root node. The yearly probability of achieving a positive total value remains unaffected and

is equal to the presented results in table 6.6, as the switching decisions remain unchanged. Additional results, including annual cash flow, transport emissions, and total chain costs, can be found in appendix E.

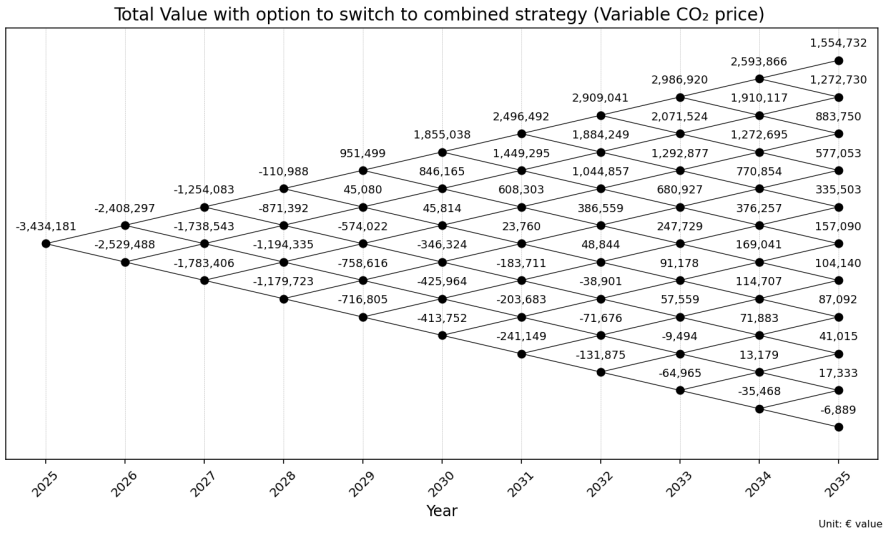

Figure 6.27: Total value with option to switch to a combined strategy under variable CO_2 price

6.3.5. Sensitivity

To assess the influence of the different parameters with a variable CO_2 price, the sensitivity analysis done in section 6.2.5 is repeated in this section. For this sensitivity analysis, the influence of the minimum required CO_2 price is excluded because this is only dependent on the cost structures and not the actual CO_2 price.

In section 6.3, the presented results revealed that the difference in the option value between average and variable CO_2 prices are minimal. Therefore, it is expected that the sensitivity results for the variable are similar to the ones obtained in section 6.2.5.

The sensitivity analysis for the option value is shown in figure 6.28. Comparing them with the average price scenario confirms that the results are identical to figure 6.18.

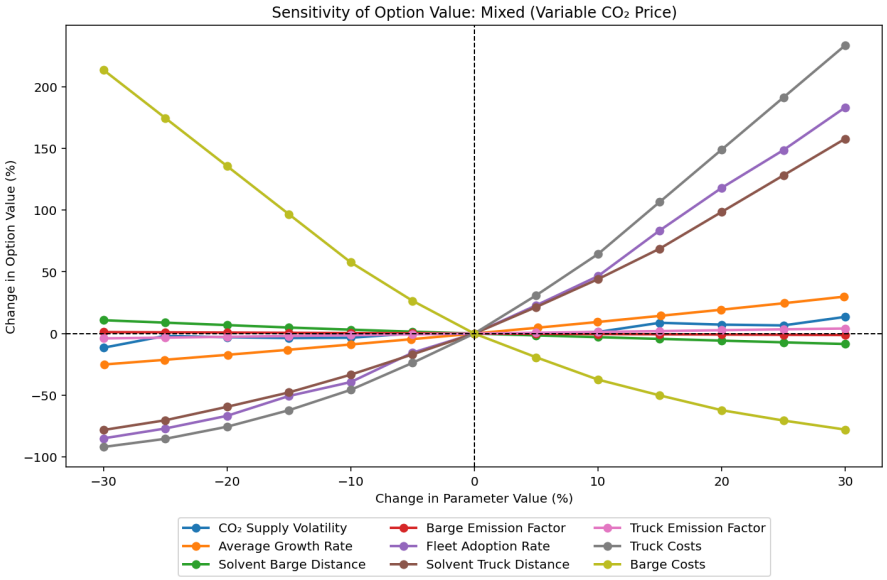

Figure 6.28: Sensitivity analysis with respect to the option value with variable CO_2 price.

The results of the sensitivity analysis with respect to the total value are presented in figure 6.29. Overall, the outcomes closely align with previous findings and exhibit similar trends as observed in the average price scenario. However, one notable difference is visible. The slope of the growth rate line is steeper under the variable CO_2 pricing scenario, indicating higher sensitivity of the total value to changes in growth rates. Several interconnected factors can explain this increased sensitivity. Under variable CO_2 pricing, the total value becomes positive in upward nodes, and as the growth rate increases, the probability of reaching these favourable upward states also increases. Additionally, option values showed modest increases in higher supply nodes compared to the average scenario due to improved margins from higher CO_2 prices.

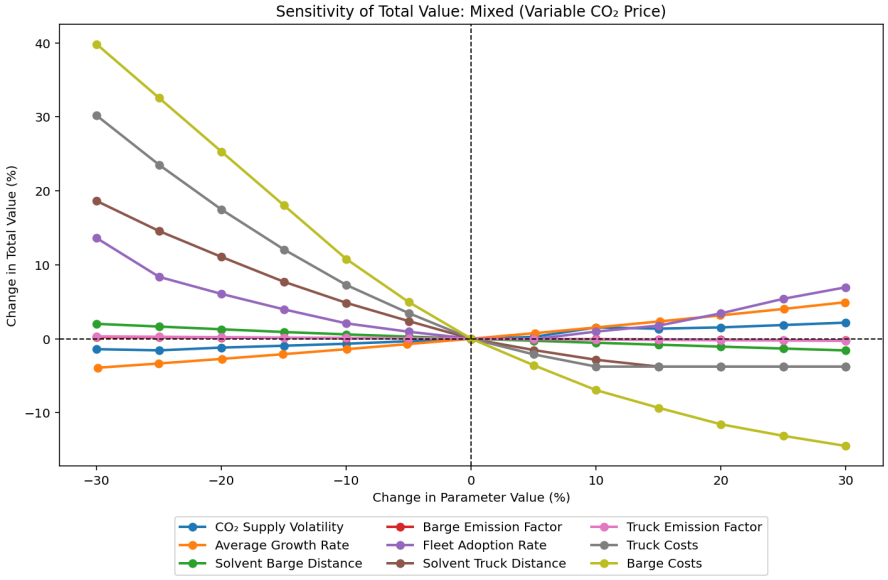

Figure 6.29: Sensitivity analysis with respect to the total value with variable CO_2 price.

6.4. Break-even prices

This section presents the minimum CO_2 prices required for the overall OCCUS supply chain to break even. These prices represent the threshold at which deploying OCC becomes economically viable, as the revenue generated is sufficient to cover the full operational costs of the supply chain. To illustrate the impact of flexibility, the break-even prices are shown for both the truck only strategy and the combined transport strategy with the option to switch. The latter, which demonstrated the highest value in the case study, reveals how the threshold price can be lowered with the switching option available.

Figure 6.30 shows the minimum required CO_2 price for the truck only transport strategy. For the upward nodes, the required price gradually decreases from €184.21/tCO_2 to a minimum of €166.02/tCO_2. A slight decrease is also observed for the middle nodes, where the supply returns to its initial value. Several factors cause these reductions. Firstly, the regeneration and liquefaction cost functions incorporate learning rates, which reduce unit costs as cumulative output increases. For the downward nodes, the reverse effect is observed. If supply decreases, the unit costs rise faster than the learning rate can offset, resulting in a higher break-even price.

The rising cost of truck transport due to increased solvent supply does not impact the upward nodes, as the unit transport costs remain constant. These scenarios still qualify for the bulk discount. However, a slight increase in the minimum required CO_2 price is visible if the CO_2 supply decreases in the following year. For the lowest supply node in 2034 and the two lowest supply nodes in 2035, a notable jump is visible. This is because the supply volume in those cases falls below the threshold required to trigger the bulk discount, resulting in higher unit transport costs.

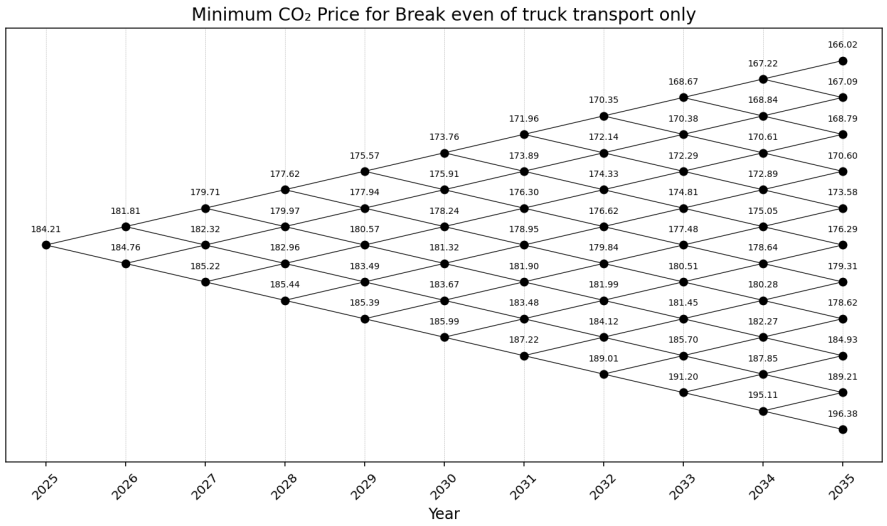

Figure 6.30: Break-even CO_2 price for truck transport only

In Figure 6.31, the minimum required CO_2 price is presented, including the option to switch to a combined transport strategy. It is important to note that all costs, except for the solvent transport, are held constant. Therefore, any differences in the minimum required CO_2 price presented in figure 6.30 can be attributed solely to the option value of incorporating barge transport.

The results show that the option to switch does reduce the minimum required CO_2 price. For the root node, the break-even price decreases by approximately €8 per tonne, representing a modest reduction of 4.3%. The downward trend in break-even price, which is also observed in the truck-only scenario, is visible here as well. However, the price decrease is larger compared to the truck-only case, highlighting that the option does indeed lower the required price as expected.

For the most probable outcomes in 2035, the results show that the break-even prices with the option are lowered from €170.60 to €152.80 and €173.50 to €164.82. These represent notable reductions of 10% and 6%, respectively. For reference, in the most upward node, the required CO_2 price could decrease up to 17% compared to the truck-only transport.

Notably, there is an increase in the break-even price for the most upward node. As discussed in section 6.2, this increase arises because the larger barge is required to transport the total solvent volume in this scenario. As a result, the unit cost of barge transport increases, outweighing the benefits of the learning rate, causing the required price to rise slightly. For the downward nodes, the required CO_2 price equals that of truck-only transport, which is logical as for these supply volumes, switching is not beneficial. Therefore, the option value is zero, adding no extra value.

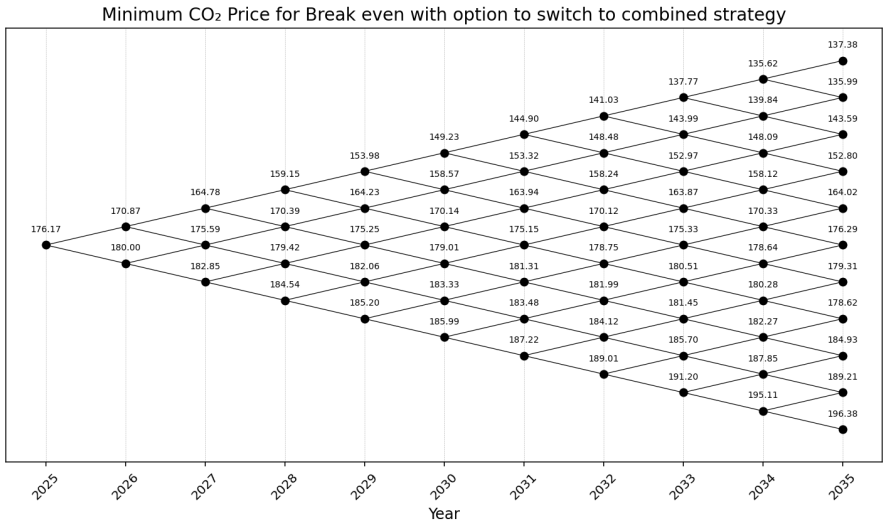

Figure 6.31: break-even CO_2 price with option to switch to combined strategy

6.5. Summary of the results

This section summarizes the key findings and conclusions from the analysed cases and different options presented in this chapter. Table 6.8 presents the break-even prices, option values, and total values at the root node for both average and variable CO_2 pricing scenarios.

The break-even price for the truck-only transport strategy at the root node is €184.21/tCO_2, which exceeds the average CO_2 price of €136/tCO_2 significantly. As demonstrated in Section section 6.4, the break-even price decreases over time, reaching a minimum of €166.02/tCO_2.

The option to switch to barge transport reduces the break-even price to €176.19/tCO_2 for the CEMT-IVa barge, €182.52/tCO_2 for the CEMT-Va barge, and €176.17/tCO_2 for the combined transport strategy. Representing reductions of 4.35 %, 0.92%, and 4.36%, respectively, compared to the truck-only scenario.

The option values at the root node are €630345 for the CEMT-IVa barge and €131,555 for the CEMT-Va barge. The combined strategy yields the highest option value of €632010, representing only a marginal 0.3% improvement over the smaller barge option. The variation in option values between average and variable pricing scenarios is minimal.

With an average CO_2 price of €136/tCO_2, all scenarios generate negative total values, indicating insufficient economic viability. Similarly, the variable increasing CO_2 price scenario also yields negative returns, demonstrating that supply chain operations remain economically unfeasible under current CO_2 supply and pricing.

Table 6.8: Summary of results for the different switch options under average and variable CO_2 pricing for the root node

		Average Price		Variable Price	
Switch option	Break-even price	OV	TV	OV	TV
Truck-only	€ 184.21	-	-€ 3,884,806	-	-€ 4,074,299
CEMT-Iva	€ 176.19	€ 630,345	-€ 3,254,461	€ 638,453	-€ 3,435,846
CEMT-Va	€ 182.52	€ 131,555	-€ 3,753,251	€ 136,095	-€ 3,938,205
Combined	€ 176.17	€ 632,010	-€ 3,252,796	€ 640,118	-€ 3,434,181

Table 6.9 presents the annual probabilities of implementing the transport mode switching decision. The CEMT-IVa barge option demonstrates initial viability in 2027 with a switching probability of 41%, subsequently fluctuating between this baseline and a maximum probability of 81%.

In contrast, the CEMT-Va barge option is triggered later, with the first switching decision in 2030 at a probability of 11%. This option shows lower overall switching frequencies, reaching a maximum probability of 49%. The combined transport strategy yields identical switching probabilities to the CEMT-IVa barge configuration.

Table 6.9: Summary of switch probabilities for the different options

Year	2025	2026	2027	2028	2029	2030	2031	2032	2033	2034	2035
CEMT-IVa	0.00	0.00	0.41	0.26	0.55	0.41	0.63	0.51	0.68	0.81	0.73
CEMT-Va	0.00	0.00	0.00	0.00	0.00	0.11	0.07	0.22	0.15	0.31	0.49
Combined	0.00	0.00	0.41	0.26	0.55	0.41	0.63	0.51	0.68	0.81	0.73

The probabilities of achieving positive economic value under average CO_2 pricing conditions are presented in table 6.10, revealing that the truck-only transport strategy and CEMT-Va barge option have zero probability of positive values across all analysed scenarios and time periods. The CEMT-IVa barge and combined transport strategies demonstrate limited viability, with positive value probabilities of 2% in 2034 and 6% in 2035. These low probabilities indicate that achieving economic viability under this average CO_2 pricing conditions is unlikely.

Table 6.10: Summary of positive value probabilities for the different options with average CO_2 price

Year	2025	2026	2027	2028	2029	2030	2031	2032	2033	2034	2035
Truck	0.00	0.00	0.00	0.00	0.00	0.00	0.00	0.00	0.00	0.00	0.00
CEMT-Iva	0.00	0.00	0.00	0.00	0.00	0.00	0.00	0.00	0.00	0.00	0.06
CEMT-Va	0.00	0.00	0.00	0.00	0.00	0.00	0.00	0.00	0.00	0.00	0.00
Combined	0.00	0.00	0.00	0.00	0.00	0.00	0.00	0.00	0.00	0.02	0.06

The probabilities of achieving positive economic value under variable increasing CO_2 pricing conditions are presented in Table table 6.10. The truck-only strategy provides a 30% probability of positive values starting from 2031. Having the option to switch to either the small CEMT-IVa or combined strategy increases both probability and advances the timing by two years to achieve positive values. For the larger barge, the probability of achieving a positive value occurs one year later than the CEMT-IVa option and at a lower probability. However, this is still a year earlier than the truck-only strategy. From 2032 onward, the probability of achieving positive value becomes equivalent across all transport options. In the final years of the analysis period, all scenarios yield positive values, indicating that the switching option and expected supply levels no longer influence economic viability if CO_2 prices reach levels sufficient to cover even the higher costs of the truck-only strategy. The results suggest that while current deployment timing is premature, economic viability could emerge in future years under conditions of increased supply and CO_2 pricing. The availability of barge transport options reduces the time required to achieve this viability.

Table 6.11: Summary of positive value probabilities for the different options with variable CO_2 price

Year	2025	2026	2027	2028	2029	2030	2031	2032	2033	2034	2035
Truck	0.00	0.00	0.00	0.00	0.00	0.00	0.30	0.94	1.00	1.00	1.00
CEMT-IVa	0.00	0.00	0.00	0.00	0.55	0.75	0.87	0.94	1.00	1.00	1.00
CEMT-Va	0.00	0.00	0.00	0.00	0.00	0.11	0.63	0.94	1.00	1.00	1.00
Combined	0.00	0.00	0.00	0.00	0.55	0.75	0.87	0.94	1.00	1.00	1.00

7

Discussion

In this chapter, a reflection is provided on the methodology, the proposed model, and the underlying assumptions and simplifications adopted throughout this study. The aim is to critically evaluate the robustness and applicability of the modelling approach and to discuss the implications of key results. By addressing both the strengths and limitations of this research, this discussion provides context for interpreting the findings and their relevance to the broader field of OCCUS supply chains.

7.1. Assumptions

To simplify the model, and due to the lack of available data, some assumptions were required, which influence the results.

First of all, this study assumes that the choice of onboard storage method has limited to no influence on the results. For instance, as discussed in section 2.4, truck transport can be done using either ISO containers or dedicated trucks, while barge transport may employ chemical barges or, in the case of containerized storage, container barges. However, in the model, only fully containerized truck transport and dedicated barge transport are compared. In reality, the supply chain is likely to involve a mix of these approaches, with some vessels storing CO_2 in containers onboard and others using dedicated tanks, depending on vessel type and size. Offloading procedures also differ. Containerized CO_2 would require cranes, while dedicated tanks would require pumping operations. These operational differences could influence the relative attractiveness of each transport option. For example, if offloading containers is significantly easier or faster, it might make truck transport more favourable, even if the overall supply volume would justify a switch to barge transport.

To estimate the initial supply, a ship database from a different research project is used. The database consists of vessels considered suitable for using ammonia as a marine fuel. According to current research, large seagoing vessels of at least 50,000 DWT are regarded as likely candidates for ammonia adoption Boersma (2024). These, however, are not necessarily the most suitable vessel types for installing and operating OCC systems. Due to the lack of more specific data, it was assumed in this study that these vessels would be equipped with OCC systems. To account for this uncertainty, a conservative fleet adoption rate of only 4% and a fixed carbon capture rate of 40% were applied. As demonstrated in figure 6.20, the initial supply influences both the total value and the option value in the model. Therefore, obtaining more accurate data on suitable vessels could further improve the reliability of the results.

Another important assumption in the model is that the supply of solvent is evenly distributed on a weekly basis. In reality, the supply is likely to fluctuate, as ship arrivals can vary significantly from week to week. Some weeks may experience a surge in arrivals and thus increased supply, while other weeks may see fewer ships and lower supply levels. This variability is not accounted for in the model, which assumes a homogeneous weekly supply. As a result, the model may overlook operational challenges related to fluctuating supply. In addition, it is assumed that transport capacity for both barges and trucks is always available to meet demand. While this is a reasonable assumption for barges due to their larger

capacities and scheduled operations, it may not hold for trucks. As supply increases, the required number of trucks may exceed what is readily available, potentially leading to logistical bottlenecks or increased transport costs due to limited capacity. By assuming uniform supply distribution and constant transport availability, the model does not account for temporary storage requirements to manage supply fluctuations. In reality, storage capacity may be necessary during periods of supply-demand imbalances or transport limitations.

In this study, fixed emission factors were assumed for both truck and barge transport. The available data indicate that the emission factor for truck transport is double that of barge transport. This assumption is more reliable for trucks because each truck carries a relatively small load, and unit emissions remain roughly constant regardless of whether the truck is fully or partially loaded. As a result, the unit emissions do not vary significantly for truck utilization. This assumption may be less accurate for the use of barges. Barges have a much larger transport capacity, and their unit emissions are likely to decrease when operating at full capacity. When barges are only partially loaded, unit emissions increase. Therefore, assuming a fixed emission factor may underestimate the efficiency gains achievable with higher barge utilization. Although the sensitivity results indicate that emission factors have limited influence on the option value, incorporating more precise emission data could improve the overall accuracy of the model.

In the model, both a fixed average CO_2 price and a variable, linearly increasing CO_2 price scenario (from the current market price to the projected 2035 price) are considered. In reality, the CO_2 price is relatively volatile with peaks and troughs. The use of yearly time intervals may justify this simplification to some extent, as it reflects longer-term investment horizons. However, in practice, supply chain operations are conducted continuously throughout the year, and substantial short-term price fluctuations could affect cash flow and the timing of operational decisions. However, since the supply chain operates continuously, fluctuations in CO_2 price could impact cash flow. There may be periods when operating the supply chain is profitable, while at other times, operation is less or not viable.

Lastly, in this research, it is assumed that regulatory factors and changes in legislation do not directly influence the outcomes of the model. The analysis does not account for the potential impact of new or evolving regulations, such as stricter emission limits or adjustments in CO_2 pricing mechanisms. In reality, future regulatory or policy developments could have affect the supply of CO_2. For example, new emission regulations could lead to sudden increases of CO_2 supply to the port.

7.2. Model limitations

The first limitation concerns the available data. Although transport companies were willing to provide cost estimates for different transport scenarios, the available data points for various distances and volumes remain relatively limited. Furthermore, the analysis relies on quotes from only one barge company and one truck transport company. As a result, and due to the linearization of these cost estimates, the accuracy for other distances and volumes may be reduced. This limitation is particularly important given that the sensitivity analysis in section 6.3.5 demonstrates that transport costs have a major influence on both the option value and the total value of the supply chain. Therefore, obtaining additional quotes from multiple transport companies and for a broader range of distances and volumes would significantly increase the reliability and robustness of the model results.

A second limitation concerns the chosen modelling approach. Real options theory is primarily developed for evaluating investment decisions, such as whether and when to invest in new or additional capacity. In this study, the real options framework is applied to strategic transport decision-making, with a focus on switching between transport modes based on provided cost data. However, since no investment data was available and penalties for contractual constraints for switching are not included, the model may not fully capture the complexities of real-world decision making. As a result, the analysis may overestimate the flexibility and economic attractiveness of switching transport modes, particularly in scenarios where additional costs or operational barriers would exist in practice.

A third limitation relates to the modelling approach of supply growth and uncertainty over time. The future evolution of CO_2 supply in the model is predicted by binomial parameters, which rely on historical data or expert opinions. As carbon capture in general, and especially OCC is not yet commonly applied, such historical data is not present. Besides, it is difficult for experts to make proper predictions

on expected captured CO_2 by maritime vessels into a port. Because of these two reasons, it could be argued that the chosen modelling approach is not the most suitable for realistically representing expected CO_2 supply growth.

Another limitation is that the model is developed for a single collection point within one port. In practice, ports often have multiple collection locations or more complex transport networks that involve various routes and combinations of transport. While the general methodology could be extended to other ports or more complex supply chains, this would require additional data and model adaptations.

Furthermore, the model is designed for an OCCUS supply chain configuration that follows the Value Maritime OCC capture approach. It could, in theory, be adapted to conventional OCCUS chains by following the steps described in DNV (2024). For example, the first transport step could be updated by sourcing new quotes for LCO_2 transport or by incorporating the transport model as outlined in Oeuvray et al. (2024). Users could also be given the option to select between LCO_2 transport or their own received quotes. In adapting the model for conventional CCUS, the regeneration costs would need to be set to zero, and a reconditioning module added in place of liquefaction. However, such modifications would make direct comparisons with the Value Maritime philosophy, and the current exclusion of OCC costs unfair. In the conventional OCC systems, liquefaction and regeneration occur on a smaller scale onboard, meaning the costs are shifted to a different part outside the scope of the model. As a result, assessing the flexibility of transport options using the break-even price could yield unrealistic values, limiting the comparability and practical relevance of the results.

7.3. Results

The results presented in chapter 6 require further critical analysis regarding their alignment with industry expectations. The total captured CO_2 and required solvent volumes are illustrated in figures 6.1 and 6.2, respectively. These projections indicate that under maximum supply scenarios, CO_2 supply would triple over the 10-year period based on the calculated binomial parameters. For the most probable outcomes, CO_2 supply increases but remains below a doubling of supply. These findings do not align with Value Maritime's projected growth expectations. They indicate that a tripling of CO_2 supply is a realistic scenario but believe it has a significantly higher probability than the 1.15% estimated in this analysis, suggesting that the current modelling approach may underestimate such outcomes.

These discrepancies raise questions regarding the model's capacity to accurately represent expected CO_2 supply growth. If tripling supply would be a more likely outcome as suggested by industry projections, the required volatility parameter would approach 30% with growth rates of approximately 15%. These values substantially exceed the calculated parameters and may not reflect realistic supply volatility expectations in practice.

The observed discrepancies between modelled outcomes and Value Maritime expectations suggest that alternative modelling frameworks might be required to capture the complex dynamics of maritime CO_2 supply growth more accurately or redefine the binomial parameters such that these values would be realistic.

If CO_2 supply trajectories align with Value Maritime's projections, the switching option would likely generate substantially higher economic value, given that significant value was added even under modest supply increases. Under such elevated volume scenarios, the CEMT-Va barge configuration would likely become more economically favourable due to its higher transport capacity.

8

Conclusion and recommendations

This chapter presents the final conclusions and recommendations. Firstly, in section 8.1, the research questions are revisited and answered using the obtained results, with each answer referenced to the corresponding section of the report for further detail. Following the conclusions, recommendations are provided in section 8.2

8.1. Conclusions

In chapter 1, the research questions were presented. To provide a structured answer to the main research question, each sub-question will be answered first:

1: What are the required steps, technologies, and sources of uncertainty associated with OCCUS supply chains?

The answer to this question is provided in chapter 2. The exact steps and technologies in the OCCUS supply chain depend on the type of carbon capture system and onboard storage method selected. In general, a carbon capture system, a regeneration and liquefaction system, transportation, and an outlet are required at a minimum. In this research, the supply chain steps are defined as follows: CO_2 is captured onboard using a post-combustion solvent-based system and temporarily stored in the solvent under ambient conditions. Upon arrival in port, the solvent is offloaded and transported by truck or barge to a conditioning facility, where the CO_2 is regenerated, liquefied, and then transported for permanent underground storage, also visualized in figure 2.5. The identified uncertainties are listed in chapter 3. The most important related to this study are the uncertainties in CO_2 supply, transport network design, and the costs associated with CCUS supply chains.

2: How have previous studies modelled OCCUS supply chains, and what methodologies have been used to incorporate uncertainty in CO_2 supply?

This research question is addressed in the literature review presented in chapter 3. Previous studies have not modelled uncertainties in OCCUS supply chains, revealing a clear research gap. As a result, the focus was shifted to land-based CCUS supply chain modelling, where two main approaches were identified: MILP combined with discrete scenarios for supply chain optimization, and RO for capturing decision making flexibility under uncertainty. For this research, RO analysis was chosen as it best aligns with the need to evaluate the value of transport mode flexibility with respect to uncertain CO_2 supply. The binomial lattice tree method was identified as the most suitable valuation method due to its intuitive structure and ease of interpretation.

3: Which parameters and criteria are needed to evaluate the influence of flexibility on the economic and environmental aspects of OCCUS supply chains?

This research question consists of two parts. The required economic and environmental input parameters are listed below the equations in chapter 4, while the actual input values are presented in chapter 5. To evaluate the influence of flexibility, the key economic criterion is the option value, which quantifies the added value of having the option to switch to different transport modes. To determine the overall feasibility of the OCCUS supply chain, the total value and break-even CO_2 price are considered.

4: What is the synthesis of a model that evaluates transport mode flexibility in glsoccus supply chains under uncertain CO_2 supply?

This research question is addressed in chapter 4. Based on the conclusions from the literature review, a binomial lattice tree real options model was developed to represent how the CO_2 supply to the port evolves yearly over time. Using this model, total yearly costs and emissions are calculated based on data from the literature and industry quotes. The main outputs of the model are the total value, option value, and break-even CO_2 prices, which together form the basis for the feasibility assessment.

5: How can the impact of transport mode switching flexibility on economic and environmental feasibility of OCCUS supply chains be demonstrated through a case study?

This research question is addressed by the case study presented in chapter 5, which models the OCCUS supply chain for a sample fleet delivering CO_2-rich solvent to the Port of Rotterdam. The study considers two scenarios: an average CO_2 price and a variable CO_2 price. Different transport strategies are evaluated, with truck-only transport serving as a baseline. Three different switch options are considered: switching to a small CEMT-Iva barge, switching to a larger CEMT-Va barge, and switching to a combination of both.

Having addressed each of the sub-research questions, it is now possible to answer the main research question of this research.

Main Research question:
How does transport mode flexibility affect the economic and environmental feasibility of onboard carbon capture utilization and storage supply chains during the early implementation phase under uncertain CO_2 supply to a port?

Based on the results, the following answer to the main research question is formulated:

Under average CO_2 price of €136 t/CO_2, the truck-only and CEMT-Va barge strategies show no economic viability, while the CEMT-IVa and combined transport strategies demonstrate minimal potential, with low probabilities of positive value. Just 2% in 2034 and 6% in 2035. This indicates that the CO_2 price is insufficient to cover the costs of operating the OCCUS supply chain. However, the option adds €630345 to the root node for CEMT-Iva barge, €131555 for the CEMT-Va barge and €632010 to the combined strategy. Highlighting that the option to switch does add value. However, from an overall economic perspective, it would not make sense to start operating the OCCUS supply chain.

Under the variable CO_2 price scenario, the option values remain almost similar. However, the total value at the root node remains negative for all cases, highlighting that OCCUS operations in the coming years are not yet viable. The truck-only strategy achieves a positive total value starting in 2031, with a probability of 30%. Introducing the option to switch to the CEMT-Iva barge improves both timing and probability, allowing a positive value in 2029, with a 55% probability. The CEMT-Va barge underperforms relative to the smaller barge, with a positive total value reached only in 2030 and a lower probability of only 11%, indicating delayed and less frequent switching. The combined strategy offers only marginal value compared to the CEMT-Iva switch option, as the larger barge is only deployed in the highest supply scenario, an unlikely event with a 1.15% probability only. Resulting in negligible overall impact.

For the truck-only case, the minimum required CO_2 price at the root node is €184.21/t. Introducing the option to switch to CEMT-Iva lowers this to €176.19/t (–4.35%). Switching to the CEMT-Va barge reduces it slightly to €182.52/t (-0.92%). The combined strategy achieves the lowest break-even price of €176.17/t (–4.36%), though this represents only a minimal improvement over the CEMT-Iva option. These results show that having the option of switching flexibility lowers the break-even CO_2 price.

8.2. Recommendations

Based on the provided conclusions, the following set of recommendations are provided:

- **Recommendation for Policymakers:** The results indicate that a break-even CO_2 price of at least €176.19 per ton is required for OCCUS operations to be viable. To accelerate the adoption of OCCUS, policymakers should ensure that the price or compensation for CO_2 reductions increases more quickly through higher carbon taxes or market mechanisms, as value significantly improves at higher (future) prices.
- **Recommendation for Value Maritime:** It is recommended to deploy barges if CO_2 volumes increase. The tipping point in which barge transport is preferred is relatively quick, supported by the results in chapter 6.

  Although this is not the primary research objective or question, it was found that the regeneration process requires a significant amount of electricity to generate the required heat for solvent regeneration. Due to high energy prices, it is a major contributor to the break-even price. Exploring opportunities to optimise or minimise the required heat supply could significantly enhance overall feasibility.
- **Recommendation for Data Collection:** It is advised to collect more detailed data on the costs of different transport options. As demonstrated in the sensitivity analysis, transport costs have a significant impact on the results. Expanding the dataset will result in more reliable cost functions and outcomes.
- **Recommendation for Model Development:** Currently, the model assesses the solvent transport leg using only truck and barge as transport modes. However, multiple transport options are possible and relevant for future applications. To enhance the model's applicability and flexibility, future development should include additional transport modes.
- **Future research:** In this study, the model was tested using a single set of binomial parameters (initial supply, volatility, and growth rate) based on available historical data. Sensitivity analysis indicates that these parameters have an impact on the option value, total value and required break-even price. Therefore, it is recommended to conduct additional tests with different sets of binomial parameters. For example, by substantially increasing the initial supply and incorporating additional transport modes, future research could explore scenarios in which switching from barge to pipeline transport becomes viable.

  In section 7.3, it was already discussed that the projected CO_2 supply over time does not align with expectations. Therefore, further research is needed on different strategies to predict or redefine the binomial parameters. The lattice tree is a powerful and easy-to-interpret strategy. If better methods could be developed, they could present more accurate results and insights.

References

Aas, K., Skagestad, R., & Mathisen, A. (2024). Full chain cases for SBCC.

ABS. (2024). *Carbon Neutral Fuel Pathways* (tech. rep.).

Agaton, C. B. (2021). Application of real options in carbon capture and storage literature: Valuation techniques and research hotspots. *Science of The Total Environment*, *795*, 148683. https://doi.org/10.1016/j.scitotenv.2021.148683

Al Baroudi, H., Awoyomi, A., Patchigolla, K., Jonnalagadda, K., & Anthony, E. (2021). A review of large-scale CO2 shipping and marine emissions management for carbon capture, utilisation and storage. *Applied Energy*, *287*, 116510. https://doi.org/10.1016/j.apenergy.2021.116510

Arning, K., Offermann-van Heek, J., Linzenich, A., Kaetelhoen, A., Sternberg, A., Bardow, A., & Ziefle, M. (2019). Same or different? Insights on public perception and acceptance of carbon capture and storage or utilization in Germany. *Energy Policy*, *125*, 235–249. https://doi.org/10.1016/j.enpol.2018.10.039

Becattini, V., Riboldi, L., Burger, J., Nöhl, J., Oeuvray, P., Reyes-Lúa, A., Anantharaman, R., Bardow, A., Frattini, L., Fu, C., Mazzotti, M., Roussanaly, S., & Zotică, C. (2024). Rolling-out pioneering carbon dioxide capture and transport chains from inland European industrial facilities: A techno-economic, environmental, and regulatory evaluation. *Renewable and Sustainable Energy Reviews*, *205*, 114803. https://doi.org/10.1016/j.rser.2024.114803

Bennæs, A., Skogset, M., Svorkdal, T., Fagerholt, K., Herlicka, L., Meisel, F., & Rickels, W. (2024). Modeling a supply chain for carbon capture and offshore storage—A German–Norwegian case study. *International Journal of Greenhouse Gas Control*, *132*, 104028. https://doi.org/10.1016/j.ijggc.2023.104028

Bloomberg. (2024, May). EU ETS Market Outlook 1H 2024: Prices Valley Before Rally [Section: Report]. Retrieved April 26, 2025, from https://about.bnef.com/blog/eu-ets-market-outlook-1h-2024-prices-valley-before-rally/

Boersma, F. T. (2024). *Operational Impact of Ammonia as Marine Fuel* [Doctoral dissertation].

Bui, M., Adjiman, C. S., Bardow, A., Anthony, E. J., Boston, A., Brown, S., Fennell, P. S., Fuss, S., Galindo, A., Hackett, L. A., Hallett, J. P., Herzog, H. J., Jackson, G., Kemper, J., Krevor, S., Maitland, G. C., Matuszewski, M., Metcalfe, I. S., Petit, C., … Mac Dowell, N. (2018). Carbon capture and storage (CCS): The way forward. *Energy & Environmental Science*, *11*(5), 1062–1176. https://doi.org/10.1039/C7EE02342A

Buirma, M., Vleugel, J., Pruyn, J., Doedée, V., & Schott, D. (2022). Ship-Based Carbon Capture and Storage: A Supply Chain Feasibility Study. *Energies*, *15*(3), 813. https://doi.org/10.3390/en15030813

BV. (2024). *ONBOARD CARBON CAPTURE AN OVERVIEW OF TECHNOLOGIES TO CAPTURE CO2 ONBOARD SHIPS* (tech. rep.).

Cox, J. C., Ross, S. A., & Rubinstein, M. (1979). Option pricing: A simplified approach. *Journal of Financial Economics*, *7*(3), 229–263. https://doi.org/10.1016/0304-405X(79)90015-1

d'Amore, F., & Bezzo, F. (2017). Economic optimisation of European supply chains for CO 2 capture, transport and sequestration. *International Journal of Greenhouse Gas Control*, *65*, 99–116. https://doi.org/10.1016/j.ijggc.2017.08.015

d'Amore, F., Lovisotto, L., & Bezzo, F. (2020). Introducing social acceptance into the design of CCS supply chains: A case study at a European level. *Journal of Cleaner Production*, *249*, 119337. https://doi.org/10.1016/j.jclepro.2019.119337

d'Amore, F., Mocellin, P., Vianello, C., Maschio, G., & Bezzo, F. (2018). Economic optimisation of European supply chains for CO 2 capture, transport and sequestration, including societal risk analysis and risk mitigation measures. *Applied Energy*, *223*, 401–415. https://doi.org/10.1016/j.apenergy.2018.04.043

d'Amore, F., Natalucci, L., & Romano, M. C. (2024). Optimisation of ship-based CO2 transport chains from Southern Europe to the North Sea. *Carbon Capture Science & Technology*, *10*, 100172. https://doi.org/10.1016/j.ccst.2023.100172

d'Amore, F., Romano, M. C., & Bezzo, F. (2021). Carbon capture and storage from energy and industrial emission sources: A Europe-wide supply chain optimisation. *Journal of Cleaner Production*, *290*, 125202. https://doi.org/10.1016/j.jclepro.2020.125202

Deng, H., Roussanaly, S., & Skaugen, G. (2019). Techno-economic analyses of CO2 liquefaction: Impact of product pressure and impurities. *International Journal of Refrigeration*, *103*, 301–315. https://doi.org/10.1016/j.ijrefrig.2019.04.011

Deutsch, H.-P., & Beinker, M. W. (2019). Binomial and Trinomial Trees. In *Derivatives and Internal Models* (pp. 139–163). Springer International Publishing. https://doi.org/10.1007/978-3-030-22899-6_9

Dixit, A., & Pindyck, R. (1994). Investment Under Uncertainty.

DNV. (2024). *THE POTENTIAL OF ONBOARD CARBON CAPTURE IN SHIPPING* (tech. rep.).

Dziejarski, B., Krzyżyńska, R., & Andersson, K. (2023). Current status of carbon capture, utilization, and storage technologies in the global economy: A survey of technical assessment. *Fuel*, *342*, 127776. https://doi.org/10.1016/j.fuel.2023.127776

Einbu, A., Pettersen, T., Morud, J., Tobiesen, A., Jayarathna, C., Skagestad, R., & Nysæther, G. (2022). Energy assessments of onboard CO2 capture from ship engines by MEA-based post combustion capture system with flue gas heat integration. *International Journal of Greenhouse Gas Control*, *113*, 103526. https://doi.org/10.1016/j.ijggc.2021.103526

Elias, R., Wahab, M., & Fang, L. (2018). Retrofitting carbon capture and storage to natural gas-fired power plants: A real-options approach. *Journal of Cleaner Production*, *192*, 722–734. https://doi.org/10.1016/j.jclepro.2018.05.019

EMSA. (2025). THETIS-MRV. Retrieved April 24, 2025, from https://mrv.emsa.europa.eu/#public/emission-report

European Commission. Joint Research Centre. (2024). *Shaping the future CO2 transport network for Europe.* Publications Office. Retrieved October 21, 2024, from https://data.europa.eu/doi/10.2760/582433

Eurostat. (2024). Electricity price statistics. Retrieved April 26, 2025, from https://ec.europa.eu/eurostat/statistics-explained/index.php?title=Electricity_price_statistics

Faber, J., Meijer, C., & Nelissen, D. (2022). Fit for 55 and 2030 milestones for maritime shipping.

Fan, J.-L., Wei, S., Zhang, X., & Yang, L. (2020). A comparison of the regional investment benefits of CCS retrofitting of coal-fired power plants and renewable power generation projects in China. *International Journal of Greenhouse Gas Control*, *92*, 102858. https://doi.org/10.1016/j.ijggc.2019.102858

Feenstra, M., Monteiro, J., Van Den Akker, J. T., Abu-Zahra, M. R., Gilling, E., & Goetheer, E. (2019). Ship-based carbon capture onboard of diesel or LNG-fuelled ships. *International Journal of Greenhouse Gas Control*, *85*, 1–10. https://doi.org/10.1016/j.ijggc.2019.03.008

Gabrielli, P., Campos, J., Becattini, V., Mazzotti, M., & Sansavini, G. (2022). Optimization and assessment of carbon capture, transport and storage supply chains for industrial sectors: The cost of resilience. *International Journal of Greenhouse Gas Control*, *121*, 103797. https://doi.org/10.1016/j.ijggc.2022.103797

GCMD. (2024). *Concept Study to Offload Onboard Captured CO2* (tech. rep.).

GCMD. (2025, April). IMO MEPC 83 - Two-tier GFI-linked pricing system - Cost and compliance calculator. Retrieved June 19, 2025, from https://www.gcformd.org/imo-mepc-83-two-tier-gfi-linked-pricing-system-cost-and-compliance-calculator/

Gerrits, B., & Blanchard, M. (2023). Senior Finance and European Affairs Manager.

Global CCS Institute. (2024a). *Global Satuts of CCS 2024* (tech. rep.).

Global CCS Institute. (2024b). *STATE OF THE ART: CCS TECHNOLOGIES 2024* (tech. rep.).

Graus, S., Ferreira, T. M., Vasconcelos, G., & Ortega, J. (2024). Changing Conditions: Global Warming-Related Hazards and Vulnerable Rural Populations in Mediterranean Europe. *Urban Science*, *8*(2), 42. https://doi.org/10.3390/urbansci8020042

Gür, T. M. (2022). Carbon Dioxide Emissions, Capture, Storage and Utilization: Review of Materials, Processes and Technologies. *Progress in Energy and Combustion Science*, *89*, 100965. https://doi.org/10.1016/j.pecs.2021.100965

Halili, G. (2025). Searoute: A python package for generating the shortest sea route between two points on Earth.

Hasan, M. F., First, E. L., Boukouvala, F., & Floudas, C. A. (2015). A multi-scale framework for CO2 capture, utilization, and sequestration: CCUS and CCU. *Computers & Chemical Engineering*, *81*, 2–21. https://doi.org/10.1016/j.compchemeng.2015.04.034

Hepburn, C., Adlen, E., Beddington, J., Carter, E. A., Fuss, S., Mac Dowell, N., Minx, J. C., Smith, P., & Williams, C. K. (2019). The technological and economic prospects for CO2 utilization and removal. *Nature*, *575*(7781), 87–97. https://doi.org/10.1038/s41586-019-1681-6

Hillier, F. S., & Lieberman, G. J. (2010). *Introduction to Operations Research* (9th ed.). Retrieved November 21, 2024, from http://pubsonline.informs.org/do/10.1287/0da64ca6-e17a-473d-b876-2df3a5ce2760/full/

Hua, W., Sha, Y., Zhang, X., & Cao, H. (2023). Research progress of carbon capture and storage (CCS) technology based on the shipping industry. *Ocean Engineering*, *281*, 114929. https://doi.org/10.1016/j.oceaneng.2023.114929

IEA. (2019, September). *Putting CO2 to Use: Creating Value from Emmisions* (tech. rep.). IEA. https://iea.blob.core.windows.net/assets/50652405-26db-4c41-82dc-c23657893059/Putting_CO2_to_Use.pdf

IEA. (2020). CCUS in clean energy transitions.

IMO. (2020). *Fourth IMO GHG Study 2020* (tech. rep.).

IMO. (2023). *Annex 15* (tech. rep.).

IMO. (2025). *Draft revised marpol annex vi* (tech. rep.). IMO. London.

ISO. (2024a). NEN-EN-ISO 14040. https://connect.nen.nl/standard/openpdf/?artfile=481642&RNR=109085&token=45bbbdf8-5ba5-423b-8977-a3badc75e825&type=pdf#pagemode=bookmarks

ISO. (2024b). NEN-EN-ISO 14044. https://connect.nen.nl/standard/openpdf/?artfile=481643&RNR=109086&token=016fafbb-e193-4458-a7ef-c4db18611163&type=pdf#pagemode=bookmarks

Jayarathna, C., Mathisen, A., Knudsen, K., Skagestad, R., Eldrup, N. H., & Nysæter, G. (2021). GHG emissions from CO2 ship transportation chain. *SSRN Electronic Journal*. https://doi.org/10.2139/ssrn.3840215

Jensen, E. H., Pedersen, R. C., Løge, I. A., Dlamini, G. M., Neerup, R., Riber, C., Elmegaard, B., Jensen, J. K., & Fosbøl, P. L. (2025). The cost of impurities: A techno-economic assessment on conditioning of captured CO 2 to commercial specifications. *International Journal of Greenhouse Gas Control*, *141*, 104309. https://doi.org/10.1016/j.ijggc.2025.104309

Kim, A. M., & Li, H. (2020). Incorporating the impacts of climate change in transportation infrastructure decision models. *Transportation Research Part A: Policy and Practice*, *134*, 271–287. https://doi.org/10.1016/j.tra.2020.02.013

Kjärstad, J., Skagestad, R., Eldrup, N. H., & Johnsson, F. (2016). Ship transport—A low cost and low risk CO 2 transport option in the Nordic countries. *International Journal of Greenhouse Gas Control*, *54*, 168–184. https://doi.org/10.1016/j.ijggc.2016.08.024

Knoope, M., Guijt, W., Ramírez, A., & Faaij, A. (2014). Improved cost models for optimizing CO2 pipeline configuration for point-to-point pipelines and simple networks. *International Journal of Greenhouse Gas Control*, *22*, 25–46. https://doi.org/10.1016/j.ijggc.2013.12.016

Knoope, M., Ramírez, A., & Faaij, A. (2015). The influence of uncertainty in the development of a CO2 infrastructure network. *Applied Energy*, *158*, 332–347. https://doi.org/10.1016/j.apenergy.2015.08.024

Kossiakoff, A., Sweet, W. N., Seymour, S. J., & Biemer, S. M. (2011). SYSTEMS ENGINEERING PRINCIPLES AND PRACTICE.

Lamberts-Van Assche, H., & Compernolle, T. (2022). Using Real Options Thinking to Value Investment Flexibility in Carbon Capture and Utilization Projects: A Review. *Sustainability*, *14*(4), 2098. https://doi.org/10.3390/su14042098

Lamberts-Van Assche, H., Lavrutich, M., Compernolle, T., Thomassen, G., Thijssen, J. J., & Kort, P. M. (2023). CO 2 storage or utilization? A real options analysis under market and technological uncertainty. *Journal of Environmental Economics and Management*, *122*, 102902. https://doi.org/10.1016/j.jeem.2023.102902

Law, L. C., Gkantonas, S., Mengoni, A., & Mastorakos, E. (2024). Onboard pre-combustion carbon capture with combined-cycle gas turbine power plant architectures for LNG-fuelled ship propulsion.

Applied Thermal Engineering, *248*, 123294. https://doi.org/10.1016/j.applthermaleng.2024.123294

Lee, S.-Y., Lee, I.-B., & Han, J. (2019). Design under uncertainty of carbon capture, utilization and storage infrastructure considering profit, environmental impact, and risk preference. *Applied Energy*, *238*, 34–44. https://doi.org/10.1016/j.apenergy.2019.01.058

Leonzio, G. (2023). Life Cycle Assessment of Carbon Dioxide Supply Chains: State of the Art and Methodology Description. *Applied Sciences*, *14*(1), 385. https://doi.org/10.3390/app14010385

Leonzio, G., Foscolo, P. U., & Zondervan, E. (2019). Sustainable utilization and storage of carbon dioxide: Analysis and design of an innovative supply chain. *Computers & Chemical Engineering*, *131*, 106569. https://doi.org/10.1016/j.compchemeng.2019.106569

Leonzio, G., Foscolo, P. U., & Zondervan, E. (2020). Optimization of CCUS Supply Chains for Some European Countries under the Uncertainty. *Processes*, *8*(8), 960. https://doi.org/10.3390/pr8080960

Lewis, N., & Spurlock, D. (2004). VOLATILITY ESTIMATION OF FORECASTED PROJECT RETURNS FOR REAL OPTIONS ANALYSIS.

Liu, H., Kearns, D., & Consoli, C. (2021). *Technology Readiness and costs of CCS* (tech. rep.).

Liu, J., Zhang, Q., Li, H., Chen, S., & Teng, F. (2022). Investment decision on carbon capture and utilization (CCU) technologies—A real option model based on technology learning effect. *Applied Energy*, *322*, 119514. https://doi.org/10.1016/j.apenergy.2022.119514

Long, N. V. D., Lee, D. Y., Kwag, C., Lee, Y. M., Lee, S. W., Hessel, V., & Lee, M. (2021). Improvement of marine carbon capture onboard diesel fueled ships. *Chemical Engineering and Processing - Process Intensification*, *168*, 108535. https://doi.org/10.1016/j.cep.2021.108535

LR. (2023). *Onboard carbon capture utilisation and storage A readiness assessment for the shipping industry* (tech. rep.).

Luo, X., & Wang, M. (2017). Study of solvent-based carbon capture for cargo ships through process modelling and simulation. *Applied Energy*, *195*, 402–413. https://doi.org/10.1016/j.apenergy.2017.03.027

MacDowell, N., Florin, N., Buchard, A., Hallett, J., Galindo, A., Jackson, G., Adjiman, C. S., Williams, C. K., Shah, N., & Fennell, P. (2010). An overview of CO2 capture technologies. *Energy & Environmental Science*, *3*(11), 1645. https://doi.org/10.1039/c004106h

Madejski, P., Chmiel, K., Subramanian, N., & Kuś, T. (2022). Methods and Techniques for CO2 Capture: Review of Potential Solutions and Applications in Modern Energy Technologies. *Energies*, *15*(3), 887. https://doi.org/10.3390/en15030887

McClarren, R. G. (2018). Closed Root Finding Methods. In *Computational Nuclear Engineering and Radiological Science Using Python* (pp. 215–228). Elsevier. https://doi.org/10.1016/B978-0-12-812253-2.00014-5

McKinnon, P. A., & Piecyk, D. M. (2010). Measuring and Managing CO2 Emissions. *ee*.

Melese, Y., Heijnen, P., Stikkelman, R., & Herder, P. (2015). Exploring for real options during CCS networks conceptual design to mitigate effects of path-dependency and lock-in. *International Journal of Greenhouse Gas Control*, *42*, 16–25. https://doi.org/10.1016/j.ijggc.2015.07.016

Metz, B., Davidson, O., Coninck, H., Loos, M., & Meyer, L. (2005). *CARBON DIOXIDE CAPTURE AND STORAGE* (tech. rep.).

Middleton, R. S., Yaw, S. P., Hoover, B. A., & Ellett, K. M. (2020). SimCCS: An open-source tool for optimizing CO2 capture, transport, and storage infrastructure. *Environmental Modelling & Software*, *124*, 104560. https://doi.org/10.1016/j.envsoft.2019.104560

Moser, P., Wiechers, G., Schmidt, S., Garcia Moretz-Sohn Monteiro, J., Charalambous, C., Garcia, S., & Sanchez Fernandez, E. (2020). Results of the 18-month test with MEA at the post-combustion capture pilot plant at Niederaussem – new impetus to solvent management, emissions and dynamic behaviour. *International Journal of Greenhouse Gas Control*, *95*, 102945. https://doi.org/10.1016/j.ijggc.2019.102945

Mulvey, J. M., Vanderbei, R. J., & Zenios, S. A. (1995). Robust Optimization of Large-Scale Systems. *Operations Research*, *43*(2), 264–281. https://doi.org/10.1287/opre.43.2.264

Myers, C. (1977). DETERMINANTS OF CORPORATE BORROWING.

Myers, C., Li, W., & Markham, G. (2024). The cost of CO2 transport by truck and rail in the United States. *International Journal of Greenhouse Gas Control*, *134*, 104123. https://doi.org/10.1016/j.ijggc.2024.104123

Neele, F., De Kler, R., Nienoord, M., Brownsort, P., Koornneef, J., Belfroid, S., Peters, L., Van Wijhe, A., & Loeve, D. (2017). CO2 Transport by Ship: The Way Forward in Europe. *Energy Procedia*, *114*, 6824–6834. https://doi.org/10.1016/j.egypro.2017.03.1813

Nie, S., Cai, G., He, J., Wang, S., Bai, R., Chen, X., Wang, W., & Zhou, Z. (2023). Economic costs and environmental benefits of deploying CCUS supply chains at scale: Insights from the source–sink matching LCA–MILP approach. *Fuel*, *344*, 128047. https://doi.org/10.1016/j.fuel.2023.128047

Oeuvray, P., Burger, J., Roussanaly, S., Mazzotti, M., & Becattini, V. (2024). Multi-criteria assessment of inland and offshore carbon dioxide transport options. *Journal of Cleaner Production*, *443*, 140781. https://doi.org/10.1016/j.jclepro.2024.140781

Oliveira, A., Couto, G., & Pimentel, P. (2021). Uncertainty and flexibility in infrastructure investments: Application of real options analysis to the Ponta Delgada airport expansion. *Research in Transportation Economics*, *90*, 100845. https://doi.org/10.1016/j.retrec.2020.100845

Osman, A. I., Hefny, M., Abdel Maksoud, M. I. A., Elgarahy, A. M., & Rooney, D. W. (2021). Recent advances in carbon capture storage and utilisation technologies: A review. *Environmental Chemistry Letters*, *19*(2), 797–849. https://doi.org/10.1007/s10311-020-01133-3

Ostovari, H., Müller, L., Mayer, F., & Bardow, A. (2022). A climate-optimal supply chain for CO2 capture, utilization, and storage by mineralization. *Journal of Cleaner Production*, *360*, 131750. https://doi.org/10.1016/j.jclepro.2022.131750

Pimentel, P., Couto, G., Tavares, A., & Oliveira, A. (2021). The impacts of real options analysis on EU co-financing policy: The case of Ponta Delgada Port in the Azores. *Research in Transportation Economics*, *90*, 100977. https://doi.org/10.1016/j.retrec.2020.100977

Port of Rotterdam. (2024). *Havenbedrijf Rotterdam - Jaarverslag 2023* (tech. rep.).

Port of Rotterdam. (2025). *Jaarverslag2024 Port of Rotterdam* (tech. rep.).

Rafiee, A., Rajab Khalilpour, K., Milani, D., & Panahi, M. (2018). Trends in CO2 conversion and utilization: A review from process systems perspective. *Journal of Environmental Chemical Engineering*, *6*(5), 5771–5794. https://doi.org/10.1016/j.jece.2018.08.065

Ravi, N. K., Van Sint Annaland, M., Fransoo, J. C., Grievink, J., & Zondervan, E. (2017). Development and implementation of supply chain optimization framework for CO 2 capture and storage in the Netherlands. *Computers & Chemical Engineering*, *102*, 40–51. https://doi.org/10.1016/j.compchemeng.2016.08.011

Reitz, L., Ros, J., Mathisen, A., Subramani, A., Skagestad, R., Farrel, G., Hellendall, M., Patel, B., Sharan, P., Akker, J. T., & Zapp, P. (2024). Life Cycle Assessment of Ship-based Carbon Capture: An Environmentally Sustainable Measure to Reduce CO2 Emissions in Shipping?

Ros, J. A., Skylogianni, E., Doedée, V., Van Den Akker, J. T., Vredeveldt, A. W., Linders, M. J., Goetheer, E. L., & G M-S Monteiro, J. (2022). Advancements in ship-based carbon capture technology on board of LNG-fuelled ships. *International Journal of Greenhouse Gas Control*, *114*, 103575. https://doi.org/10.1016/j.ijggc.2021.103575

Roussanaly, S., Berghout, N., Fout, T., Garcia, M., Gardarsdottir, S., Nazir, S. M., Ramirez, A., & Rubin, E. S. (2021a). Towards improved cost evaluation of Carbon Capture and Storage from industry. *International Journal of Greenhouse Gas Control*, *106*, 103263. https://doi.org/10.1016/j.ijggc.2021.103263

Roussanaly, S., Deng, H., Skaugen, G., & Gundersen, T. (2021b). At what Pressure Shall CO2 Be Transported by Ship? An in-Depth Cost Comparison of 7 and 15 Barg Shipping. *Energies*, *14*(18), 5635. https://doi.org/10.3390/en14185635

Rubin, E., Abanades, J. C., Akai, M., Benson, S., Keith, D., Mazzotti, M., Metz, B., Osman-Elasha, B., Palmer, A., Smekens, K., & Soltanieh, M. (2005). Coordinating Lead Authors.

Seo, Y., Huh, C., Lee, S., & Chang, D. (2016). Comparison of CO 2 liquefaction pressures for ship-based carbon capture and storage (CCS) chain. *International Journal of Greenhouse Gas Control*, *52*, 1–12. https://doi.org/10.1016/j.ijggc.2016.06.011

Skagestad, R., Mathisen, A., & Aas, K. (2024). CO2 offloading alternatives and guidelines.

Sødal, S., Koekebakker, S., & Aadland, R. (2008). Market switching in shipping — A real option model applied to the valuation of combination carriers. *Review of Financial Economics*, *17*(3), 183–203. https://doi.org/10.1016/j.rfe.2007.04.001

Solomon, M. D., Scheffler, M., Heineken, W., Ashkavand, M., & Birth-Reichert, T. (2024). Pipeline Infrastructure for CO2 Transport: Cost Analysis and Design Optimization. *Energies*, *17*(12), 2911. https://doi.org/10.3390/en17122911

Statista. (2023). Netherlands: Power sector carbon intensity 2023. Retrieved May 8, 2025, from https://www.statista.com/statistics/1290441/carbon-intensity-power-sector-netherlands/

Stec, M., Tatarczuk, A., Iluk, T., & Szul, M. (2021). Reducing the energy efficiency design index for ships through a post-combustion carbon capture process. *International Journal of Greenhouse Gas Control*, *108*, 103333. https://doi.org/10.1016/j.ijggc.2021.103333

Tavakoli, S., Gamlem, G. M., Kim, D., Roussanaly, S., Anantharaman, R., Yum, K. K., & Valland, A. (2024). Exploring the technical feasibility of carbon capture onboard ships. *Journal of Cleaner Production*, *452*, 142032. https://doi.org/10.1016/j.jclepro.2024.142032

Thaler, B., Kanchiralla, F. M., Posch, S., Pirker, G., Wimmer, A., Brynolf, S., & Wermuth, N. (2022). Optimal design and operation of maritime energy systems based on renewable methanol and closed carbon cycles. *Energy Conversion and Management*, *269*, 116064. https://doi.org/10.1016/j.enconman.2022.116064

The Economist Group. (2023). *Global Maritime Trends 2050* (tech. rep.).

Van Der Spek, M., Fout, T., Garcia, M., Kuncheekanna, V. N., Matuszewski, M., McCoy, S., Morgan, J., Nazir, S. M., Ramirez, A., Roussanaly, S., & Rubin, E. S. (2020). Uncertainty analysis in the techno-economic assessment of CO2 capture and storage technologies. Critical review and guidelines for use. *International Journal of Greenhouse Gas Control*, *100*, 103113. https://doi.org/10.1016/j.ijggc.2020.103113

VCS. (2024a, October). *Storage in Saline Aquifers and Depleted Hydrocarbon Reservoirs, v1.0* (tech. rep.). Verified Carbon Standard.

VCS. (2024b, October). *TRANSPORT FOR CCS PROJECTS* (tech. rep.). Verified Carbon Standard.

Visonà, M., Bezzo, F., & d'Amore, F. (2024). Techno-economic analysis of onboard CO 2 capture for ultra-large container ships. *Chemical Engineering Journal*, *485*, 149982. https://doi.org/10.1016/j.cej.2024.149982

Wang, X., & Du, L. (2016). Study on carbon capture and storage (CCS) investment decision-making based on real options for China's coal-fired power plants. *Journal of Cleaner Production*, *112*, 4123–4131. https://doi.org/10.1016/j.jclepro.2015.07.112

Wang, X., & Qie, S. (2018). When to invest in carbon capture and storage: A perspective of supply chain. *Computers & Industrial Engineering*, *123*, 26–32. https://doi.org/10.1016/j.cie.2018.06.006

Wilberforce, T., Baroutaji, A., Soudan, B., Al-Alami, A. H., & Olabi, A. G. (2019). Outlook of carbon capture technology and challenges. *Science of The Total Environment*, *657*, 56–72. https://doi.org/10.1016/j.scitotenv.2018.11.424

Wohlthan, M., Thaler, B., Helf, A., Keller, F., Kaub, V., Span, R., Gräbner, M., & Pirker, G. (2024). Oxyfuel combustion based carbon capture onboard ships. *International Journal of Greenhouse Gas Control*, *137*, 104234. https://doi.org/10.1016/j.ijggc.2024.104234

WPI. (2025). Maritime Safety Information. Retrieved April 24, 2025, from https://msi.nga.mil/Publications/WPI

Zhang, S., Zhuang, Y., Tao, R., Liu, L., Zhang, L., & Du, J. (2020). Multi-objective optimization for the deployment of carbon capture utilization and storage supply chain considering economic and environmental performance. *Journal of Cleaner Production*, *270*, 122481. https://doi.org/10.1016/j.jclepro.2020.122481

Zhang, X., Wang, X., Chen, J., Xie, X., Wang, K., & Wei, Y. (2014). A novel modeling based real option approach for CCS investment evaluation under multiple uncertainties. *Applied Energy*, *113*, 1059–1067. https://doi.org/10.1016/j.apenergy.2013.08.047

Zhao, T., Li, R., Zhang, Z., & Song, C. (2025). Current status of onboard carbon capture and storage (OCCS) system: A survey of technical assessment. *Carbon Capture Science & Technology*, *15*, 100402. https://doi.org/10.1016/j.ccst.2025.100402

Zheng, S., & Jiang, C. (2023). Real options in transportation research: A review. *Transport Economics and Management*, *1*, 22–31. https://doi.org/10.1016/j.team.2023.06.001

A

Additional results for common supply chain steps

The presented additional lattices show the total costs and emissions for the regeneration, liquefaction, LCO_2 Transport and permanent storage costs.

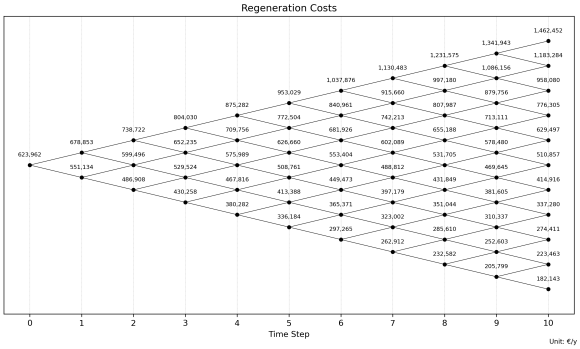

(a) Regeneration Costs

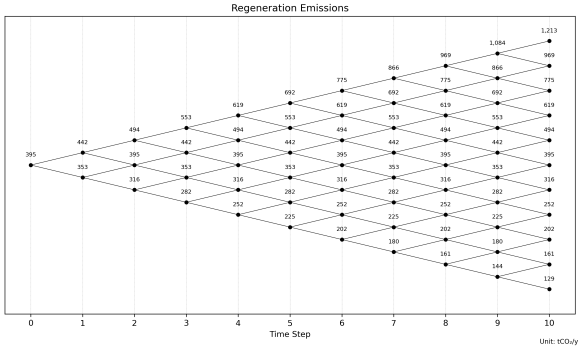

(b) Regeneration Emissions

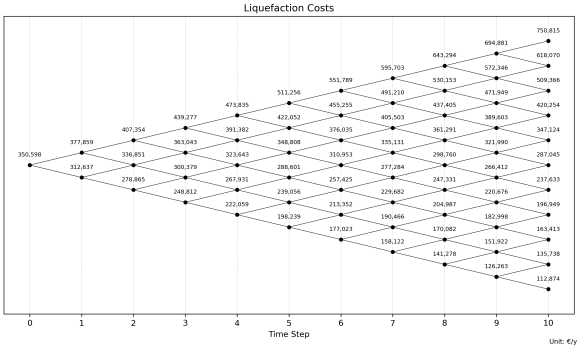

(c) Liquefaction Costs

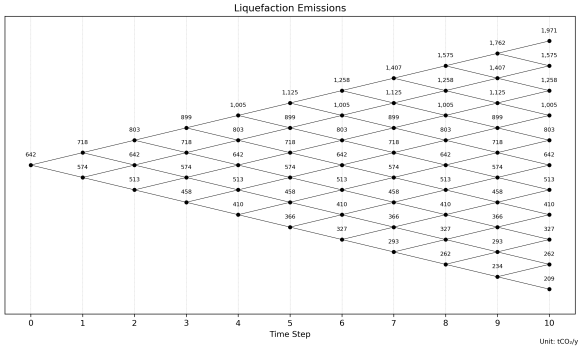

(d) Liquefaction Emissions

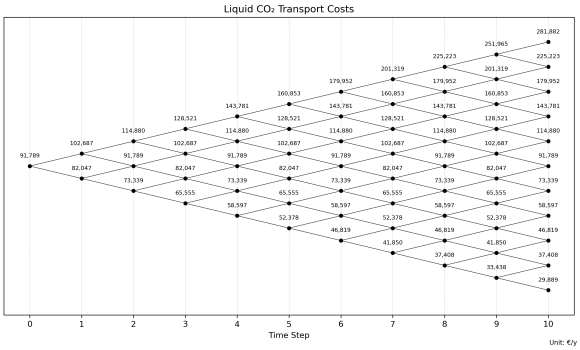

(e) Liquid CO_2 Transport Costs

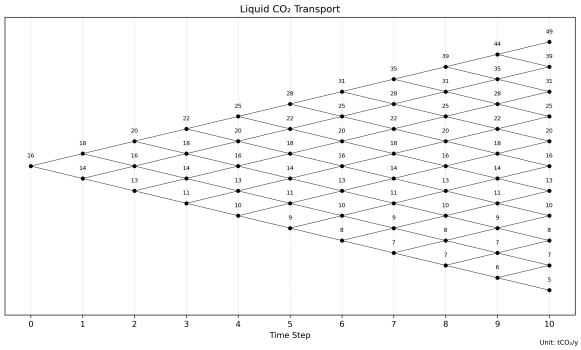

(f) Liquid CO_2 Transport Emissions

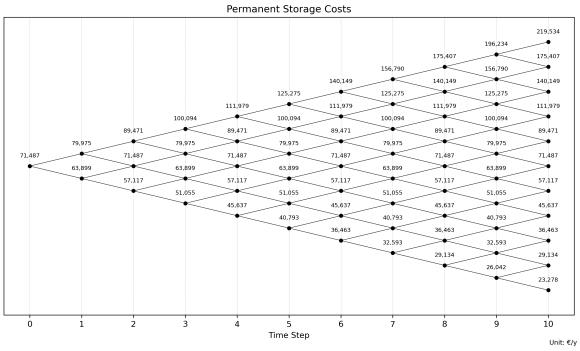

(g) Permanent Storage Costs

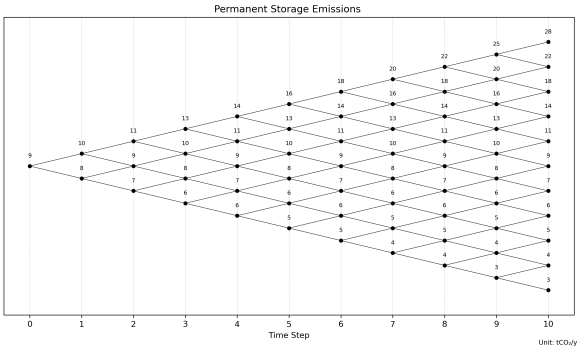

(h) Permanent Storage Emissions

B

Additional results Truck-only

The additional presented lattices show intermediate results for the supply chain in case solvent transport is carried out by truck for the entire period.

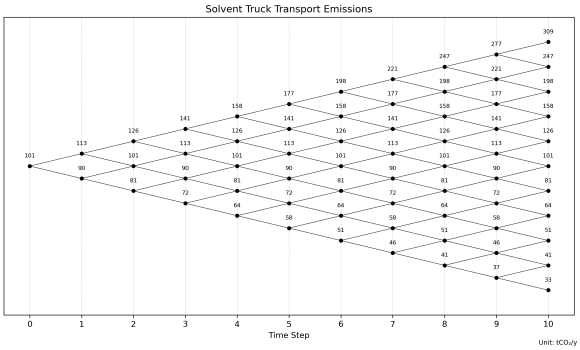

(a) Solvent Truck Transport Emissions

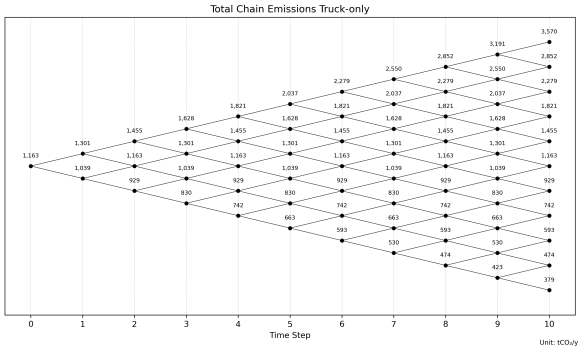

(b) Total Chain Emissions Truck-only

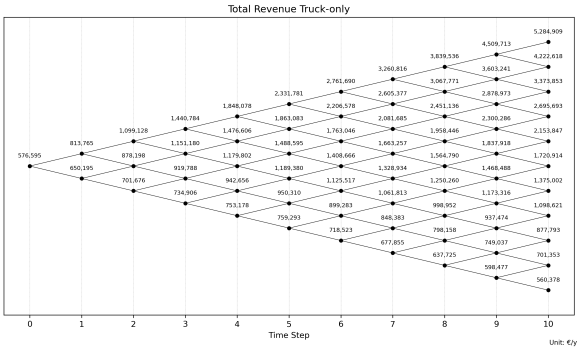

(c) Total Revenue Truck-only

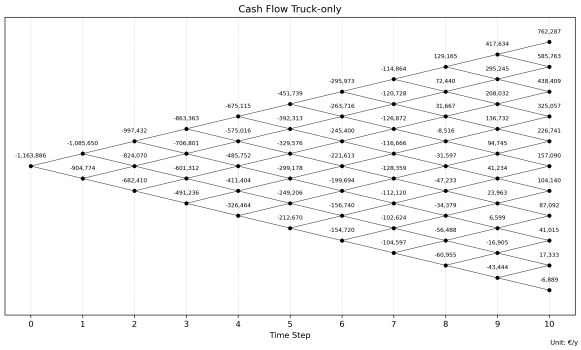

(d) Cash Flow Truck-only

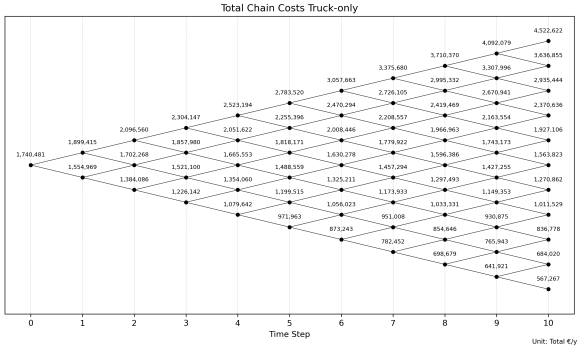

(e) Total Chain Costs Truck-only

C

Additional results CEMT-IVa

The additional presented lattices show intermediate results for the supply chain in case solvent transport is carried out by the CEMT-IVa barge for the entire period.

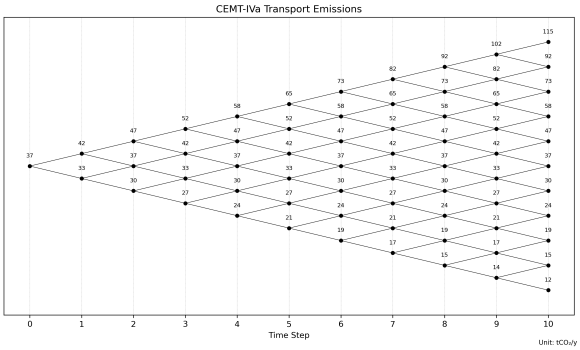

(a) CEMT-IVa Transport Emissions

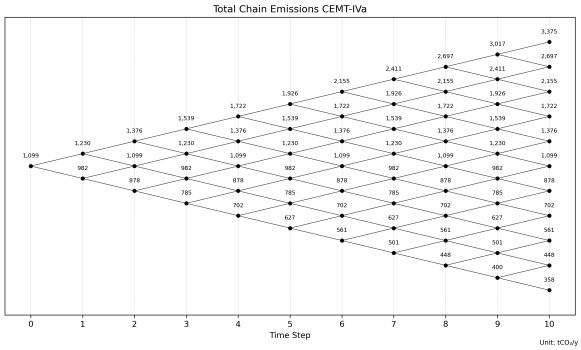

(b) Total Chain Emissions CEMT-IVa

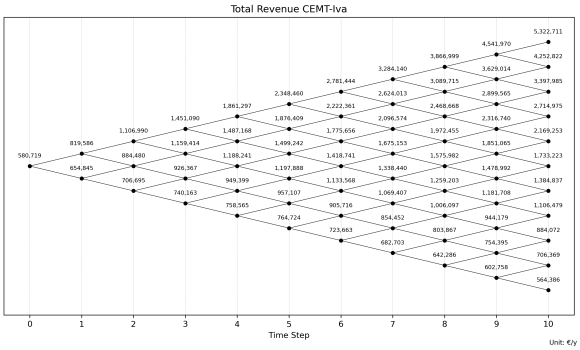

(c) Total Revenue CEMT-IVa

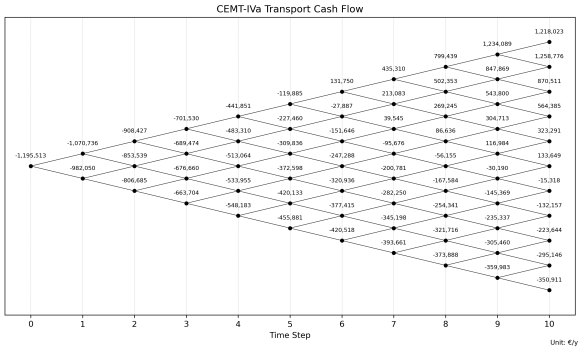

(d) Cash Flow CEMT-IVa

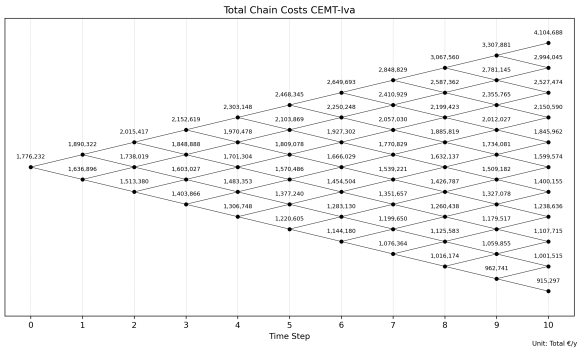

(e) Total Chain Costs CEMT-Iva

D

Additional results CEMT-Va

The additional presented lattices show intermediate results for the supply chain in case solvent transport is carried out by the CEMT-Va barge for the entire period.

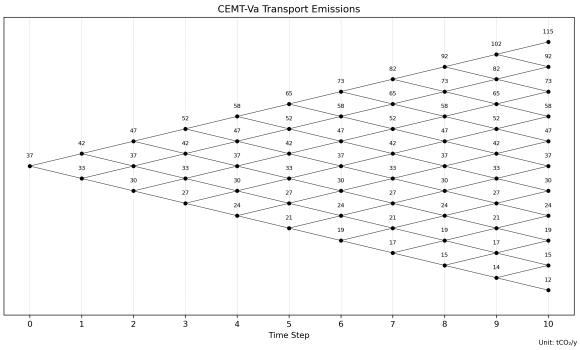

(a) CEMT-Va Transport Emissions

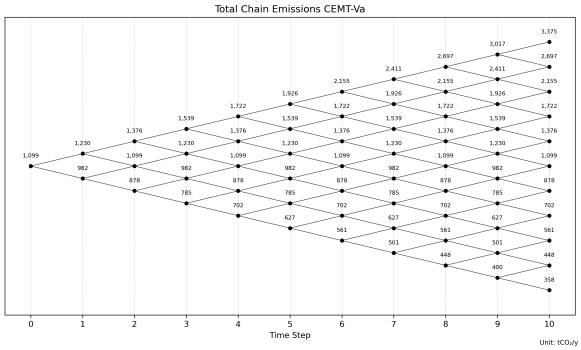

(b) Total Chain Emissions CEMT-Va

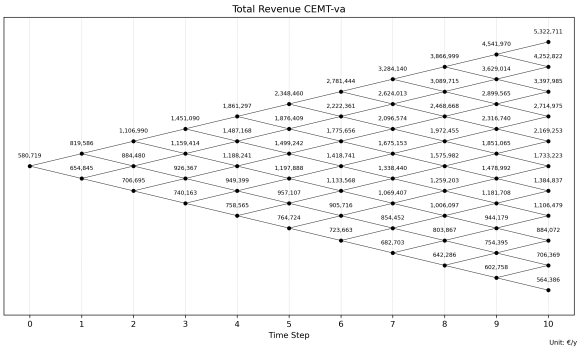

(c) Total Revenue CEMT-Va

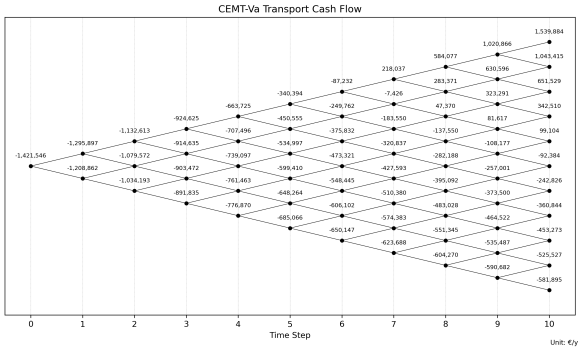

(d) CEMT-Va Transport Cash Flow

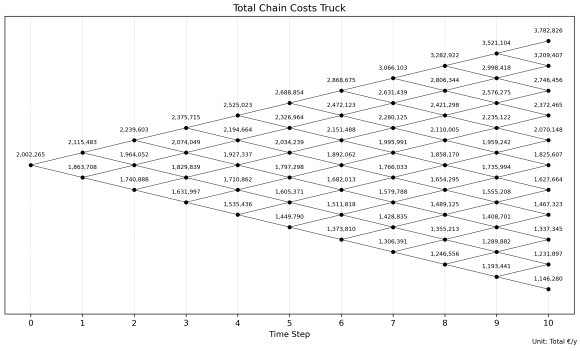

(e) Total Chain Costs CEMT-Va

E

Additional results Combined barge strategy

The additional presented lattices show intermediate results for the supply chain in case solvent transport is carried out by the combined barge strategy for the entire period.

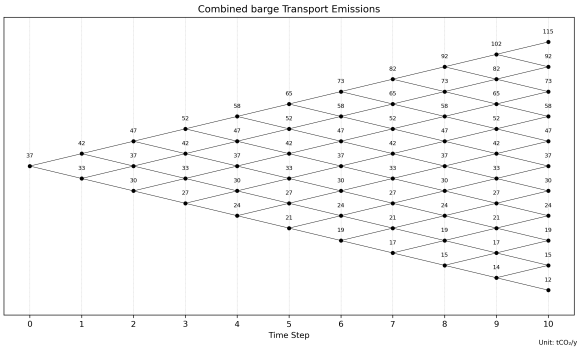

(a) Combined Barge Transport Emissions

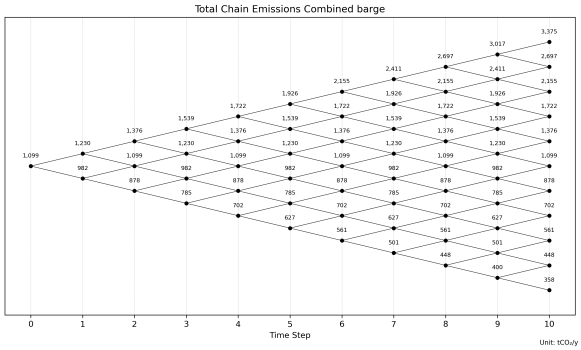

(b) Total Chain Emissions Combined Barge

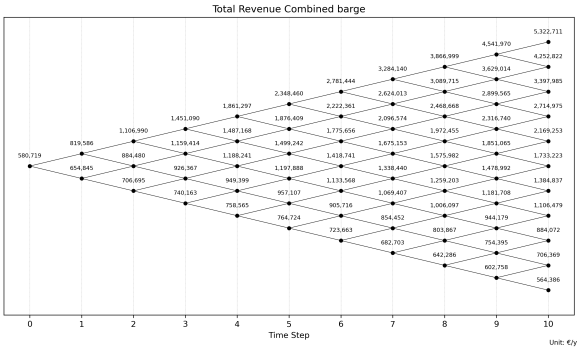

(c) Total Revenue Combined Barge

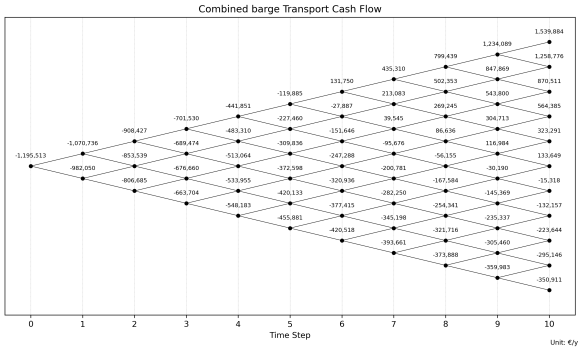

(d) Combined Barge Transport Cash Flow

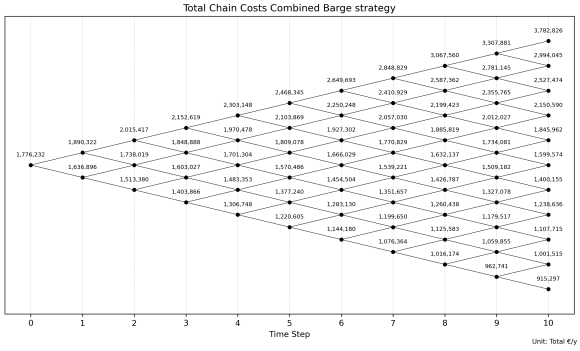

(e) Total Chain Costs Combined Barge